

**A Combined Membrane Filtration - Aeration Approach for the Treatment of Hydraulic
Fracturing - Flowback and Produced Water from the Duvernay Formation**

by

Isabel Plata Enriquez

A thesis submitted in partial fulfillment of the requirements for the degree of

Master of Science

Department of Earth and Atmospheric Sciences
University of Alberta

© Isabel Plata Enriquez, 2018

Abstract

Membrane filtration technologies have been successfully applied for the treatment of many types of wastewater. In hydraulic fracturing operations, membrane processes can be applied as a cost-effective way of removing unwanted substances from flowback and produced water (FPW) and promoting its reuse in subsequent fractured wells. High degrees of fouling has been reported when raw FPW has been passed through membranes, suggesting the need for fluid pre-treatment. In this study, aeration was used as a pre-treatment method to improve filtration flux of polymeric membranes in microfiltration (MF) and ultrafiltration (UF) processes for an FPW sample collected from the Duvernay shale play located in Alberta, Canada. The pre-treatment not only enhanced FPW flux but also increased the rejection of targeted particles (Fe, Si), and reduced some of the potentially toxic organic and inorganic compounds in the filtered fluid. Additionally, the performance of four polymeric membranes including two polyvinylidene fluoride (PVDF) MF membranes (0.2 and 0.1 μm), one polyethersulfone (PES) MF membrane (0.22 μm) and one polyethersulfone UF membrane (0.03 μm) were compared using a dead-end filtration cell. In the first test, raw FPW was used as the feed water during the experiments, and in the second stage, aeration was first applied to the raw FPW, and the aerated water was then passed through the membranes.

For all membranes, severe membrane fouling was found in the first 15 min when using the untreated FPW, with a very low rejection of Fe and Si (<10%). After the aeration treatment, the filtration flux decreased by less than 20%, as compared to more than 40% in the raw FPW, while rejection of Fe and Si increased to more than 70%. No significant differences were found in the fouling mechanisms before and after filtration. The predominant fouling mechanisms were

cake layer and intermediate pore blocking. Comparison of the four polymeric membranes revealed that the 0.2 PES membrane had the best flux and a similar rejection to the UF membrane. Therefore, the 0.2 PES membrane was used for further analysis such as quantification of polycyclic aromatic hydrocarbons (PAHs) and determination of the reduction of adverse effects on zebrafish embryos following aeration and filtration. This study highlights the key importance of pre-treatment when using membrane technologies to treat FPW, and further demonstrates the positive environmental implications of the two-step process developed here.

Acknowledgments

I would like to thank, first and foremost, my supervisor Dr. Daniel S. Alessi who gave me the opportunity to be part of his talented group and for providing me with extensive support both academically and economical throughout my entire graduate studies. I would also like to thank Dr. Mohtada Sadrzadeh for providing valuable tools and comments for the development of this research.

Additionally, I want to express my sincere gratitude to every person in the Alessi's lab, especially to Konstantin von Gunten and Dr. Shannon Flynn whose ideas contributed immensely to the richness of this project. Special thanks to the people in the Advanced Water Research Lab who also contributed to essential parts of this study. Finally, thanks to my husband and family for every word of encouragement to never give up in the process.

Table of Contents

Abstract	ii
Table of Contents	v
List of Figures	vii
List of Tables	x
1. Introduction.....	1
1.1 Overview.....	1
1.2.1 Hydraulic Fracturing and Extraction of Unconventional Oil and Gas.....	3
1.2.2 Water Demand and Fracturing Fluids.....	6
1.2.3 Flowback and Produced Water.....	8
1.2 Research Purpose and Objectives.....	15
2. Methods.....	17
2.1 Experimental Procedure and Materials.....	17
2.1.1 FPW Sample Location.....	17
2.1.2 Membranes Selection and Characterization.....	18
2.1.3 Membrane Filtration Experiments.....	20
2.2 Analytical Procedures.....	26
2.2.1 Inorganic Solution Chemistry.....	26
2.2.2 Organic Solution Chemistry.....	27
2.2.3 Solids Characterization.....	28
2.3 Developmental Toxicity in Exposed Zebrafish Embryos.....	32
2.4 Microbial Communities from Flowback Precipitates.....	34
3. Results and Discussion.....	35
3.1 Flowback and Produced Water Physicochemical Characterization.....	35
3.2 Membrane Filtration.....	38
3.2.1 Membrane Resistance and Contact Angle Measurements.....	38
3.2.2 Flux and Rejection of Untreated Flowback and Produced Water.....	41
3.2.3 Optimization of the Membrane Filtration Process for Flowback and Produced Water: Application of an Aeration Pre-treatment.....	49
3.2.4 Flux and Rejection of Aeration-treated Flowback and Produced Water.....	55
3.2.5 Fouling Characterization Before and After Aeration Treatment.....	60

3.3 Environmental Implications of FPW treatment.....	77
3.3.1 Total Digestion and Sequential Extraction from Solids Before and After Aeration Treatment	77
3.3.2 Polycyclic Aromatic Hydrocarbons (PAHs) analysis	81
3.3.3 Toxicological Analysis on Zebrafish Embryos (<i>Danio rerio</i>).....	85
3.3.4 Microbial Communities Present in FPW Solids	89
4. Conclusions	91
5. Future Work	94
References	96
Appendix A.	110
Appendix B.	112

List of Figures

Figure 1. Location of unconventional deposits of oil and natural gas in Canada. (Adapted from Network, C.W., 2015).....	4
Figure 2. Volume of water used in hydraulic fracturing by source in Alberta. Adapted from Alberta Energy Regulator (AER, 2017).....	7
Figure 3. Priority of target constituents considered in the treatment of FPW. Adapted from Bromley, 2015.....	13
Figure 4. Location map of the gas well where the FPW sample was collected.....	17
Figure 5. Experimental bench-scale setup for MF and UF operations.....	21
Figure 6. Experimental setup of the aeration tests.	25
Figure 7. Schematic of the zebrafish embryos exposure (Modified from Lammer et al., 2009)..	33
Figure 8. Hydraulic resistance of the four polymeric membranes.	39
Figure 9. Pore structure of the 0.2 PVDF and 0.2 PES membranes. Figures A and B correspond to the 0.2 PVDF membranes “top” and “bottom” sides, respectively. C and D images show the shiny side of the 0.2 PES membrane with narrow pores and the matte side with wider pores, respectively.	40
Figure 10. Comparison of permeate flux for polymeric MF and UF membranes at a TMP of 8 and 20 psi, respectively.	43
Figure 11. Normalized flux and time after filtration of 1 L of FPW sample.....	45
Figure 12. Comparison of filtration flux of the 0.2 PES membrane at different TMP at 5 psi and 8 psi and the 0.2 PVDF membrane at 8 psi.	46
Figure 13. Comparison of permeation flux of the 0.2 PES and 0.2 PVDF membranes with initial fluxes at TMP of 8 and 14 psi, respectively.....	47
Figure 14. Concentration of Fe (II) and total Fe after 24 hr aeration, determined by the ferrozine method (Stookey, 1970).....	51
Figure 15. First-order rate of oxidation of ferrous iron after 24 h aeration using the raw FPW sample.	52
Figure 16. Log of the rate constant as a function of log of Fe (II).....	53
Figure 17. pH changes of the raw FPW sample during the 24-hr aeration experiment at room temperature.....	54

Figure 18. TOC changes during 24 h aeration with compressed air of an FPW sample from the Duvernay play.	55
Figure 19. Permeate flux of four different polymeric MF-UF membranes after the aeration treatment.	57
Figure 20. Normalized flux of four different polymeric membranes after filtration of 1 L of FPW sample.	57
Figure 21. Flux decline of the 0.2 PVDF and 0.2 PES membranes at a pressure of 14 psi and 8 psi, respectively, and similar initial flux.	58
Figure 22. A) Appearance of the feed (raw FPW) and non-aerated permeate (NAP) solutions. B) Appearance of the FPW after the aeration treatment (oxidized FPW) used as a feed in MF and UF analysis, and the aerated permeate (AP) solution.....	60
Figure 23. Fouling mechanisms at the initial stage after filtration of non-aerated FPW according to Hermia's model.....	63
Figure 24. Fouling mechanisms at the later stages of the non-aerated FPW for the 0.2 PVDF and 0.2 PES membranes.....	64
Figure 25. Fouling mechanisms after the aeration treatment for the 0.2 PVDF and 0.2 PES membranes.	67
Figure 26. Particles deposited on the surface of the MF membranes before and after the aeration treatment.	69
Figure 27. Overall composition of particles retained on the 0.2 PES membrane before and after aeration.....	70
Figure 28. A) clusters of iron oxides smaller than 1 micron and tubular iron oxides. A) clusters of needle-like shapes of Ba/Sr-SO ₄ (possibly barite and celestine). Similar particles were observed before and after the aeration treatment for all the membrane filtrations.	72
Figure 29. XRD of the samples before and after aeration treatment.....	73
Figure 30. Surface of the 0.2 PES membrane before and after the aeration treatment.	74
Figure 31. Cross section of the 0.2 PVDF (left side) and 0.2 PES (right side) membranes. A. cross-section of the unused 0.2 PVDF membrane. B. Cross-section of the 0.2 PVDF membrane after filtration of raw FPW. C. Cross-section of the 0.2 PVDF membrane after filtration of the oxidized FPW. D. Cross-section of the 0.2 PES membrane after filtration of raw FPW. D. Cross-section of the 0.2 PES membrane after filtration of the oxidized FPW.	76

Figure 32. Sequential extraction results of solids before and after the aeration treatment. Total digestion for each sample is presented above the graph..... 80

Figure 33. Total PAHs concentration. A) shows the total PAHs concentration from the untreated (Raw) FPW, the treated FPW by only-membrane filtration (Non-Aerated Permeate, NAP), and the FPW with the combined aeration-filtration treatment (Aerated Permeate, AP). B) shows the distribution of the total PAHs in the aqueous (W) and suspended sediment (S) fractions of the total in each FPW sample, respectively..... 83

Figure 34. Effects in zebrafish embryo of the filtration and filtration-aeration treatments compared to the raw FPW sample after 96 h of exposure. A control water was also compared. NAP: non-aerated permeate, AP: aerated permeate A) Mortality of exposed embryos. B) Pericardial Edema results. Significant differences ($p < 0.05$) among each dilution are shown by different letters using one-way ANOVA. Significant differences between the control and dilutions is represented by (*).
..... 87

Figure 35. LC₅₀ curves for the exposed zebrafish embryos to the three different FPW solutions.
..... 88

Figure 36. Microbial communities of the treated and untreated sediments collected after microfiltration with the 0.2 PES membrane..... 90

List of Tables

Table 1. Properties of membranes used in the filtration experiments.	20
Table 2. Fouling mechanisms according to Hermia's Model. (Adapted from Cassini et al., 2011).	24
Table 3. Types of water based on TDS concentrations. Adapted from Carrol (in Todd and Mays, 2005).	35
Table 4. Flowback and produced water characteristics of a hydraulically fractured well in the Duvernay play.	37
Table 5. Comparison of the chemical composition from two gas plays in the US and the Duvernay play in Canada. *Data collected from Ziemkiewicz and He (2015), Stepan et al., (2010), and Li (2013).	37
Table 6. Contact angle measurement of each membrane by the sessile drop method.	41
Table 7. Observed rejection of Fe, Si, and TOC after FPW micro and ultrafiltration of FPW. Only the 0.2 µm membranes were done in duplicates due to limited water samples.	48
Table 8. Rejection of iron, silica, and TOC after aeration of the raw FPW.	59
Table 9. Concentration of 13 USEPA priority parent PAHs, and 4 alkylated PAHs present in the FPW samples. Concentration in the aqueous (W) and the sediment (S) fractions, respectively. ND = Not Detected; MDL = Method Detection Limit.	84
Table 10. LC50 data and analysis through the Litchfield-Wilcoxon method where significant differences are shown by different letters.	88
Table 11. Richness and diversity of the microbial community for the two FPW solids (before and after aeration).	90

1. Introduction

1.1 Overview

Oil and gas operations generally utilize large volumes of fresh water, especially vast amounts are required in the development of hydraulically fractured horizontal wells in unconventional reservoirs (Cheremisinoff and Davletshin, 2015; Jackson et al., 2015). The potential of generating high volumes of wastewater, which is known in the industry as flowback and produced water (FPW), after drilling a single well presents major management challenges due to its complex chemical composition and the potential toxicity of some of the constituents (Bai et al., 2013; Jackson et al., 2015). Additionally, the creation of strict new regulations to protect the environment have increased the pressure on the oil and gas industry to develop sustainable strategies to reuse and recycle this type of wastewater. In Alberta, disposal of FPW is mainly through deep-well injection because of the lack of cost-effective treatment technologies capable of producing a treated fluid stream with acceptable parameters for reuse in hydraulic fracturing (Rokosh et al., 2012). Recently, membrane filtration technologies are gaining more attention as potential water treatment options that can produce water of an acceptable quality for reuse in further operations. Pressure-driven membrane processes such as microfiltration (MF) and ultrafiltration (UF) are intended to fractionate wastewater constituents reducing the use of more aggressive chemical treatments (Alzahrani and Mohammad, 2014). Although this technology is a feasible alternative for FPW treatment, a common drawback is encountered by a reduction in the performance of the membranes due to fouling. This phenomenon may rapidly decrease the membrane flux, which in turn can increase operational costs due to frequent cleaning procedures and/or replacing of membranes. Some authors (Kong et al., 2017; Sick, 2015; Howe and Clark,

2006) have addressed this issue by applying a pre-treatment method to the feed solution, namely a coagulation process. Nonetheless, these authors found that a lower coagulant dose of aluminum increased fouling compared to the raw water (Salt Lake water), but a higher dose seemed to improve permeate flux (i.e., fluid which passes through the membrane). Their results suggest that interactions among foulants, coagulants, and membrane materials are challenging to foresee and may sometimes not achieve the expected improvements in permeate flux. Therefore, the goal of this study is to test aeration as a pre-treatment method for not only improving the flux in MF and UF operations, but also to accelerate the formation of iron hydroxides onto which some potentially toxic constituents present in FPW might be adsorbed, as it has been reported by He et al. (2017b) that suspended solids from FPW are associated to some organic components. Application of these two technologies in the treatment of FPW has promise in decreasing the consumption of fresh water sources and may also prevent the release of contaminants into the environment.

1.2 Development of the Oil and Gas Industry

Fossil fuels such as coal, petroleum and natural gas remain the primary energy source around the world, with an annual consumption accounting for more than 80% of the total of energy produced worldwide in the last two decades (IEA, 2014). However, as more attention and efforts are being made towards decreasing the levels of harmful greenhouse gases emissions, mainly from the combustion of coal and petroleum products, natural gas is among the proposed answers in a transition toward low-carbon energy sources (O.E.C.D., 2011). Natural gas is a mixture of hydrocarbons, containing more than 90% of methane (CH_4), and small proportions of non-hydrocarbon substances including nitrogen and hydrogen sulfide (Cheremisinoff and Davletshin, 2015; Arthur et al., 2009). Although natural gas can be mined from conventional deposits, in recent years, it is typically extracted from unconventional reservoirs (Drogos, 2015). In conventional

deposits, oil and gas can flow easily through sedimentary rocks due to the formation characteristics, i.e., high porosity and well-connected pores. Unconventional deposits, on the other hand, are constrained by the low porosity and reduced permeability of the rocks, such as shales, siltstones, very fine-grained sandstones, and carbonates (Speigh, 2016, Drogos, 2015).

1.2.1 Hydraulic Fracturing and Extraction of Unconventional Oil and Gas

Hydraulic fracturing is a revolutionary technique that has been employed for over six decades to stimulate underground sedimentary rocks enhancing the recovery of oil and gas reserves (U.S.EPA, 2016; Drogos, 2015). Initially, this technology was used in conventional deposits, but a decline in the reserves boosted the need to turn towards other natural gas deposits which were previously inaccessible (U.S.EPA, 2016). Recently, technological innovations through the combined use of directional drilling and hydraulic fracturing techniques have allowed access to unconventional deposits, increasing production rates considerably of not only natural gas but also for oil. The United States, for example, had a steep increase in production of natural gas as a consequence of the technical improvements made in hydraulic fracturing rising from about 18 trillion cubic feet (tcf) in 2005 to more than 25 tcf in 2015 (U.S.EIA, 2016). Other countries with abundant natural gas reserves such as China, Argentina, Mexico, and Canada could further raise global production by an additional 50% by 2035 (IER, 2012).

In Canada, the fifth producer of natural gas in the world, resources have also increased due to hydraulic fracturing and have been estimated to be over 1,000 tcf (CAAP, 2018; NEB, 2017). However, resource assessments may vary, and the full potential of gas reserves might not be fully discovered as unconventional deposits are still under exploration in many regions of Canada (Chong and Simikian, 2014). Currently, resources have been identified in the provinces of British Columbia, Alberta, Saskatchewan, New Brunswick, Ontario, and Quebec (Figure 1). The majority

of natural gas production comes from the Western Canadian Sedimentary Basin (WCSB), specifically from the province of Alberta where the production accounted for about 67% of the total natural gas in Canada (Alberta oil and gas, 2017; NRCAN, 2018). Although the total production of natural gas is projected to decrease slightly by 2021 due to low prices, it is projected to rise 11% approximately by 2040 (NEB, 2017).



Figure 1. Location of unconventional deposits of oil and natural gas in Canada. (Adapted from Network, C.W., 2015).

The potential of natural gas deposits in the province of Alberta includes the Nordegg Member, the Muskwa Formation, the Colorado Group, the Montney Formation, and the Duvernay Formation. The latter two plays (the Montney and Duvernay Formations) also produce liquified natural gas (LNG, containing ethane and butane), which has increased the interest in their exploration and exploitation (NRCAN, 2018; NEB, 2017; Network, C.W., 2015). In the Duvernay Formation, which fracturing activities have been rapidly increasing in recent years, the estimated

natural gas resources average 443 tcf (Rokosh et al., 2012). According to the Alberta Energy Regulator (AER, 2016), by the end of 2015 more than 220 gas wells were drilled using hydraulic fracturing technologies, and it is expected that approximately 8,200 new wells will be drilled in the next 30 years (Alberta oil and gas industry, 2017).

The process of hydraulic fracturing and horizontal drilling starts with the perforation of vertical wells at depths of 1 to 5 km until the target formation is reached, and then the wellbore is angled horizontally for several miles (Cheremisinoff and Davletshin, 2015). Next, fracturing of the low-permeable rocks is carried out by injecting large amounts of water, and a variety of chemicals at high pressures in order to create a flow path for oil and gas. A solid proppant (typically sand or ceramic beads) is also added into the well to keep the fractures open, which enables oil and gas to move towards the wellbore and up to the surface. The mixture of these three elements (water, chemical additives, and proppant) is known as hydraulic fracturing fluid (U.S.EPA, 2016; Drogos, 2015). Fracturing operations are generally conducted in more than one stage per well where, and depending on the number, they can be classified as short (less than 25) or large (more than 35 stages) (Bai et al., 2015). The number of stages is determined mainly on well-length, reservoir characteristics, and the operator's fracturing design. Depending on the number of stages required to hydraulically fractured a well the volume of water will also differ. After the fracturing process is completed, the pressure in the well is reduced allowing the flow of oil and gas to the surface along with the fracturing fluids and naturally occurring water that was also trapped underground. The returning of both waters, mainly fracturing fluids and some formation water, is termed as flowback water, which can flow for the first two weeks and up to 2 months (Bai et al., 2015; Alessi et al., 2017). The term produced water is often applied to the returning water after the flowback period, and it is characterized by a higher content of formation water (Kondash et al.,

2017). However, the distinction between these two terms is not objective in the industry or the scientific literature, thus in this thesis the term of flowback and produced water (FPW) is used here to describe the whole wastewater product, and it is not differentiated.

1.2.2 Water Demand and Fracturing Fluids

Water is a crucial element for the development of a hydraulically fractured well in unconventional deposits, where consumption is considerably higher compared to conventional operations (CCA, 2014). The supply of water in hydraulic fracturing can be taken from different sources depending on the geographic location, fresh water (lakes, rivers, groundwater) being the main source; other types include groundwater (fresh and saline), recycled/reused FPW or other types of wastewater (Goss et al., 2015; Alessi et al., 2017). In Alberta, for instance, in 2016, the use of non-saline water sources accounted for about 90% of the total use, while only 6% and 1% were recycled from fracturing operations and other types of wastewater, respectively (Figure 2; AER, 2017). Large volumes of water are usually required to drill a single well, varying from less than 10,000 m³ to more than 30,000 m³ in the U.S. and Canada. The exact amounts of water use for drilling a well may fluctuate depending on multiple factors such as the geology of the target formation, the types of fracturing fluids, the water sources available in the region, and the number of fracture stages (Stringfellow et al., 2014; Clark et al., 2013; Network, C.E., 2015). In the Duvernay play specifically, Alessi et al. (2017) reported that the volume of water used per well between 2011 and 2014 was around 10,000 m³, while PTAC (2017) indicated values from 15,000 m³ to more than 100,000 m³ which varied depending on the length of the well and the operator's technology.

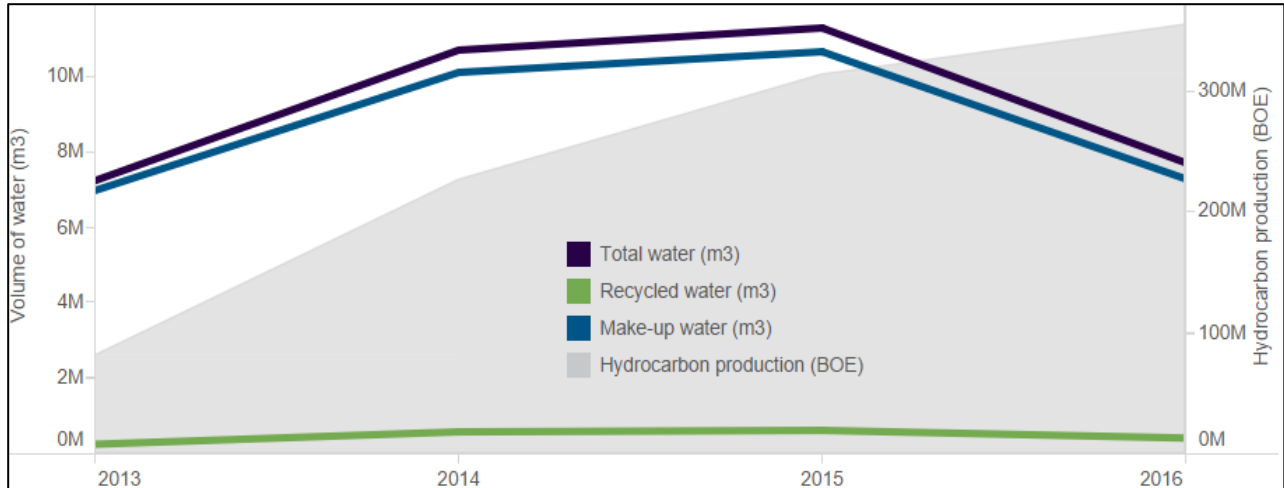


Figure 2. Volume of water used in hydraulic fracturing by source in Alberta. Adapted from Alberta Energy Regulator (AER, 2017).

The type of hydraulic fracturing fluids used in horizontal drilling can be classified into four categories: slickwater, gel, energized, and hybrids (a combination of energized slickwater, and gel slickwater) (Alessi et al., 2017). Slickwater fracturing fluids, which are suitable for brittle formations and are commonly used across the United States and in the Duvernay Formation in Alberta (Canada), usually requires a higher volume of water than the other three types (PTAC, 2017; Rivard et al., 2014). Other fracturing fluids are primarily used in more ductile deposits such as the Montney Formation (Speight, 2016). Over a thousand chemical additives, e.g., acids, alcohols, aromatic hydrocarbons, surfactants, etc., can be employed in the fracturing fluids in varying combinations, although the exact chemical concentration of the mixtures and their component concentrations are often not entirely disclosed, as they are proprietary information (Alessi et al., 2017; U.S.EPA, 2015; Stringfellow et al., 2014). The purpose of adding these chemicals include reduction of mineral and biological scaling, adjusting pH, increasing the

viscosity to carry proppant, and generally for maintaining the fracture network and thereby improving the production of natural gas (U.S.EPA, 2016).

1.2.3 Flowback and Produced Water

As previously mentioned, flowback is the water that returns to the surface immediately after the fracturing process is completed. Its composition is differentiated by lower concentrations of salts and more fracturing fluids components as compared to produced water or returned water at later stages. Produced water is often inferred to reflect typical conditions of naturally occurring formation water (CCA, 2014). The total production of FPW may fluctuate in every well just as the amount of water required for fracturing a well varies among plays. Kondash et al. (2017) reported a production range from about 1,000 m³ to more than 14,000 m³ in some of the most active basins of the U.S. Similarly, in western Canada, FPW generation has been estimated to be around 10,000 and 50,000 m³ between 2011 and 2013 in the Montney and the Duvernay formations, respectively (Goss et al., 2015). Some studies (e.g., Kondash et al., 2017; Kim et al., 2016; Bai et al., 2015; Arthur et al., 2009) have indicated that most of the injected fluids are kept in the target formation and that only a low percentage (below 50 to 40%) will return to the surface, thus FPW consists mainly of formation water at later stages. For instance, Rivard et al. (2013) reported FPW recoveries between 15 to 70% in British Columbia, while in eastern Canada, the recovery was around 45%.

In general, the geochemical composition of these waters is highly complex and can vary depending on several factors such as the geology of the target formation, the source water, the fracturing fluids, and also the time of water collection, i.e., lower total dissolved solids (TDS) has been reported in the initial returned water (first couple of weeks) and gradually increasing its concentration at later stages (Goss et al., 2015; Zolfaghari et al., 2015). Generally, TDS ranges

from below 10,000 mg/L to more than 300,000 mg/L (CCA, 2014; Benko and Drewes, 2008). Common inorganic constituents include Na, Ca, Mg, Ba, Fe, B, As, Cu, Si, Pb, halides (Cl, Br), as well as naturally occurring radioactive materials (NORMS) (Haluszczak et al., 2012; Abualfaraj et al., 2014). Organic compounds are also found in FPW, usually in trace amounts, such as xylenes, acetone, 2-butanone, Cocamidopropyl dimethylamine, ethoxylate groups, polyethylene glycols (PEGs), polycyclic aromatic hydrocarbons (PAHs), phenols, aliphatic hydrocarbons, BTEX compounds, ethane, propane, etc. (Lester, et al., 2015; Annevelink et al., 2016; Ferrer and Thurman, 2015). Wide ranges of total organic carbon (TOC) concentrations have been reported from less than 50 mg/L to 5500 mg/L in the U.S. (Orem et al., 2014). In Canada, TOC concentrations in FPW samples have been reported from the Duvernay formation with values of 211 mg/L and 734 mg/L (He et al., 2017a; He et al., 2018). The primary source of the high TDS concentrations and also some of the organic compounds found in FPW has been suggested to be the result of natural constituents from the formation water, or the product of chemical reactions between the fracturing fluids with the formation water, and the dissolution of rock constituents (minerals and organics) (Ziemkiewicz and He, 2015).

1.2.3.1 Environmental Implications of FPW Releases on Landscapes

Potential risks of contamination to surface and groundwater ecosystems which can occur from accidental spills of FPW during transportation, releases at the well pad, or from inappropriate disposal activities is one of the major concerns related to hydraulic fracturing technologies (U.S.EPA, 2016; Annevelink et al., 2016). The prediction of harmful effects from those FPW releases on living organisms has been difficult to measure due to uncertainties on the mechanisms and transformation of some of the organic e inorganic components present in water when reaches the soil surface or comes in contact with rivers, or lakes. A few studies, mainly from the U.S. and

Canada, have directly reported the toxicity effects of FPW samples on aquatic organisms. In the U.S., Kassotis et al. (2016) showed disruptive reproduction and development in fish downstream of a wastewater injection facility in West Virginia. Cozzareli et al. (2017) described the adverse effects, including endocrine disrupting activity and high mortality, in several aquatic species in a small stream in North Dakota (U.S) as a result of a wastewater pipeline leak from hydraulic fracturing operations. In Canada, He et al. (2017a, 2017b, 2018), Folkerts et al. (2017), and Blewett et al. (2018) reported the acute toxicity (median lethal concentration, MLC_{50}) and other lethal and sublethal points on rainbow trout, zebrafish embryos, and *Daphnia Magna* species, respectively, exposed to FPW samples collected from the Duvernay play in Alberta. Their findings quantified harmful effects in the normal development of the species such as biotransformation, oxidative stress, and endocrine disruption. Interestingly, some of the studies highlighted that the adverse effects were diminished when the FPW was previously treated by removing the suspended solids. These results address the relevance of investigating treatment options to remove potential toxic components from FPW samples.

1.2.3.2 Management of FPW and Treatment Options

As the rate of hydraulic fracturing and horizontal drilling to extract natural gas is expected to grow over the next 30 years, governmental agencies, as well as the industry, face new technological and environmental challenges emerging from the necessity to treat and reuse produced FPW while reducing the use of fresh water. Currently, due to the physicochemical complexities of FPW and mainly to economic factors, the most commonly used methods to manage this type of wastewater in the U.S. and Canada is through deep-well injection, at depths of ~4000 ft (1200m) (Alessi et al., 2017; Saba, 2014; Clark and Veil, 2009; U.S.EPA, 2016). However, the limited number of available injection wells nearby some fracturing areas coupled to

the need of reducing the use of fresh water sources have increased the interest of treating and reusing FPW in new hydraulic fracturing operations (Gregory et al., 2011). Other FPW handling options are direct reuse with no treatment, on-site treatment and reuse, off-site treatment and reuse, and off-site treatment and disposal (Boschee, 2014). From these alternatives and depending on the chemical composition of the FPW, direct reuse might not be considered an option as some of the constituents can present considerable obstacles during well development such as scaling, well plugging, and inhibition of some additives. Thus, applying a pre-treatment method might offer cost-saving benefits to the industry. On-site treatment, which uses a combination of treatment methods in serial, would likely be the preferred choice, although identifying adequate treatment technologies that can meet the required water specifications is a demanding task due to compositional variations in each well and basin.

Global FPW management practices are not well documented, which makes it difficult to assess and compare the efficiency of the treatment options applied to each area. The Marcellus play, however, has reported more information about the strategies used for FPW handling where the primary management method is direct reuse by mixing of untreated FPW with fresh water. Direct reuse is only employed when the FPW to be reused contains low TDS (Boschee, 2014). The second common treatment method for FPW is the use of centralized waste treatment facilities (CWT). These methods have increased FPW reuse in the Marcellus play from 5% in 2008 to about 90% in 2013 (Rahm et al., 2013; U.S.EPA, 2016). Other examples are the Barnett play, where reuse of FPW is also becoming an integral part of the management strategy for reducing freshwater use (Mantell, 2011; Clark et al., 2013). In the Montney and the Duvernay formations in British Columbia and Alberta, respectively, underground injection is still considered the preferred disposal option with little water reuse (Alessi et al., 2017).

Treatment technologies to remove inorganic and organic constituents from wastewaters may include biological, physical, and chemical methods (Fakhru'l-Razi et al., 2009). However, biological treatments might not be suitable in the management of FPW because of its high salinity and the presence of other toxic compounds, which can be harmful and affect the performance of microorganisms (Butkovsky et al., 2017). Water treatment technologies can be further classified into two categories: conventional and advanced treatment technologies. Conventional methods usually do not require high energy consumption and can include techniques such as flocculation, coagulation, granular media filtration, sedimentation, microfiltration and ultrafiltration, and lime softening. These methods are used for removal of suspended solids, oil and grease. On the other hand, advanced treatments such as nanofiltration, reverse osmosis membrane filtration, thermal distillation, evaporation, and advanced oxidation are more expensive as they require higher energy to operate (Mantell, 2011; Boschee, 2014; U.S.EPA, 2018). Removal of dissolved species is the main target of these advanced technologies. Since the primary goal is to reuse FPW in similar hydraulic fracturing processes (due to the high TDS concentrations) rather than reuse in other industries (agricultural) or to achieve contaminants levels that meet drinking water standards, conventional methods might be more convenient and feasible to develop. Some studies have shown that waters with high TDS levels (up to 285,000 mg/L) were suitable for hydraulic fracturing wells (Lebas et al., 2013), demonstrating that the focus should be on removing suspended solids and scaling elements. Figure 3 illustrates constituents in FPW that are of primary concern for its treatment (Bromley, 2015). For instance, removal of suspended solids from FPW by membrane filtration processes was suggested as a more environmentally friendly approach than the use of chemical treatments (Mantell, 2011). Hussain et al. (2014) also noted that membrane

filtration operations are more efficient for the removal of suspended particles compared to other types of filtration such as sand filtration or filtration by other media.

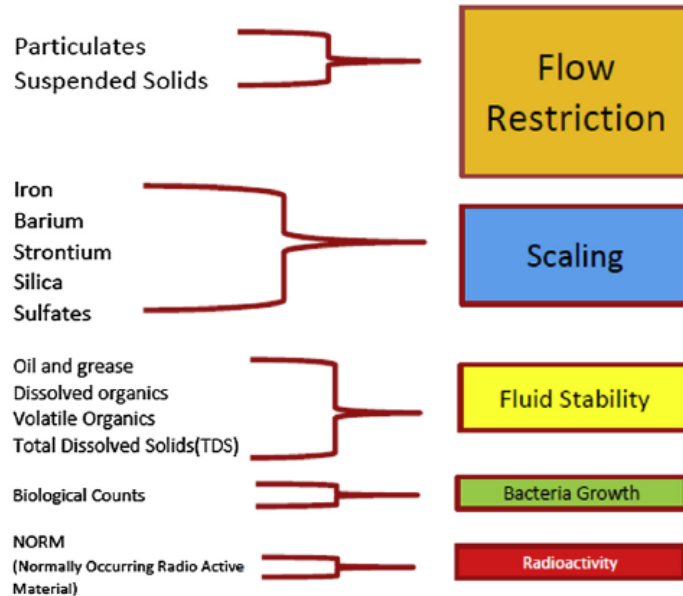


Figure 3. Priority of target constituents considered in the treatment of FPW. Adapted from Bromley, 2015.

Membrane filtration technologies, particularly MF and UF, could be a promising alternative in the treatment of FPW to remove effectively suspended solids for subsequent reuse in the fracturing fluids mixture or as a pre-treatment preceding more advanced technologies such as reverse osmosis for other beneficial reuse (Hussain et al., 2014). Extensive research has been carried out on MF and UF operations from municipal wastewater treatments (Mallevalle et al., 1996), but few studies have been published that investigate membrane filtration operations in the treatment of real FPW. Most of the published research has been conducted mainly in the Marcellus and Barnett plays in the U.S. and one example from the Fuling play in China, but no data has been published on FPW treatment by MF and UF in Canada. Importantly, previous results reported

severe fouling of MF and UF membranes without previous conditioning of FPW. Fajt et al. (2013) compared different types of MF membranes to evaluate removal of iron and suspended solids by including an aeration pretreatment to an FPW sample obtained in the Barnett Shale. These treatments proved effective for removing iron from solution, although no studies were performed in the analysis of flux or fouling of the membranes. Jiang et al. (2013) evaluated the flux performance and fouling mechanisms of MF and UF ceramic membranes with different pore sizes (1.4 μm , 0.8 μm , 0.2 μm , 0.02 μm , 5 nm). The authors also tested a combination of treatments, i.e., MF, UF, and subsequent ion-exchange, to treat flowback water from the Marcellus play. Their results showed a rapid flux decline for all the membranes (MF-UF) due to fouling, exhibiting differing clogging mechanisms such as complete pore block and cake filtration mechanisms, but also demonstrated a high removal of suspended solids. In the serial treatments, the authors also compared the efficiency between MF and UF techniques, concluding that removal of suspended solids was similar (near 100%) in both processes; therefore, MF was proposed as a more cost-effective operation. He et al. (2014) investigated the fouling phenomenon in MF using a hydrophilic polymeric membrane (polyvinylidene, PVDF) with a pore size of 0.22 μm . The authors suggested that the main reason of membrane fouling was the presence of organic-coated particles of submicron size similar to the pore size of the membranes in the early flowback. He and Vidic (2016) tested two MF (0.2 μm and 0.25 μm) ceramic membranes in a crossflow filtration system using flowback water from the Marcellus play. The study revealed that disaggregation of bigger particles and formation of colloids was the cause for fouling. Xiong et al. (2016) also analyzed the fouling characteristics of polymeric MF membranes with different pore sizes (0.2, 0.4, 0.8, and 1.2 μm). High degrees of membrane fouling was attributed mainly to the stable colloidal material present in flowback water from the Marcellus shale. Kong et al. (2017) studied

the feasibility of applying chemical coagulation before an UF operation using a flowback sample from the Fuling play in China. The study showed that the removal of organics improved considerably by applying coagulation as a pre-treatment. The coagulation method consisted of adding a high chemical dose of poly aluminum chloride (PAC) to the FPW sample. The purpose of the PAC was to form larger particles by agglomeration of colloidal species, which then they could be retained on a membrane, and at the same time was able to decrease membrane fouling considerably. The most recent study by Maguire-Boyle (2017) showed that modifying the surface of a ceramic MF membrane by increasing its hydrophilicity, improved the rejection of organics to more than 90%, and resulted in negligible fouling. These previous results demonstrate the complexity and variations found in the FPW samples from different wells and plays, where further characterization is necessary to improve our understanding of the possible benefits of using membrane technologies in the treatment of FPW.

1.2 Research Purpose and Objectives

The need for reusing FPW in the oil and gas industry for making the water cycle more sustainable has increased in recent years. Evaluation of treatment options and an understanding of the underlying physical and chemical mechanisms behind them are fundamental in addressing some of the obstacles and drawbacks that might arise during the use of these processes. Therefore, the focus of my study was to evaluate feasible and cost-effective membrane filtration and aeration methods that could be applied in the treatment of an FPW sample from the Duvernay Formation, Alberta. The main objectives are as follows:

1. To assess the performance of commercially available microfiltration and ultrafiltration membranes that includes parameters such as flux decline, fouling mechanisms, and rejection of particles mainly Fe and Si from an FPW sample. This assessment will be

conducted directly on the raw FPW as well as the treated FPW through the aeration process as a pre-treatment to optimize the membrane filtration operations.

2. To investigate the effects of employing aeration directly to the FPW sample and understanding some of the reactions that may occur. For instance, if the precipitation of ferric iron particles, e.g., amorphous ferric hydroxides, could promote the removal of organic compounds from the solution.
3. To characterize solids obtained from the membrane filtrations, before and after the aeration treatment. Precipitates before and after aeration are compared by sequential extraction methods, total digestion, and alkaline fusion to identify changes in trace metals fractionation and mobility.
4. To evaluate the effectiveness of the combined treatment (aeration – membrane filtration) by conducting toxicity tests on zebrafish embryos exposed to various dilutions of treated and untreated FPW, recording mortality and anomalies in their development.

2. Methods

2.1 Experimental Procedure and Materials

2.1.1 FPW Sample Location

In this study, a flowback and produced water (FPW) sample from an unconventional well was used to assess the effectiveness of combined aeration-membrane treatment strategies, and their implications for membrane performance, solution chemistry, and toxicity. The FPW sample was collected from a well drilled in 2016 by Encana Corporation, which is located in central Alberta, Canada (Figure 4). The well was fractured into the Duvernay Formation using slickwater fluids, reaching an approximate depth of 3,200 m, having 37 stages, and producing only gas. Once collected after the oil-water separator, the FPW sample was stored in two sealed 20 L polypropylene buckets and kept at room temperature at the University of Alberta. The FPW sample corresponds to the initial retrieved water in the subsurface (first eight hours of the flowback period).

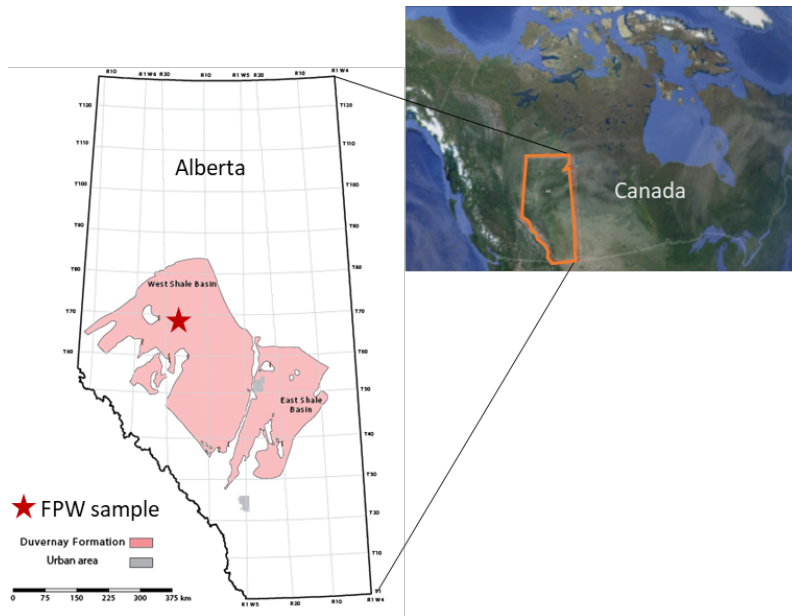


Figure 4. Location map of the gas well where the FPW sample was collected.

2.1.2 Membranes Selection and Characterization

Four commercial membranes were selected to conduct the experimental filtrations. Two types of polymeric materials were tested, polyvinylidene fluoride (PVDF) and polyethersulfone (PES), as these are the most widely used polymers in wastewater treatment (Howe and Clark, 2002; Mallevalle et al., 1996). These two types of membrane materials were chosen because of their outstanding chemical resistance, thermal stability, resistance to solutions with a wide range of pH, and are often more affordable than other commercially available materials, e.g., inorganic membranes (Ladewig and Al-Shaeli, 2017). Three of the membranes used in this research corresponded to microfiltration (MF) and only one was tested for ultrafiltration (UF). Two flat sheet MF membranes were comprised of PVDF, with pore sizes of 0.22 μm and 0.1 μm (EMD Millipore, Durapore). The other two membrane materials corresponded to PES, one of them having a pore size of 0.22 μm was applied in MF, and the other membrane was used for UF tests, having a pore size of 0.03 μm (Sterlitech Corporation). The main purpose in MF operations is to remove suspended solids (particles larger than 0.1 μm), while in UF operations, the target is meant to not only remove suspended particles, but also to retain macromolecules, e.g., proteins, clays, and colloids (Cheryan, 1986). Table 1 presents the specifications of the polymeric MF and UF membranes used in this study, as obtained from the manufacturers.

All purchased membranes had a hydrophilic surface according to their manufacturer specifications. Hydrophilic membranes are usually preferred in water treatment applications because they are less prone to fouling than hydrophobic membranes (Cheryan, 1986). Thus, to determine the hydrophilicity, or wettability, of the surface of the clean, unused PVDF and PES (MF and UF) membranes, contact angle measurements were conducted using a Drop Shape Analyzer (KRUSS - DSA100) with an accuracy of ± 0.3 degrees according to the manufacturer.

Analysis of the contact angle was determined through the Advance software (Kruss Scientific) using the sessile drop method, by depositing a liquid (deionized water) onto a solid, in this case, the polymeric membranes. The membranes were first cleaned with ultrapure water to remove any residues, as recommended by the manufacturer. Before analysis, the membranes were air-dried, cut into 5x25 mm pieces and fixed on microscope slides. A volume of 5 to 6 μL of ultrapure water was deposited onto the solid surface (membranes) using a 1 mL-syringe. Contact angles were measured at five points of each membrane at random locations, and the average and standard deviation are reported here. At every point of measurement, several pictures were taken, but only one was chosen, where there was no observed vibration of the water droplet on the membrane, to report the most accurate angle. Measurements were performed at room temperature.

The cross-section and surface of the membranes were imaged using a Zeiss Sigma Field Emission scanning electron microscope (FESEM), before and after the aeration treatment, as well as the unused membranes. The elemental composition was confirmed using energy dispersive X-ray spectroscopy (EDS; Bruker). To analyze the cross-section of each membrane (used and unused), they were first cut into small strips and placed into liquid nitrogen for about 10 min. Then, each membrane was carefully split in half, making sure not to damage the pores. The membranes were placed on carbon tape and carbon-coated before analysis.

Table 1. Properties of membranes used in the filtration experiments.

Membrane	MF	MF	MF	UF
Material	Polyvinylidene Fluoride (PVDF)	Polyvinylidene Fluoride (PVDF)	Polyether Sulfone (PES)	Polyether Sulfone (PES)
Pore size, μm	0.22	0.1	0.2	0.03
Diameter, mm	90	76	90	90
Thickness, μm	125	125	110-115	110-115
Max. Operating Temp, $^{\circ}\text{C}$	85	85	130	130
Max. Operating Pressure, psi	50	75	50	90
pH range	2-11	2-11	2-11	2-11
Wettability	Hydrophilic	Hydrophilic	Hydrophilic	Hydrophilic
Manufacturer	Durapore	Durapore	Sterlitech Corp.	Sterlitech Corp.

2.1.3 Membrane Filtration Experiments

Filtration experiments were conducted using a bench-scale setup (Figure 5) that consisted of a dead-end filtration unit cell (Amicon 8400, Millipore) with an effective surface area of 41.8 cm^2 , which was used for filtration of the flowback and produced water sample before and after aeration tests. MF and UF experiments were performed under constant pressure at approximately 8 and 20 psi, respectively, by applying compressed nitrogen gas. The pressure was adjusted manually with a pressure gauge (4-100 psi). The permeate weight was recorded every 30 s with a Mettler Toledo balance (0.1 g resolution, ME4001E). Membrane flux was calculated using Eq. 1.

$$J = Q / (A \cdot t) \quad (1)$$

Where J is the transient permeate flux (L/m^2h or LMH), Q is the permeate rate (L), A is the effective membrane area (m^2), and t refers to filtration time (h).

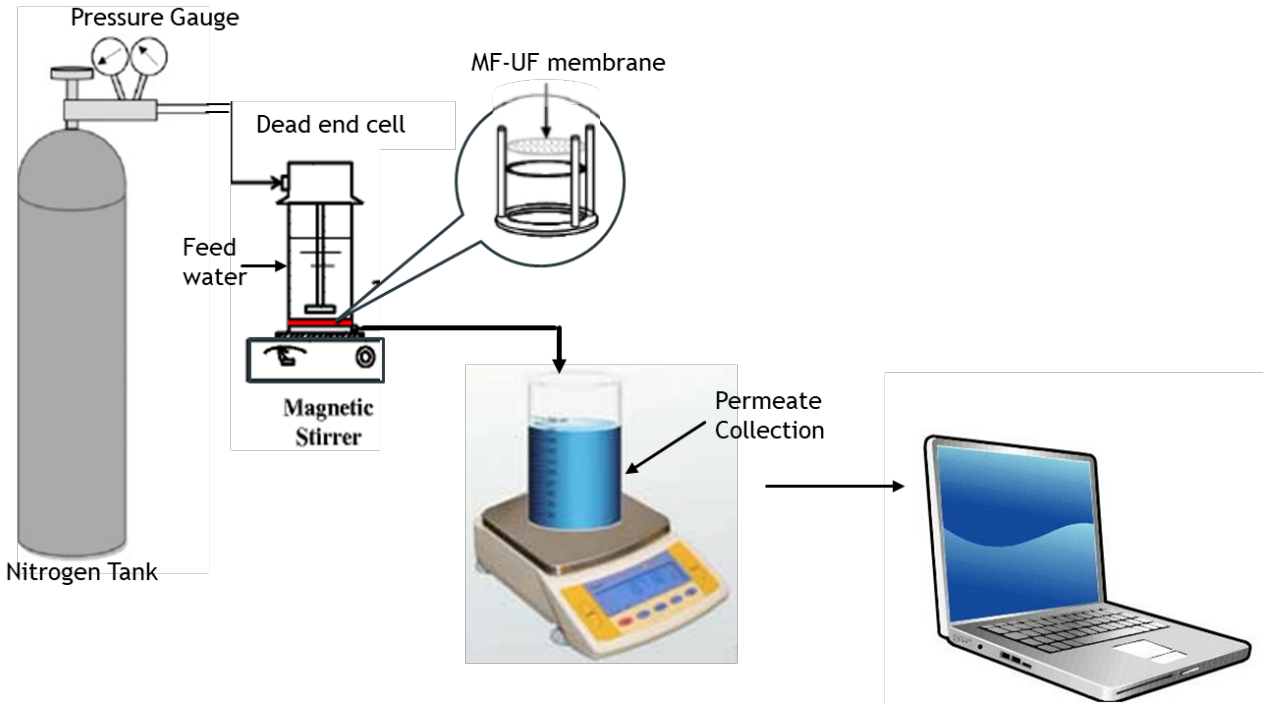


Figure 5. Experimental bench-scale setup for MF and UF operations.

Dead-end filtration experiments were conducted at room temperature under unstirred conditions, and new membranes were used for each test. Prior to the filtration of FPW, each membrane was pre-compacted for at least 20 min at 40 psi. This step is usually performed to obtain a stable flux during the actual filtration experiments (Dang et al., 2006). Next, the resistance of the membranes was measured by recording the water flux at different pressures (10, 20, 30, 40 psi), followed by filtration of ultrapure water for about 20 min. Subsequently, one liter of FPW was directly filled into the filtration cell to conduct the MF and UF tests, respectively. Smaller volumes of FPW were used to run duplicates using only one membrane due to the limited available volume

of the FPW sample. Rejection analysis, which is the ratio of concentrations in the permeate and the feed solution (Mallevalle et al., 1996), were correlated through Eq. 2.

$$R (\%) = [1 - (C_p/C_f)] \cdot 100 \quad (2)$$

Where C_p and C_f are the permeate and feed concentrations, respectively.

Fouling analyses were conducted following Hermia's model (Hermia, 1982) to identify the primary mechanisms that can affect flux variations during dead-end microfiltration and ultrafiltration. Membrane fouling is a phenomenon responsible for the reduction of permeate flux due to an accumulation of particulates on the membrane surface or inside the membrane's pores (Mallevalle et al., 1996; Howe et al., 2007; Sampath et al., 2014), which has been one of the major obstacles encountered in membrane technologies applied to wastewater treatment (Mondal, 2016). Four different models (Table 2) were developed for flux decline at constant pressure following the general blocking filtration law (Eq. 3).

$$\frac{d^2t}{dV^2} = k \left(\frac{dt}{dV} \right)^n \quad (3)$$

Where t is the filtration time, V is the total permeate volume, k is a constant, and n is a blocking index that defines the fouling type as shown in Table 2, and are described as follows:

- a. The *complete blocking model* ($n = 2$) is defined by the complete obstruction of the membrane pores due to molecules depositing only on the membrane surface and not inside of the pores. In this type of fouling, particles do not deposit on other particulates that were previously accumulated on the membrane surface. Eq. 3 was integrated to yield a linearized equation of permeate flux and time (Eq. 4) (Lim and Bai, 2003).

$$\ln J_p = \ln J_0 - k_c t \quad (4)$$

K_c is a function of the membrane surface blocked per unit of the total volume that permeates through the membrane, k_A , and as a function of the initial permeate flux (J_0) according to Eq. 5 (Bowen et al., 1995).

$$k_c = k_A J_0 \quad (5)$$

b. The *standard blocking model* ($n = 1.5$) is characterized by particles with a smaller size than the pores which can enter the membrane surface and deposit on the pore walls. Eq. 6 is the linearized expression of this model (Bowen et al., 1995).

$$\frac{1}{J_p^{1/2}} = \frac{1}{J_0^{1/2}} + K_s t \quad (6)$$

The parameter, K_s , is defined in Eq. 7.

$$K_s = 2 \frac{K_B}{A_0} A J_0^{1/2} \quad (7)$$

Where K_B is the decrease in the cross-sectional area of the membrane pores per unit of permeate volume, A_0 is the porous membrane surface, and A is the area of the clean membrane.

c. *Intermediate blocking model* ($n = 1$), similar to the complete blocking model, is defined by the accumulation of particles on the membrane surface and blocking of the pores. The difference with this model is that particles can deposit on previously settled particles. The linearized function is given by Eq. 8 (Mohammadi et al., 2003).

$$\frac{1}{J_p} = \frac{1}{J_0} + K_i t \quad (8)$$

Where $K_i = K_A$, which represents the surface of the membrane blocked per unit of total of permeate volume (Bowen et al., 1995).

d. *Cake filtration (layer) model* ($n = 0$) represents a layer of solutes deposited on the membrane surface. The particles are usually bigger than the pore size and do not deposit within them.

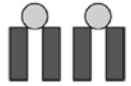
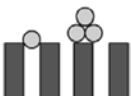
The linearized Eq.9 is as follow (Lim and Bai, 2003):

$$\frac{1}{J_p^2} = \frac{1}{J_0^2} + K_{gl}t \quad (9)$$

The parameter K_{gl} is given by Eq 10 (Bowen et al., 1995):

$$K_{gl} = \frac{2 R_g K_D}{J_0 R_m} \quad (10)$$

Table 2. Fouling mechanisms according to Hermia's Model. (Adapted from Cassini et al., 2011).

	Pore blocking model	Illustration	Linear equation
$n = 2$	Complete blocking		$\ln J = \ln J_0 - K_c t$
$n = 1.5$	Standard blocking		$\frac{1}{J^{0.5}} = \frac{1}{J_0^{0.5}} - K_p t$
$n = 1$	Intermediate blocking		$\frac{1}{J} = \frac{1}{J_0} - K_i t$
$n = 0$	Cake layer formation		$\frac{1}{J^2} = \frac{1}{J_0^2} - K_t t$

Due to the observed rapid fouling and sharp reduction of flux from MF and UF experiments conducted with raw FPW from previous studies (He et al., 2014; Xiong et al., 2016), the need to limit the fouling phenomena might be attained by applying pre-treatment techniques such as pre-filtration, coagulation/flocculation, or pre-oxidation (aeration) (Mallevalle et al., 1996). Aeration was selected as the pre-treatment method in this study, as this operation is typically used in wastewater applications to degrade organic pollutants, precipitate dissolved iron and manganese

ions (Hongprasith et al., 2016; Mallevalle et al., 1996) and it is a simple and reliable process that can be applied at small or large scales (Oliveira and Franca, 1998).

The aeration tests were carried out in a graduated 2 L polypropylene cylinder with a diameter of 84 mm and a height of 531 mm. The experimental setup is shown in Figure 6. Compressed air was used as the delivered gas, and the flow rate was set at approximately 0.3 liters per minute (LPM) using a flow meter. A stainless-steel (ss) bubbling stone (air diffuser) with a 2 μm pore size was installed at the bottom of the cylinder to generate fine air bubbles. The graduated cylinder was filled with 2 L of FPW and sealed with parafilm paper through the entire experiments. Each aeration experiment was conducted for 24 h at room temperature. Samples were collected at certain times to evaluate chemical changes in the solution for the total aeration time.

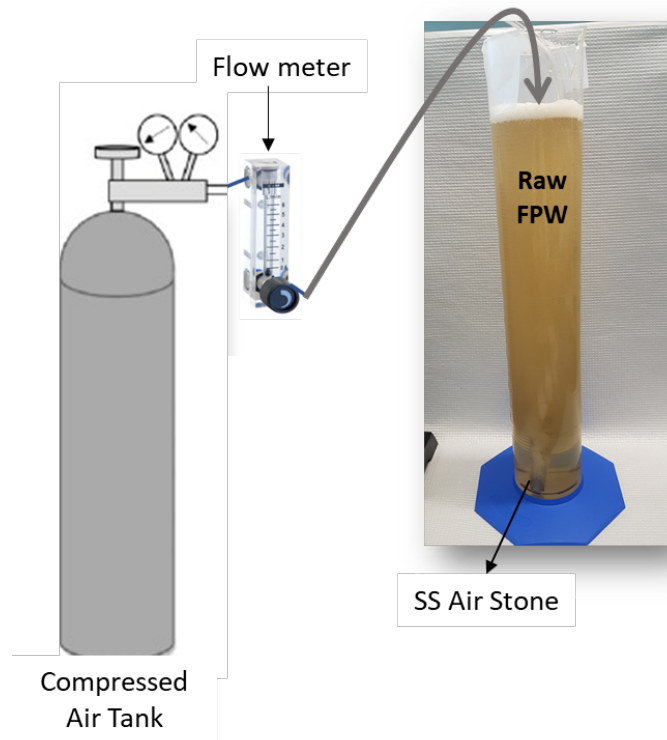


Figure 6. Experimental setup of the aeration tests.

2.2 Analytical Procedures

2.2.1 Inorganic Solution Chemistry

Multi-elemental analyses of the Raw FPW solution, as well as FPW treated either by filtration or aeration-filtration, were determined using an Agilent 8800 Triple Quadrupole Inductively Coupled Plasma Double Mass Spectrometer (ICP-MS/MS). Prior to analysis, raw solutions were filtered through a 0.2 μm nylon membranes (Agilent Technologies), and then diluted and acidified with 18M Ω ultrapure water and trace metal grade nitric acid (HNO_3 , 70%), respectively. Single-element standards (Spex CertiPrep, CPI International, Ricca Chemical Company) were used for external calibration following a standard addition method (He et al., 2017b), and indium (0.5 ppm) was used for internal calibration (in-line injection). Argon was used as the carrier gas. At least three measurements were performed for each element in MS/MS mode, and additionally, He (3 mL/min) and O_2 (10%) gas were introduced as collision gases to minimize polyatomic interferences. A similar procedure was used to determine the elemental composition in the total digestion, alkaline fusion, and sequential extraction methods, modifying only the matrix for standards and the solution dilutions using 2% HNO_3 and 0.5% HCl . Analysis of anions was carried out in the Natural Resources Analytical Lab (NRAL) at the University of Alberta. Determination of Cl^- , Br^- , and SO_4^{2-} was performed using a Dionex Ion chromatograph (model DX 600) with a 4 mm analytical column (AS9-HC), a guard column (AG9-HC), and a suppressor (ASRS Ultra – 4mm). The samples were diluted using ultrapure water in 50 mL centrifuge tubes.

Total dissolved solids (TDS) analysis were carried out by evaporating 10 mL of the FPW solution in an oven at 80°C until the sample was completely dry. Then the temperature was raised to 250°C to dehydrate residual salts and the final precipitates were weighed. Total suspended solids

(TSS) were determined gravimetrically by passing the raw solution through a 0.22 μm nylon membrane (Fisher Scientific), and the remaining solids were weighted.

During the aeration experiments, changes in the concentration of dissolved ferrous iron (Fe^{2+}) was monitored by applying a modified ferrozine (Na_2 -3-(2-pyridyl)-5,6-bis (4-phenylsulfonate)-1,2,3-(triazine) colorimetric assay (Stookey, 1970). Quantification of the Fe (II) concentration was performed using a UV-Vis Spectrophotometer (Thermo Scientific Evolution 60S) at an absorbance of 562 nm. The FPW solutions were diluted 20 times with 1 M HCl to obtain measurements within the instrument analytical range. pH was also monitored throughout the aeration experiment using a Mettler Toledo (Easy Five dual) FEP 20 pH meter.

2.2.2 Organic Solution Chemistry

The raw and treated FPW samples, were analyzed for total organic carbon (TOC), measured as non-purgeable organic carbon (NPOC), at the NRAL using a Shimadzu TOC-V CHS/CSN Model TOC Analyzer (Shimadzu Corporation). Samples were diluted with ultrapure water.

Determination of polycyclic aromatic hydrocarbons (PAHs) was conducted by Dr. Yifeng Zhang in the Department of Laboratory Medicine and Pathology at the University of Alberta. After selection of a suitable membrane, the permeates obtained using the 0.2 PES membrane were analyzed to compare and evaluate the non-aerated filtration and the aeration-filtration treatments as well as the raw FPW. It has been previously determined by He et al. (2017a, b) that suspended solids, particularly Fe-Si oxyhydroxides, are closely associated with heavy organic compounds, and therefore removing those particulates from the solution could decrease the potential toxicity of FPW. Constituents analyzed included 16 parent PAHs and 4 alkyl-PAHs. Briefly, the raw FPW

and the permeates obtained from both filtration and aeration-filtration treatments were filtered using 0.4 μm glass fiber filters (Glass Fiber Store, 90 mm diameter). Deuterium-labeled PAHs (10 ng) was added as an internal standard to each sample. The aqueous filtrate was liquid-liquid extracted using 50 mL dichloromethane (DCM). The used filters with sediment were freeze-dried for 2 days. Accelerated solvent extractor (ASE) was used for PAHs extraction from these dried sediment filters.

The extracts were concentrated by nitrogen gas evaporation, and then 3 mL hexane was added and vortexed with precleaned copper powder and anhydrous sodium sulfate. Next, silica solid phase extraction (Water, 1g/6cc) in cartridges was performed. After this, PAHs were eluted with 5 mL hexane/DCM 7:3 (v/v), then concentrated and reconstituted by 200 μL hexane and placed into vials for GC-MS analysis. Targeted analytes were analyzed in selected ion monitoring (SIM) mode, and concentrations were determined by relative response to the respective internal standard. The details of GC-MS analysis have been described elsewhere (Zhang et al., 2016).

2.2.3 Solids Characterization

Suspended solids and precipitates obtained from the membrane filtration (no aeration) and aeration-filtration experiments were subjected to total digestion using hydrofluoric acid (HF) to determine total metals concentrations, and alkaline fusion was performed to quantify the Si content following a method described by GBC Scientific Equipment (2013). Due to the low mass of solids recovered after performing the raw FPW filtration, no duplicates were carried out; only one sample was subjected to each analysis. Conversely, after applying aeration-filtration to the FPW sample, Fe (III) precipitates formed, increasing the amounts of solids retained on the membranes, and all digestion procedures for these samples were performed in triplicate. Blanks, with no solids added to the centrifuge tube (only addition of the digestion chemicals), were also analyzed for each

method to identify if there was any type of contamination. The accuracy of the methods was examined by the analysis of a certified reference material STSD-3 (CANMET Mining and Mineral Sciences Laboratories).

For the HF digestions, 0.05 to 0.1g of sample was first mixed for one hour with 5 mL concentrated hydrogen peroxide (H_2O_2 , ACS certified, Fisher Scientific) and 5 mL 70% HNO_3 in a 50 mL Teflon® FEP tubes (Thermo Scientific) at room temperature. Next, the samples were evaporated until near dryness at 130°C in a heating block. Then, 70% HNO_3 (5 mL) and 47-51% HF (5 mL) were added to the tubes and left at 175°C until all liquid was evaporated. After the tube is completely dry, another treatment was completed by adding 3 mL of 37% HCl and 1 mL 70% HNO_3 . The liquids were evaporated at 130°C until near dryness. Finally, the remaining solution was diluted in a solution comprised of 2% HNO_3 and 0.5% HCl in a 50 mL centrifuge tube.

In the alkaline fusion method, 0.05 g of sample, 0.2 g of sodium hydroxide (NaOH), and 0.2 g of sodium peroxide (Na_2O_2 , ACS certified, Fisher Scientific) were added to a nickel crucible where 0.8 g NaOH was previously melted and cooled. Then with the crucibles covered, the reagents and sample were heated over a Bunsen burner for about 5 min. After the crucibles were allowed to cool down slightly, the outside was flushed with 6 M HCl in 250 mL polypropylene beakers. Then, approximately 5 mL of 6 M HCl was added to the mixture of FPW solids and chemicals in the crucibles and left until a violent reaction occurred, and all particles were dissolved. Finally, 18M Ω ultrapure water was used to rinse the crucibles and to dilute the solution to 50 mL.

A sequential extraction procedure was also used to characterize and compare any variations in the metal fractionation of the FPW solids obtained from the membrane filtrations before and after the aeration treatment. A modified Tessier et al. (1979) method by Krishnamurti et al. (1995) and Li et al. (1995), was adapted and applied for FPW suspended solids, differentiating a total of

six fractions. The sequential extraction follows a stepwise process starting from the most labile fraction (1, exchangeable) finishing with the more recalcitrant (6, residual). Solids obtained from the filtrations with the untreated and treated FPW were air dried and homogenized before the extractions.

To obtain fraction 1 (exchangeable), a total of 0.5 g of solids were placed into 50 mL polypropylene centrifuge tubes with 8 mL of 0.5 M magnesium chloride (MgCl_2 , ACS certified, Fisher Scientific). This solution was left to react for 30 min at room temperature under continuous agitation on a rugged rotator (Glas-Col) at 50 rpm. Next, the tubes were centrifuged (Sorvall LYNX 4000, Fisher Scientific) at 15,000 relative centrifugal force (rcf) for 15 min. 5 mL of supernatant was taken into a new 50 mL tube, and the remaining liquid was discarded. In fraction 2 (metals bound to carbonate), the solid residues from fraction 1 were leached with 8 mL of 1 M sodium acetate ($\text{C}_2\text{H}_3\text{NaO}_2$, Fisher Scientific, adjusted to pH 5 with acetic acid) for 5 h at room temperature and under continuous agitation (50 rpm). The liquid was extracted in the same way as described in fraction 1. To obtain fraction 3 (metals bound to Fe-Mn-oxides), the remaining solids from fraction 2 were extracted using 20 mL of 0.04 M hydroxylamine hydrochloride ($\text{NH}_2\text{OH} \cdot \text{HCl}$, ACS grade, Fisher Scientific) at 95°C in a heating block for 6 h with occasional agitation. The samples were centrifuged, and 15 mL of supernatant was taken into the new 50 mL tubes. For fraction 4 (metals bound to organic matter and sulfides), 3 mL of 0.02 M HNO_3 and 5 mL 30% H_2O_2 (adjusted to pH 2 with HNO_3) were added to the residues from fraction 3. The sample was heated at 85°C for 2 h with occasional agitation, and 3 mL of 30% H_2O_2 was added again maintaining the same temperature for 3 h. Next, when the samples were cooled, a final 5 mL of 3.2 M ammonium acetate ($\text{C}_2\text{H}_3\text{O}_2\text{NH}_4$, HPLC grade, Fisher Scientific) in 20% (v/v) HNO_3 was added and adjusted to 20 mL with ultrapure water. The mixture was continuously agitated for 30

min, followed by centrifugation and collection of the supernatant (15 mL). To obtain fraction 5 (metals bound to crystalline Fe oxides), 20 mL of a solution of 0.2 M ammonium oxalate ((NH₄)₂C₂O₄, ACS grade, Fisher Scientific) in 0.1 M ascorbic acid (C₆H₈O₆, ACS grade, Fisher Scientific) adjusted to pH 3 with oxalic acid (C₂H₂O₄, ACS grade, Fisher Scientific) was added to the residue from fraction 4. The sample was heated at 95°C for 1.5 h and occasionally agitated. After centrifugation, 10 mL of supernatant was taken. For the final fraction 6 (residual), the solids from fraction 5 were transferred into 50 mL Teflon® FEP tubes where total digestion was performed following the HF procedure as described above. The final product was diluted to 50 mL with ultrapure water in centrifuge tubes.

After retrieving the supernatant, the residues from fractions 1 to 5 were washed with 10 mL ultrapure water, followed by centrifugation at 15,000 rcf for 10 min. To matrix match for ICP-MS/MS analysis, the supernatants were digested with 1 mL 70% HNO₃ and heated until near dryness on a heating block at 120°C. The samples were then adjusted to a final volume of 50 mL with 2% HNO₃ and 0.5% HCl. The residual fraction for Si was calculated by subtracting the concentrations obtained in fractions 1 to 5 from the total concentration results determined by alkaline fusion.

Morphologies of the particles collected from each of the MF and UF experiments, before and after aeration, were characterized using the FESEM with a resolution of ~10 nm. Samples were prepared for imaging by depositing coatings of carbon using a Leica EM SCD005. Images were obtained with secondary, in-lens, and backscattered electron detectors at different magnifications to capture particle size variations. To examine the chemical composition from selected spots as well as the average composition of the bulk sample, EDS was used with dual silicon drift detectors and a resolution of 123 eV.

X-ray diffraction (XRD) patterns were collected for solid samples before and after aeration using a Rigaku Geigerflex Powder Diffractometer in the XRD Lab at the University of Alberta. The diffractometer is equipped with a cobalt tube, graphite monochromator, and scintillation detector. Interpretation of the results was performed using JADE 9.1 program and by matching with the reference files International Centre for Diffraction Data (ICDD) and the Inorganic Crystal Structure Database (ICSD) databases.

2.3 Developmental Toxicity in Exposed Zebrafish Embryos

Disturbance of aquatic environments by potentially toxic substances is often assessed through laboratory experiments by conducting toxicological tests on freshwater species such as zebrafish, fathead minnow, and daphnids (Lammer et al., 2009). In this study, exposure tests on zebrafish embryos were conducted in collaboration of Dr. Yuhe He of the Department of Biological Sciences (University of Alberta) to evaluate the effects of the membrane filtrations and aeration experiments on the toxicity of the FPW permeate. Zebrafish embryos were obtained after one-hour post fertilization (hpf) from a breeding tank with two mature females and one male Zebrafish. A semi-static experiment was conducted with four samples (raw, non-aerated permeate (NAP), and aerated permeate (AP), and a control sample which corresponds to water from the initial breeding tank), and 4 different FPW dilutions (0.28%, 0.83%, 2.5%, and 7.5%) were tested. In the exposure, 10 embryos were randomly selected and placed in every well (of a 6-well plate) that was filled with 5 mL of the prepared FPW dilutions (Figure 7). The six-well plates were then covered and incubated at 26 °C for 96 h. The FPW dilutions in the well-plates were exchanged with new FPW having the same dilution factor after 48 h of incubation, and experiments were performed in triplicates. The exposed embryos were observed every 24 h in a 4 day-period to determine mortality and any irregular modification of each embryo (e.g., pericardial edema, spinal

malformation, unhatched embryos, and yolk sac.). Any non-fertilized eggs were discarded after each verification of the well-plates.

At the end of the exposure, the mortality rate of embryos and LC₅₀ values (median lethal concentrations resulting in 50% mortality of a population) were calculated using the Toxicity Relationship Analysis Program (TRAP) version 1.30a (EPA, Washington, DC, USA). Statistical analyses were conducted using the software package SPSS 24.0. Statistical differences of mortality among the three different treatment samples were analyzed by one-way ANOVA analysis followed by Tukey's post hoc test. Differences between groups were considered significant when $p < 0.05$. Also, the standard Environment Canada protocols using the Litchfield-Wilcoxon methodology were applied to determine significant differences for LC₅₀ values among the samples (Wheeler et al., 2006).

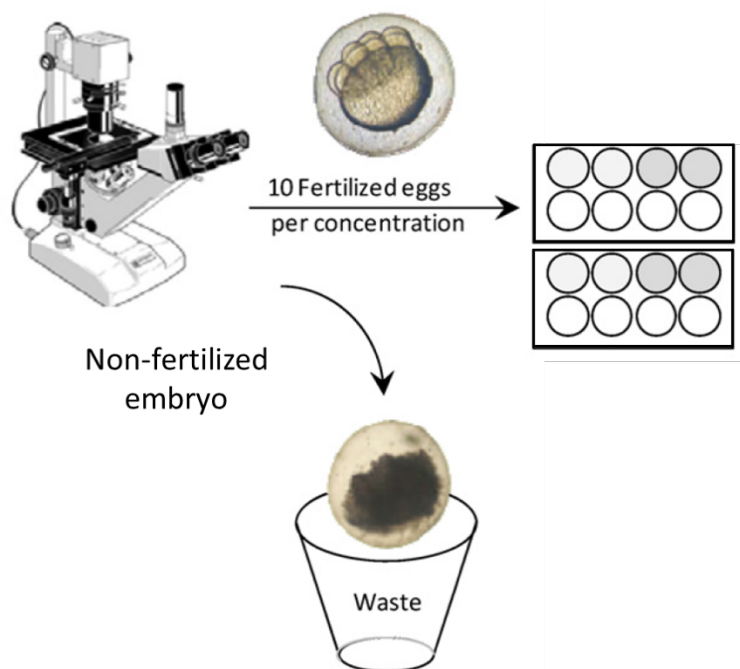


Figure 7. Schematic of the zebrafish embryos exposure (Modified from Lammer et al., 2009).

2.4 Microbial Communities from Flowback Precipitates

The microbiological analyses were conducted by Konstantin von Gunten at the University of Alberta. DNA was extracted from the air-dried hydraulic fracturing precipitates obtained by filtration of aerated and non-aerated FPW sample and through the different membranes. The FastDNA SPIN Kit for Soil was used (MP Biomedicals) for DNA extraction using approximately 50 mg of sample. Microbial community analyses were performed by 16S rRNA gene sequencing using universal bacterial and archaeal primers (for details see von Gunten *et al.*, 2018). Sequencing was performed on the Illumina MiSeq platform for pair-end reads and using the Illumina NexteraXT library preparation kit (Illumina), and data processing was performed using the MetaAmp version 2.0 (Dong *et al.*, 2017). The amplicons length was set to 250 base pairs, and a length overlap of 50 base pairs was chosen. Reference alignment was done to the SILVA database (Quast *et al.*, 2013; Yilmaz *et al.*, 2014) with an operational taxonomic unit (OTU) clustering at the 97% similarity level. Plots were prepared with R version 3.5.1 and the PHYLOSEQ package (McMurdie and Holmes, 2013; R Core Team, 2017).

3. Results and Discussion

3.1 Flowback and Produced Water Physicochemical Characterization

The chemistry of flowback and produced water partially reflects the nature of the hydraulic fracturing fluids (FF) employed in the drilling operations as well as the subsurface geochemical conditions of the target formation (King, 2012). The FPW sample used in this study had a high concentration of total dissolved solids (TDS) of 167,022 mg/L (± 314 , in duplicate samples) which can be classified as brine according to Table 3. For comparison, average seawater has a TDS concentration of around 35,000 ppm.

Table 3. Types of water based on TDS concentrations. Adapted from Carrol (in Todd and Mays, 2005).

Type of Water	Total dissolved solids (mg/L)
Fresh water	0-1,000
Brackish water	1,000-10,000
Saline Water	10,000-100,000
Brine	>100,000

A summary of the FPW composition is shown in Table 4. Major dissolved cations determined in the sample included sodium (being the most abundant), calcium, potassium, strontium, magnesium, iron, and boron. Representative trace elements were silica and manganese. The main anions detected in the sample were chloride and bromide. Radioactive elements were not detected in the analyzed water. A charge balance (<2%) is also presented in Table B.1 (Appendix B) to validate the elemental analysis. The source of the dissolved salts found in most FPW samples has been suggested to be from the dissolution of salts in the target geologic formation or unit, and/or migration from adjacent brines (Blauch et al., 2009).

Table 5 shows a comparison of three different FPW samples from the U.S. and the sample used in this study. Higher TDS concentrations from the Marcellus and Bakken formations in the U.S and the Duvernay Formation in Canada seem to be correlated to ancient sedimentary rocks, composed of organic-rich, shales limestones, and mudstones, i.e., deposited during the middle Paleozoic where depositional environments are associated with evaporitic events (Blauch et al., 2009; Stoakes and Creaney, 1985; Ettensohn and Barron, 1981). The Duvernay Formation (central Alberta), where the FPW sample was recovered and analyzed here, was deposited in the middle Paleozoic (Late Devonian) about 385 million years ago (Stoakes and Creaney, 1985). In contrast, a sample collected from the Niobrara Formation of an early Cretaceous-age shows a considerably lower TDS concentration (Li, 2013). This comparison demonstrates the close relationship between the geologic conditions and the wastewater generated by hydraulic fracturing operations.

The organic content of this FPW sample, measured as total organic carbon (TOC, Table 4), had substantially elevated concentrations compared to natural surface and ground waters which can range from 0.5 to 60 mg/L (Mullholland, 2003; Gooddy and Hinsby, 2008). TOC values were approximately similar to those reported in the Marcellus play (170-630 ppm) by Xiong et al. (2016). High concentrations of organics are a concern in the petroleum industry because it can detrimentally impact the performance of some of the additives used in the drilling process. Moreover, high concentrations of organic material usually represent a challenge in many water treatments methods and potential risks to the environment in the case of a surface spill (Hussein et al., 2014; Butkovsky et al., 2017). It is worth noting that the measured TOC concentration may not be representative of the total organic content of the sample due to the formation of a thin, immiscible oil layer at the top of the fluid sample.

Table 4. Flowback and produced water characteristics of a hydraulically fractured well in the Duvernay play.

Parameter	Unit	Duvernay-FPW
pH		6.15 ± 0.016
TN	mg/L	399
TOC	mg/L	400 ± 1.6
TDS	mg/L	167,022 ± 314
TSS	mg/L	264
Na	mg/L	53,545 ± 622
Ca	mg/L	7650 ± 56.4
K	mg/L	1909 ± 3.7
Sr	mg/L	888 ± 6.9
Mg	mg/L	692 ± 1.21
Fe	mg/L	210 ± 4.7
B	mg/L	80.5 ± 3.7
Si	mg/L	23.2 ± 1.8
Ba	mg/L	9.4 ± 0.12
Mn	mg/L	5.3 ± 0.14
Zn	mg/L	1.2 ± 0.12
Pb	mg/L	0.13 ± 0.02
Cl	mg/L	101,287 ± 2317
Br	mg/L	220 ± 3.9

Table 5. Comparison of the chemical composition from two gas plays in the US and the Duvernay play in Canada. *Data collected from Ziemkiewicz and He (2015), Stepan et al., (2010), and Li (2013).

Parameter	Unit	*Marcellus	*Bakken	Duvernay	*Niobrara
TDS	mg/L	8840-154000	158000-219000	167022	18285
Na	mg/L	2440-119000	47100-74600	53545	5754.8
Ca	mg/L	1010-19900	7540-13500	7650	380.6
Sr	mg/L	117-4660	518-1010	888	55.4
Mg	mg/L	107-2260	630-1750	692	42.9
Fe	mg/L	14.7-149	72-120	210	80.7
Ba	mg/L	10.2-2580	0-24.6	9.4	18.2
Cl	mg/L	4700-79000	90000-133000	101287	10798.6

3.2 Membrane Filtration

3.2.1 Membrane Resistance and Contact Angle Measurements

Prior to evaluating the performance of the different polymeric membranes with the raw FPW sample, the intrinsic membrane resistance or hydraulic resistance (R_m) was determined for each membrane using ultrapure water as the feed. R_m is a useful parameter for assessing the stability of a membrane, although it should be noted that R_m cannot be used to compare the expected performance of different membranes when using the real feed sample (Cheryan, 1998).

R_m was calculated through the equation:

$$R_m = \frac{\Delta P_T}{J\mu} \quad (11)$$

Where ΔP_T is the transmembrane pressure (N/m^2), J is the pure water permeation flux (m^3/m^2s) and μ is the viscosity of the water (Ns/m^2).

First, the membranes were compacted at higher pressure (up to 60 psi) for at least 30 minutes, then the R_m was determined by varying the transmembrane pressure (TMP) at over a particular interval of time and while recording the pure water flux. Figure 8 shows the difference in the resistance for all tested membranes, ranging from approximately $2 \times 10^9 m^{-1}$ to $4 \times 10^9 m^{-1}$. The highest hydraulic resistance was observed for the 0.1 PVDF MF membrane, a parameter which is inversely proportional to the flux, i.e., having the lowest flux. The lowest resistance and the highest permeation rate was obtained for the 0.2 PES MF membrane. The 0.2 PES membrane and the 0.2 PVDF membrane had slightly different resistance values of $2.3 \times 10^9 m^{-1}$ and $2.8 \times 10^9 m^{-1}$,

respectively. The difference in resistance between these two types of materials might be the result of different pore structures and their hydrophilicity.

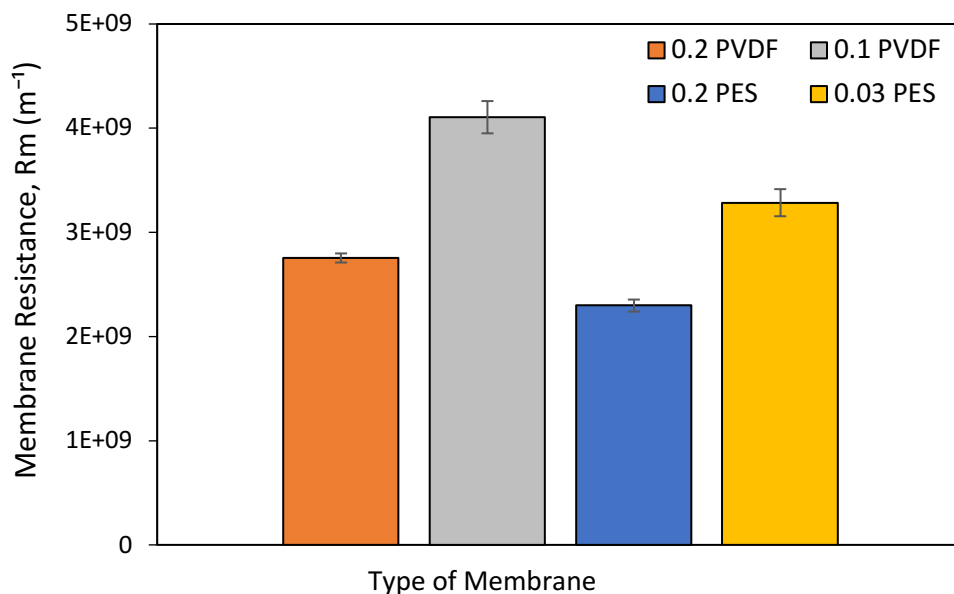


Figure 8. Hydraulic resistance of the four polymeric membranes.

In order to determine major differences related to the pore structure of the membranes, SEM images were taken of the surface of the commercial 0.2 PVDF and 0.2 PES membranes (Figure 9). Images were taken for both sides of each membrane. The PVDF membranes (Figures 9A and 9B) displayed a morphology of interconnected pores with a fibrous network (sponge-like structure), and it is considered to have a symmetric pore structure throughout the membrane. The aperture of the pores on both sides of the PVDF membrane did not differ substantially. The characteristics of this membrane are similar to the microporous isotropic structure described by Ho and Zidney (1999). On the other hand, the PES membranes have an asymmetric pore structure, i.e., where the smallest openings of the pores appear on one side of the membrane (Figure 9C) that usually has a shiny appearance. The matte side of the membrane usually has wider pores (Figure

9D), an observation which is also confirmed by the manufacturers. Both materials have a uniformly distributed semicircular shapes across both sides of the membranes. These results evidenced that although the membranes present some discrepancies on their pore structure which could affect the flow of water and the rejection of particles, this is not likely to represent the major factor affecting the hydraulic resistance, as the two membrane materials have interconnected pore structures (Ho and Zidney, 1999).

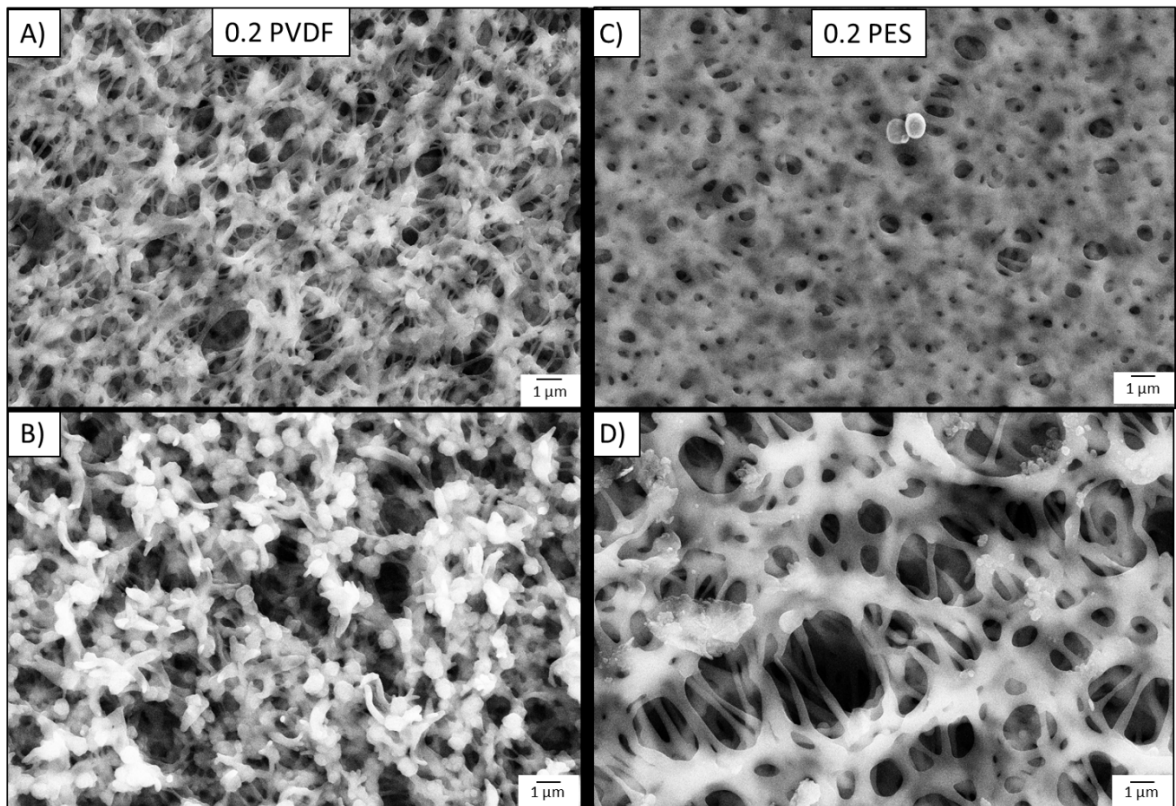


Figure 9. Pore structure of the 0.2 PVDF and 0.2 PES membranes. Figures A and B correspond to the 0.2 PVDF membranes “top” and “bottom” sides, respectively. C and D images show the shiny side of the 0.2 PES membrane with narrow pores and the matte side with wider pores, respectively.

The hydrophilicity, on the other hand, could be the most significant parameter affecting membrane resistance. The results showed that both tested PES membranes reflected a more

hydrophilic surface, with values below 50°, in comparison to the PVDF material which had a higher contact angle (>80°), as seen in Table 6. Generally, a membrane with a contact angle of over 50° is considered to be a hydrophobic membrane (Lee et al., 2004). This difference is important as hydrophilic membranes are deemed less prone to fouling which might be due to the presence of larger number of hydrophilic functional groups (e.g., OH⁻) on the membrane surface, and these membranes are therefore often preferred in the treatment of wastewaters (Cheryan, 1998).

Table 6. Contact angle measurement of each membrane by the sessile drop method.

No.	Membrane Type	Measured Contact Angle (°)	Thickness (µm)
1	0.2 PVDF	82.24 ± 0.70	125
2	0.1 PVDF	80.51 ± 0.96	125
3	0.2 PES	46.25 ± 0.37	110-115
4	0.03 PES	44.60 ± 0.72	110-115

3.2.2 Flux and Rejection of Untreated Flowback and Produced Water

The purpose of the first part of the research was to evaluate and compare the filtration flux for the different pore size membranes as well as to test various membrane materials using the raw FPW sample described above. The results of these analyses will lead to further studies selecting the most appropriate membrane, i.e., the membrane with the higher flux and better removal of

target particles. Figure 10 shows the variation of permeate fluxes of the MF and UF membranes versus time. The operating conditions for the three polymeric MF membranes were the same, i.e., a constant transmembrane pressure of 8 psi, during the entire filtration time. Generally, to compare the performance of several membranes with similar pore size but made of different material, all operating conditions should be held constant (Cheryan, 1998). The permeate flux for the UF membrane is also shown in the same figure, although the pressure used in the UF experiments was about 20 psi, two times higher than the MF filtrations, as it is the typical value used according to the literature. Additionally, the same feed volume of 1 L was used throughout the experiments.

In the graph, a high variability of the initial fluxes and the total filtration time is evident for all the membranes. Initial flux ranges from 930 to 2692 liters per square meter per hour (L/m^2h) and filtration time varies from less than 20 minutes to more than 4 h among the four membranes. The highest initial flux was observed for the 0.03 PES membrane, which might seem unexpected as this membrane had the smallest pore size, i.e., being the only UF membrane used in the experiments. This high flux could be explained by the difference in operating conditions where higher TMP (20 psi) was applied compared to the other three MF membranes. Although the 0.03 PES membrane had the highest initial flux, it rapidly decreased from about 2900 L/m^2h to less than 400 L/m^2h in the first ten minutes with a total filtration time of 2 h. The 0.2 PES, having a bigger pore size than the 0.03 PES membrane, had the second highest initial flux and followed a similar flux decline pattern, but with a total filtration time of only 45 minutes. The 0.2 PVDF membrane had the shortest filtration time of only 20 minutes and lower flux decline, and a relatively lower initial flux of only 1150 L/m^2h . The worst performance was observed for the 0.1 PVDF membrane, having both the lowest initial flux (below 1000 L/m^2h) and the longest filtration time of approximately 4 h. The higher initial fluxes in the two PES membranes as compared to the PVDF

may be explained as a result of their more hydrophilic surface characteristics, as shown from previous results. Jiang et al. (2013) also observed this variability in the initial flux when testing several ceramic MF and UF membranes with one flowback water sample obtained from the Marcellus play. The authors attributed this difference in membrane flux to the multiple fouling mechanisms found for each membrane which was highly dependent with the pore size. In the case of this study, one of the main reasons of flux variability could be the membrane material.

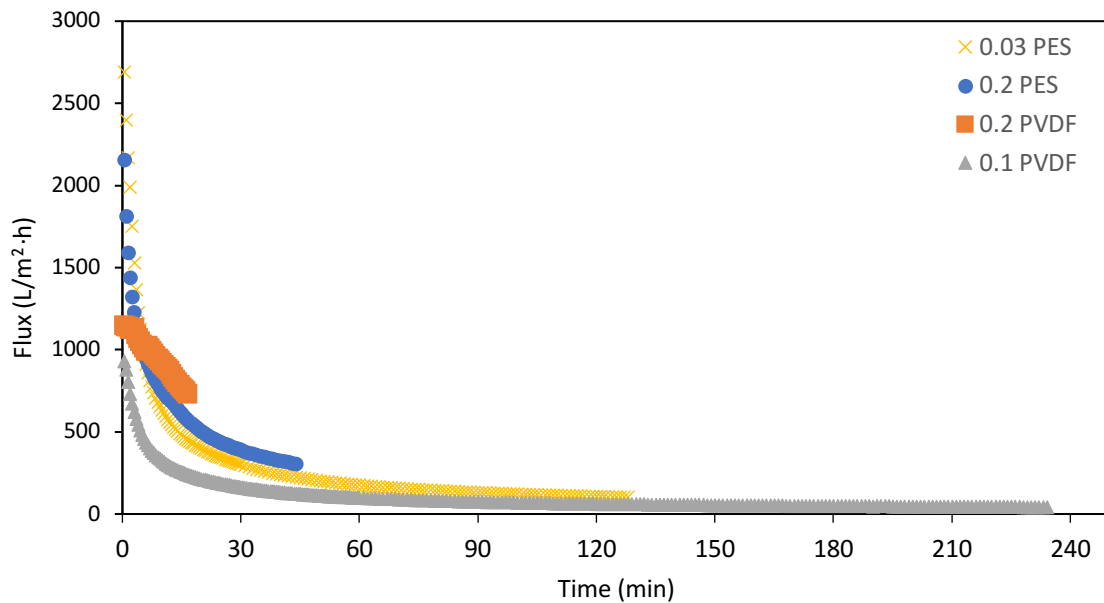


Figure 10. Comparison of permeate flux for polymeric MF and UF membranes at a TMP of 8 and 20 psi, respectively.

Due to the substantial differences in the initial fluxes for all the membranes, which might difficult their comparison, and consequently to elaborate a fair assessment of the membrane performance, the normalized flux was assessed as a more appropriate alternative. Researchers typically prefer the use of normalized plots, with normalized flux and sometimes normalized time, to gain a better understanding of the flux decline from different types of membranes. The

normalized flux measurement can then be evaluated to obtain an approximate reference of the membrane performance (Kim et al., 2015; Howe and Clark, 2002).

Figure 11 shows the normalized permeate fluxes as a function of normalized filtration time using 1 L of FPW. The 0.1 PVDF and 0.03 PES membranes showed a greater flux decline of about 96% and had similar decline patterns versus the two membranes with a bigger pore size (0.2 μm). Even though the 0.03 PES membrane had a more hydrophilic character than the 0.1 PVDF membrane, it is likely that the smaller pore size contributed to the drop-in flux. The lowest rate of flux decline was observed for the 0.2 PVDF membrane, with a reduction of only 40% of the initial flux. In general, the MF membranes with the 0.2 pore size presented less flux declined than the other two membranes.

A comparison of the performance between the 0.2 PES and the 0.2 PVDF membranes, reflects an apparent lower performance for the 0.2 PES membrane which had a considerable lower flux than the 0.2 PVDF membrane. Instead, the 0.2 PES membrane had a flux trend similar to the smaller pore size membranes, i.e., having a flux decline of about 85%, two times lower than that of the 0.2 PVDF membrane. This might seem unexpected as this membrane presented the lowest hydraulic resistance and a more hydrophilic surface than the 0.2 PVDF membrane. The lower flux for the 0.2 PES membrane might be explained as a result of the transmembrane pressure (TMP) applied in the first experiment, which might be exceedingly high for this type of membrane. It has been noted previously by some authors that a high TMP could result in higher flux, but at the same time, a more rapid deposition of particles on the membrane might occur, or what is known as the effect of concentration polarization, which might cause a rapid reduction of flux (Cheryan, 1999; Zhou et al., 2015). Therefore, while a high TMP might improve the driving force of the solution,

it may ultimately result in a greater deposition of particles and major resistance, which could be the reason for the highest flux decline in the 0.2 PES membrane.

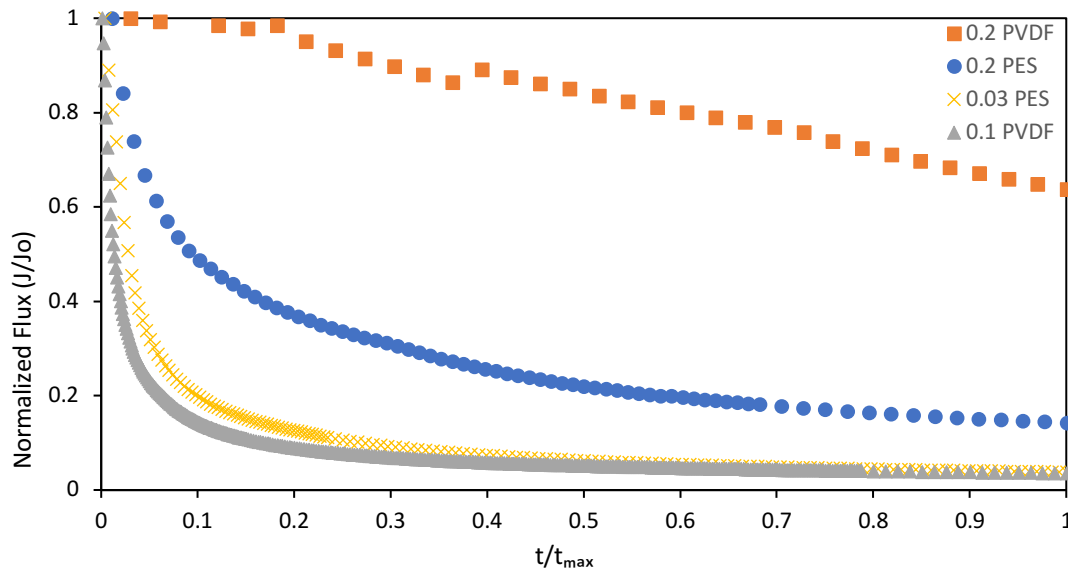


Figure 11. Normalized flux and time after filtration of 1 L of FPW sample.

In order to evaluate the effects of the TMP on the 0.2 PES membrane, a lower pressure (5 psi approx.) was tested, and the filtration flux was recorded. Figure 12 shows the permeate flux for the 0.2 PSE membrane at a lower pressure (5 psi) as compared to the 0.2 PVDF membrane and the 0.2 PES with a TMP of 8 psi. When the pressure was decreased, the flux decline in the 0.2 PES membrane was less steep and followed a similar trend to the 0.2 PVDF membrane. The volume of the feed for this experiment was approximately 500 mL. It was observed that by decreasing the pressure, the effects of concentration polarization could be minimized, maintaining a more stable flux at the beginning of the filtration. These observations suggest that flux decline is affected for multiple parameters such as differences in membrane properties including their hydrophilicity, and also for the conditions of the system, e.g., variations of pressure, concentration polarization, and

membrane fouling (deposition and interactions of particles such as colloids, dissolved inorganic and organic substances, etc.).

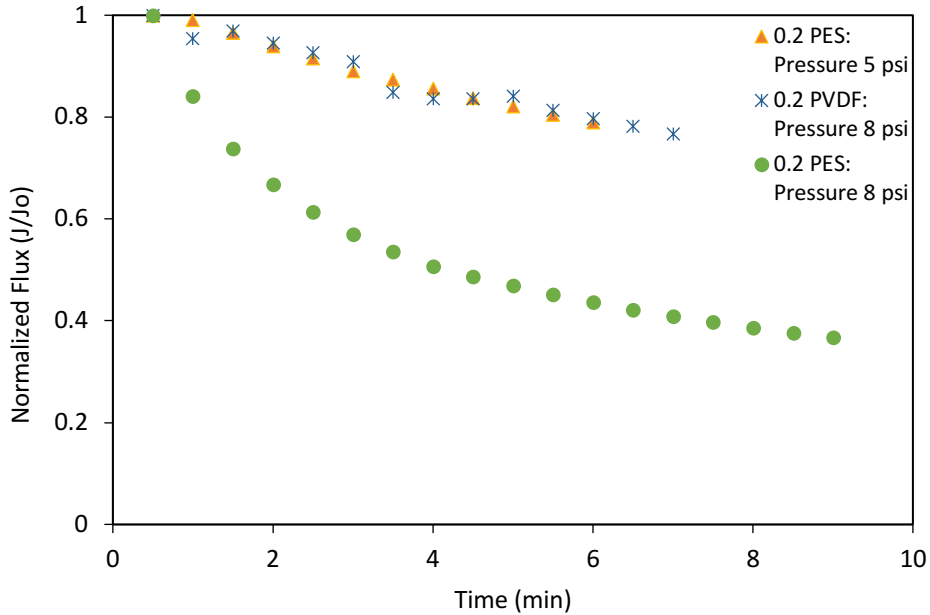


Figure 12. Comparison of filtration flux of the 0.2 PES membrane at different TMP at 5 psi and 8 psi and the 0.2 PVDF membrane at 8 psi.

Additional filtration experiments, matching the initial fluxes, were performed using the 0.2 PVDF and 0.2 PES membranes. These two membranes were chosen to conduct additional experiments as they showed higher performance with less flux decline as compared to the smaller pore size membranes (0.1 and 0.03 μm). This examination allowed for a further assessment of their tendency to foul. To achieve this, the filtration experiments using the two polymeric membranes were adjusted to different TMP of 14 psi and 8 psi for the 0.2 PVDF and the 0.2 PES membranes, respectively (Figure 13). As a result, the initial flux of the two membranes was well-matched at approximately 2200 L/m²h. The permeate flux decline for the 0.2 PES membrane observed in the initial test decreased considerably, being around 64% of the initial flux. A similar trend was observed for the 0.2 PVDF membrane, but it had a further flux reduction of 87%. These

results demonstrate that the 0.2 PES membrane has a lower flux reduction than the 0.2 PVDF when applying the same initial flux. Overall, experiments with the raw FPW showed a significant flux reduction, similar to results published by several authors (Xiong et al., 2016; He et al., 2014; Jiang et al., 2013) which also noticed low flux in MF experiments using different raw FPW samples obtained from the U.S. The authors attributed such low flux the result of high inorganic and organic concentrations present in the feed solution.

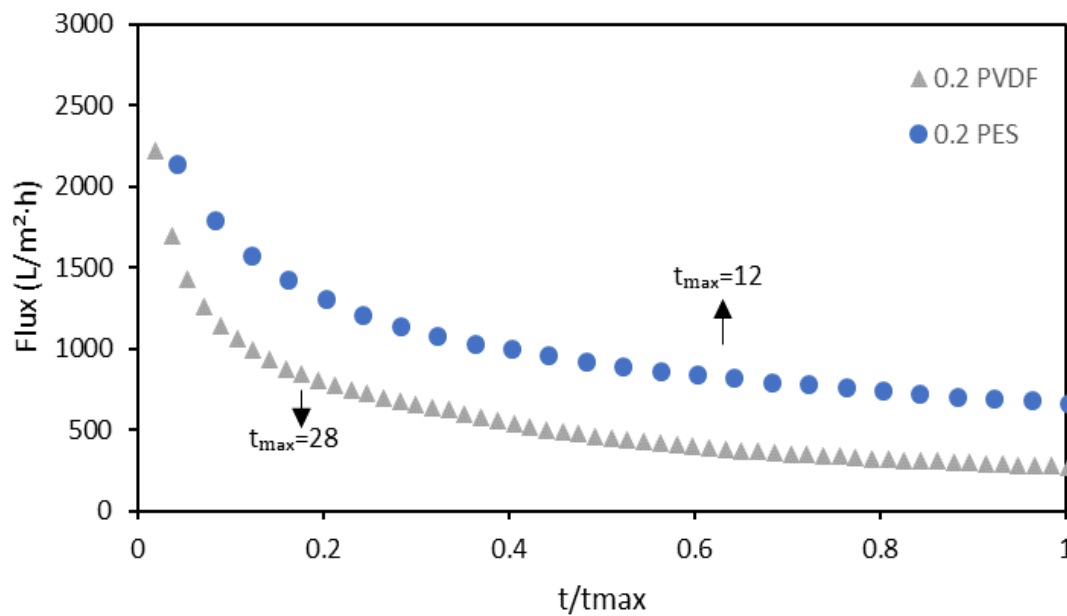


Figure 13. Comparison of permeation flux of the 0.2 PES and 0.2 PVDF membranes with initial fluxes at TMP of 8 and 14 psi, respectively.

Besides filtration flux, rejection of solutes has been commonly used as the second most important parameter for selecting the most suitable membrane in the water treatment (Cheryan, 1998). In this study, rejection was evaluated for each of the four polymeric membranes focusing on the removal of iron, silica, and TOC. Table 7 shows the concentration of the permeates obtained with the four membranes and their respective rejection percentages. The removal of the three targets (Fe, Si, and TOC) from the raw FPW was similar in all four membranes with no significant

differences found between the UF and the MF types. This result may have significant economic implications, as the MF membranes with bigger pore sizes could be used to remove solutes with comparable results to those of the UF membranes, using lower energy and thereby potentially reducing operational costs. The overall rejection of particles for all the four membranes tested was relatively low with values below 10% for each solute target and each membrane. The lowest rejection was seen in the 0.2 PVDF membrane likely because of the larger pore size and membrane material. Although the 0.2 PES membrane had the same pore size than the PVDF membrane, it showed a slightly better rejection of iron and silica. The highest removal percentage was for the two membranes with the smallest pore size, i.e., the 0.1 PVDF (MF) and 0.03 PES (UF) membranes. It is worth noting that part of the removal of TOC is likely due to adsorption on the gel layer formed on the membrane surface during the filtration period, which may have contributed to the decrease of the permeate flux and also altering the membrane surface, becoming more hydrophobic, and thus attracting more hydrophobic species from the feed solution.

Table 7. Observed rejection of Fe, Si, and TOC after FPW micro and ultrafiltration of FPW. Only the 0.2 μm membranes were done in duplicates due to limited water samples.

Sample	Rejection of Iron (Fe)		Rejection of Silica (Si)		Rejection of TOC	
	Concentration (mg/L)	Observed Rejection %	Concentration (mg/L)	Observed Rejection %	Concentration (mg/L)	Observed Rejection %
Raw FPW	210 \pm 4.7		23.2 \pm 1.8		400 \pm 1.6	
0.2 PVDF	207 \pm 4.5	1.3 \pm 1.02	22.3 \pm 0.5	3.9 \pm 5.8	372	7.0
0.1 PVDF	195	6.9	20.5	11.5	369	7.7
0.2 PES	200 \pm 4.6	4.7 \pm 1.2	20.1 \pm 2.3	10.6 \pm 4.2	376	6.1
0.03 PES	194	7.4	19	18	369	7.8

3.2.3 Optimization of the Membrane Filtration Process for Flowback and Produced Water:

Application of an Aeration Pre-treatment

The above experiments demonstrated that using membrane filtration technologies alone to treat hydraulic fracturing flowback and produced water may present several challenges due to the rapid flux decline in the first ten minutes of operation. The low removal of the target materials also revealed that using only low-pressure membrane processes might not be entirely effective to get an acceptable water quality for reuse. Hence, a pre-treatment method applied before the membrane process may be necessary to improve the filtration process and the quality of water for future reuse in the petroleum industry.

Aeration was selected as a pre-treatment method to be employed prior to membrane filtration for multiple reasons such as environmental, operational, and economic considerations. First, environmental implications of FPW have been studied recently by He et al., 2017 (a), and He et al., 2017 (b) where the authors noted that the majority of suspended solids found in FPW samples from the Duvernay play (Alberta) were composed of iron oxides coated by silica which were associated with some organic compounds, e.g., polycyclic aromatic hydrocarbons (PAHs). Speciation analysis conducted on the FPW sample using the ferrozine assay (Stookey, 1970) revealed that most of the iron concentration (> 100 mg/L) present in the solution was in the reduced and dissolved form, Fe (II), and therefore it was hypothesized that if the formation of more iron oxides particles was induced, perhaps more organics would be adsorbed onto the surfaces of these oxides. Muller et al. (2007) suggested that hydrophobic organic contaminants have a sorption affinity to minerals with polar surfaces such as quartz and goethite-coated quartz. A second consideration was for operational reasons. As revealed in the previous results wherein raw FPW was filtered, removing ferrous iron was not an efficient process. Thus, by increasing the particle

size by precipitating iron hydroxides through aeration, more solutes could be retained on the membrane surface improving the rejection of unwanted particles such as iron and silica, which are of concern in the oil and gas industry because they can cause scaling on pipes and in geologic formations. Third, aeration is a low-cost and conventional treatment in the wastewater industry that employs no harsh chemicals. The process involves the operation of simple equipment that includes the use of fine air diffusers to augment oxygen transfer by introducing air through small bubbles, resulting in greater bubble surface area and increased liquid-gas contact (U.S.EPA, Aeration and Air Stripping).

Kinetics of the iron oxidation during the aeration experiments were first modeled to determine the order of the reaction at a constant temperature (ambient room temperature). Figure 14 shows the changes observed during the 24 h experiment where the reduction of Fe (II) followed an exponential decay trend, along with the total concentration of iron. The kinetics data showed a rapid decline of Fe (II) concentration in the first two hours of the experiment, with as much as 80% of ferrous iron being oxidized and most likely precipitated as amorphous iron hydroxides. At the end of the experiment, some of the Fe (II) remained in solution, perhaps due to various aqueous complexes that ferrous iron can form with ligands present in the complex FPW solution. This phenomenon was also suggested in other aeration experiments carried out with natural waters (Millero et al., 1986).

The chemical reaction between Fe (II) and oxygen has been reviewed previously by Burke and Banwart (2002) and is presented in Eq. 12, which is in agreement with the experimental conditions of this study. Previous studies on the oxidation kinetics of $\text{Fe}^{2+}(\text{aq})$ demonstrated that iron oxidation follows a first-order reaction (Eq. 13) with respect to the concentration of Fe (II), and is independent of the Fe (III) concentration (Stumm and Lee, 1961). The overall oxidation rate

of Fe (II) (Eq. 14) has also been reported by other authors (Stumm and Lee, 1961; Tamura et al., 1976) which demonstrates that the rate might be sensitive to changes of solution such as pH and oxygen concentration.



$$\frac{-d\text{Fe(II)}}{dt} = k[\text{Fe(II)}] \quad (13)$$

$$\frac{-d\text{Fe(II)}}{dt} = k[\text{Fe(II)}][\text{OH}^-]^2[\text{O}_2] \quad (14)$$

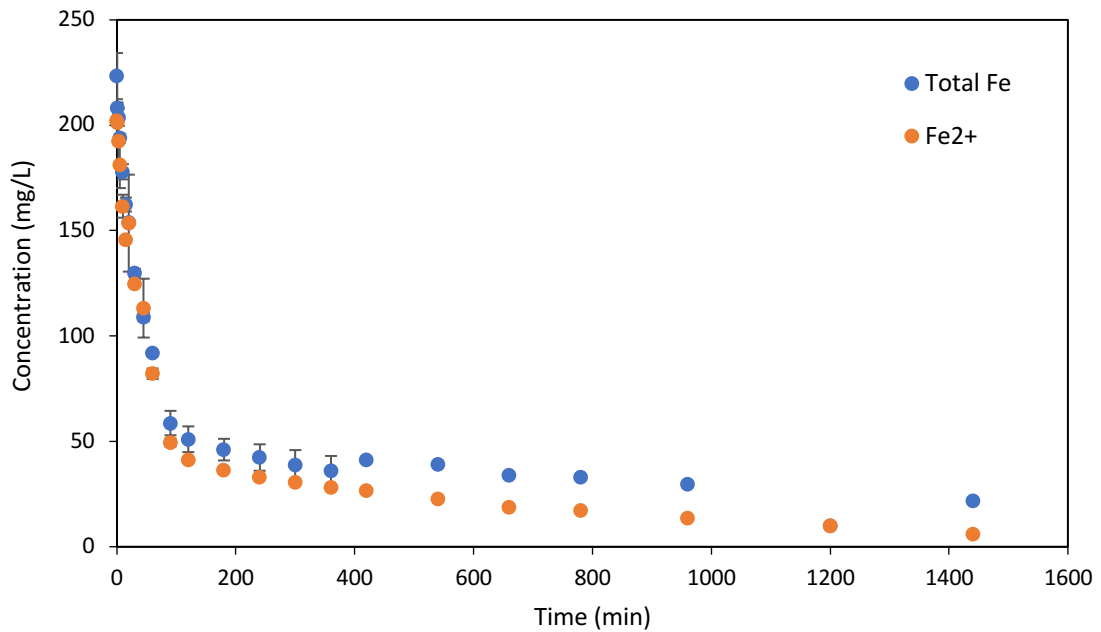


Figure 14. Concentration of Fe (II) and total Fe after 24 hr aeration, determined by the ferrozine method (Stookey, 1970).

In this research, a first-order reaction (k in units of min^{-1}) was established by plotting the data in $\text{Ln}(C/C_0)$ vs. time format, where C_0 is the initial concentration of Fe (II) at $t=0$ and C is the concentration of Fe (II) at a given time (Figure 15). The linear correlation observed demonstrated that the reaction was first-order, having an excellent fit with a coefficient (R^2) of 0.98. The order of reaction and the concentration-independent rate constant (K_{int}) was also calculated by plotting the experimental data using the log Rate vs. the log concentration of Fe (II), which yielded a straight line. The slope of this plot also had a good fit, with an R^2 of 0.98 and a slope of 1 which indicates a first-order reaction (Figure 16). The rate constant (K_{int}) was calculated to be 0.0138 min^{-1} . It has been suggested that the oxidation rate of ferrous iron can be enhanced by the adsorption of dissolved iron species to hydrous oxide surfaces (Morgan and Lahav, 2007), which could be the case in our experiments.

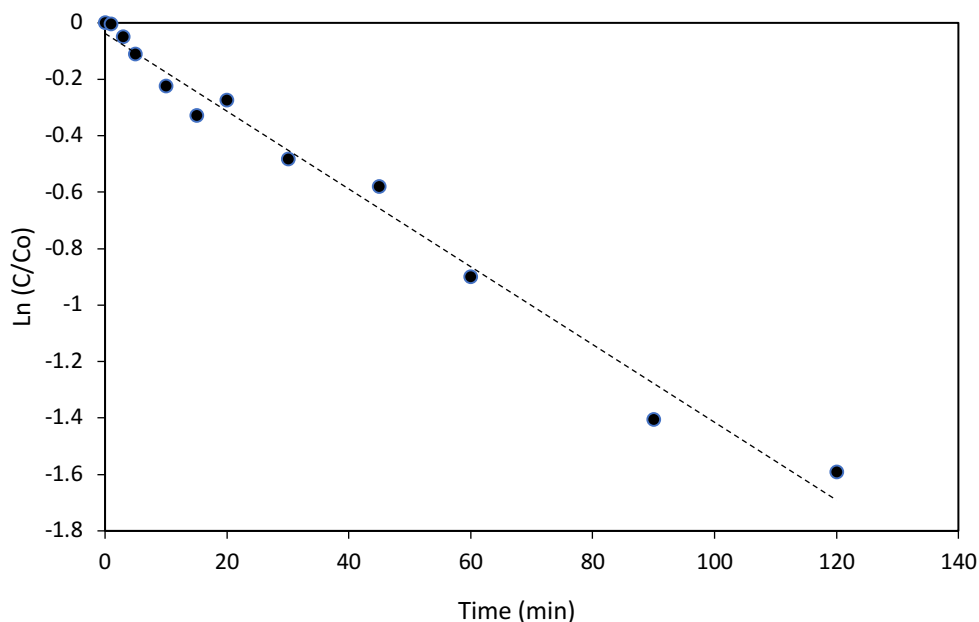


Figure 15. First-order rate of oxidation of ferrous iron after 24 h aeration using the raw FPW sample.

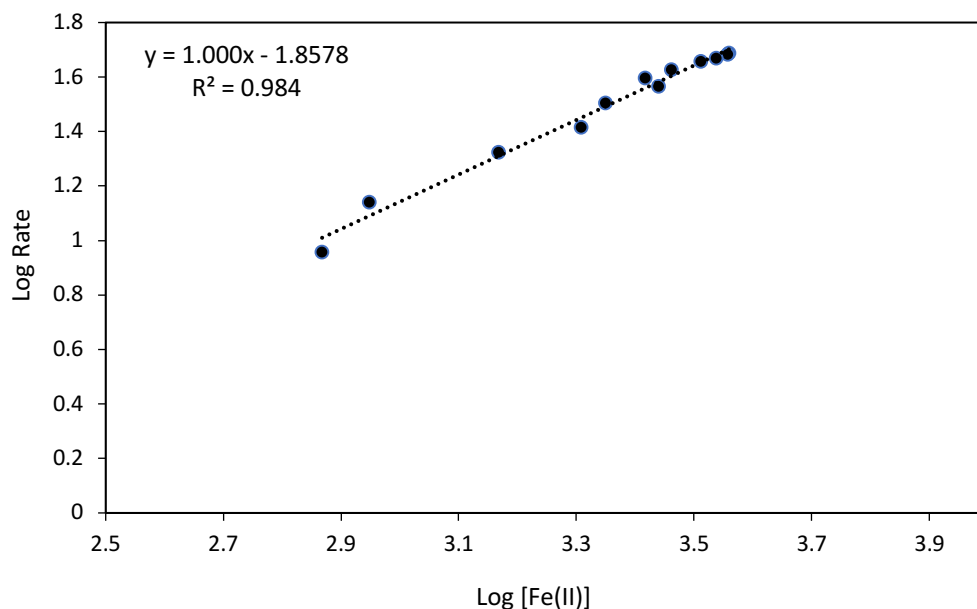


Figure 16. Log of the rate constant as a function of log of Fe (II).

Changes in pH were also evaluated through the aeration experiments (Figure 17). The initial pH of the FPW sample was 6.1, and after 24 hours of aeration, it dropped to 4.9. A rapid decline was observed in the first 4 h of the experiments, after which pH plateaus. These results are comparable to the sharp decrease of the ferrous iron concentration, evidencing the dependence between these two components in the system, where the reduction in pH is likely due to the high concentration of dissolved iron, and consequent precipitation of iron hydroxides. In this chemical reaction, OH^- are being consumed during iron precipitation, producing acidity by the concomitant production of H^+ ions, as shown in Eq. 12, which has also been observed previously by some authors (e.g., Burke and Banwart, 2002).

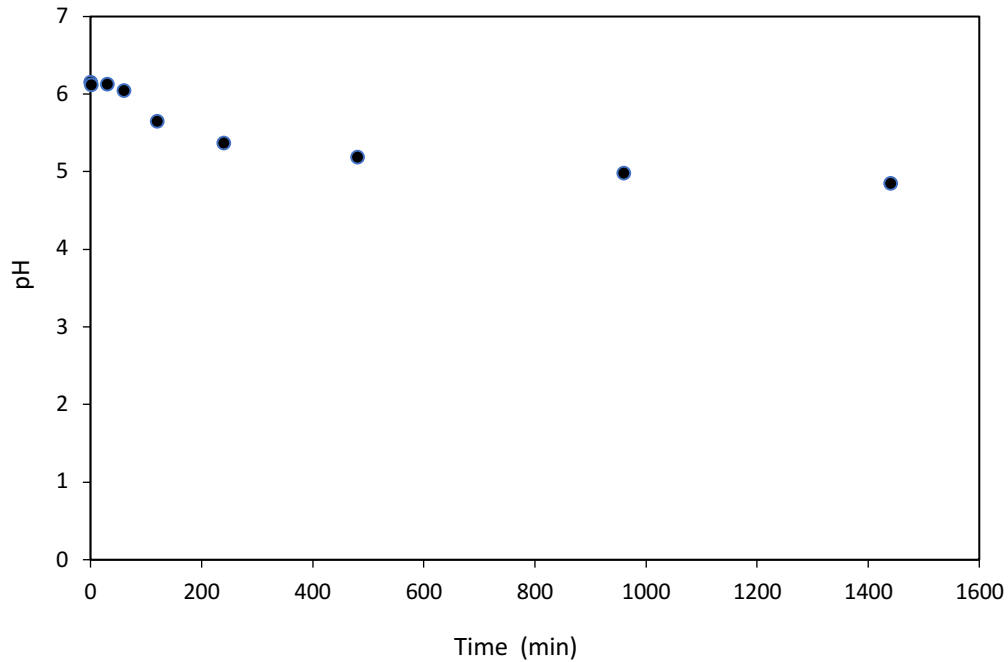


Figure 17. pH changes of the raw FPW sample during the 24-hr aeration experiment at room temperature.

TOC changes were also monitored during the 24 hr aeration experiments. Figure 18 shows a sharp TOC decrease in the first 60 m of aeration from 400 ppm to 345 ppm, which then reaches a plateau with a total TOC reduction of 21.5% with respect to the raw FPW solution. The decrease in the organic content could be attributed to different factors such as adsorption on the iron oxides surfaces and volatilization of the lower molecular weight organic compounds (Muller et al., 2007; Radhi and Borghei, 2017). These results demonstrate that the aeration treatment alone could also improve the quality of the FPW reducing the levels of some organic compounds.

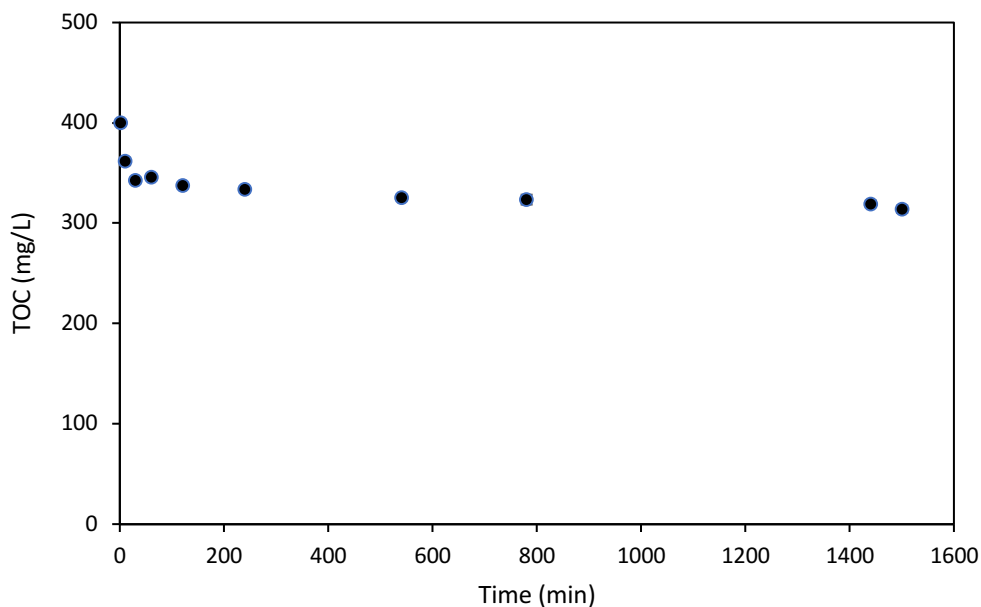


Figure 18. TOC changes during 24 h aeration with compressed air of an FPW sample from the Duvernay play.

3.2.4 Flux and Rejection of Aeration-treated Flowback and Produced Water

Figure 19 shows the permeation flux of the FPW sample after the aeration treatment using the four tested commercial MF (0.2 μm PVDF, 0.1 μm PVDF, 0.2 μm PES) and UF (0.03 μm PES) membranes. In subsequent sections, the terms NAP and AP will be used to refer the non-aerated permeate and the aerated permeate for the untreated FPW samples and the FPW pre-treated through aeration, respectively. The operating conditions in this test were the same as the previous experiments for the non-aerated FPW (constant pressure of 8 psi and 1 L of solution) to compare the performance of the different membranes before and after the aeration treatment. Some similarities were observed on the initial fluxes of the 4 membranes, but significant differences are

reported regarding the filtration flux (flux decline and time), and rejection of target particles (iron and silica) after the aeration pre-treatment compared to the filtrations with the untreated FPW.

Like the filtration results of the non-aerated sample, the initial flux for the treated FPW presented high variations among the four membranes. This difference is most notable depending on the type of membrane material, i.e., the highest initial flux belonging to the PES membranes and the lowest values corresponding to the PVDF membranes. The PES membranes had higher initial flux with an average of 2700 L/M²H, almost twice as much as the initial flux of the PVDF membranes with an average of 1576 L/M²H. The initial flux of the samples after the aeration treatment had a marked increase, of at least 10%, in all the membranes versus their non-aerated counterparts. The flux declines also decreased substantially for each membrane during the filtration of 1 L of solution, with percentages of 11.5%, 11.8%, 5.4%, 19.4% for the 0.2 PVDF, 0.1 PVDF, 0.03 PES, 0.2 PES, respectively, compared to higher values (>40%) in the non-aerated FPW. One of the most relevant improvements with the aeration treatment is observed in the total filtration time, which decreased from more than 2 hrs for the membranes with the smallest pore size (0.1 PVDF and 0.03 PES) to less than 30 minutes. The filtration time, therefore, improved 62.5%, 48.5%, 96.5%, and 95.3% for the 0.2 PES, 0.2 PVDF, 0.1 PVDF, and 0.03 PES membranes, respectively.

The normalized filtration flux of the four membranes is shown in Figure 20 so that the flux declines can be more easily compared. The data show an improvement in the flux after the aeration of the FPW sample, which is negligible compared to the non-aerated sample. No significant flux decline was observed on the three polymeric MF membranes and one UF membrane after filtration of 1 L, as compared to the non-aerated FPW. These results clearly revealed how the recovery of flux was enhanced by the aeration pre-treatment.

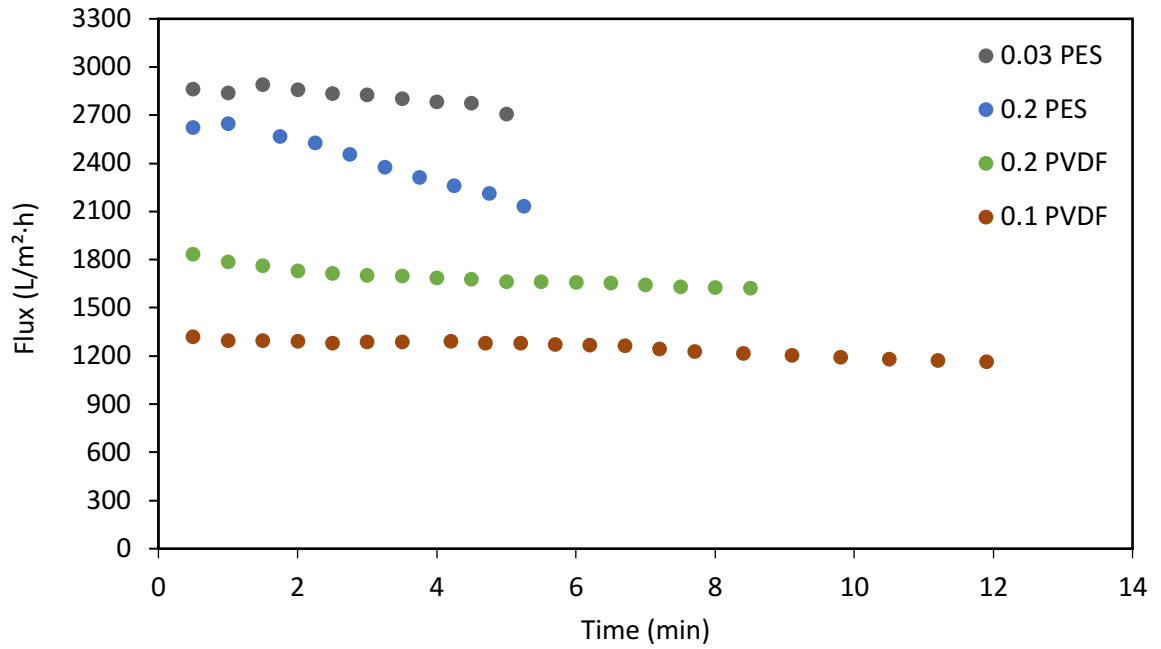


Figure 19. Permeate flux of four different polymeric MF-UF membranes after the aeration treatment.

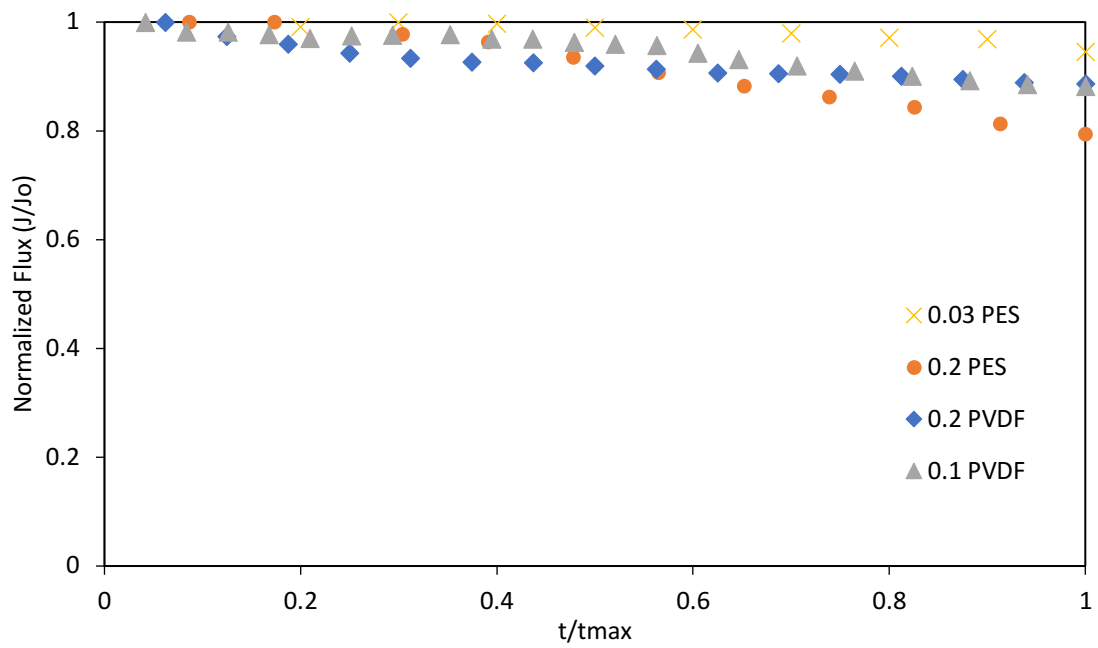


Figure 20. Normalized flux of four different polymeric membranes after filtration of 1 L of FPW sample.

Further experiments were performed using only the two MF (PVDF and PES) membranes with the bigger pore size (0.2 μm) by matching their initial flux at 2500 (Figure 21). This experiment was conducted in order to have a better estimation of the flux performance between these two membranes. These membranes were selected, as mentioned previously, because they presented better flux rates and rejection of the target particles (Fe and Si) during the initial testing, with the lowest energy consumption (lower pressure values). The feed volume for this experiment was about 0.6 L. After the aeration pre-treatment the total filtration time was only about four minutes compared to more than 12 min for the non-aerated sample. Moreover, the flux decline reduces considerably to 20% and 9% for the 0.2 PVDF and 0.2 PES membranes, respectively. These results demonstrate the higher performance for the 0.2 PES membrane having less flux reduction in a relatively shorter filtration time.

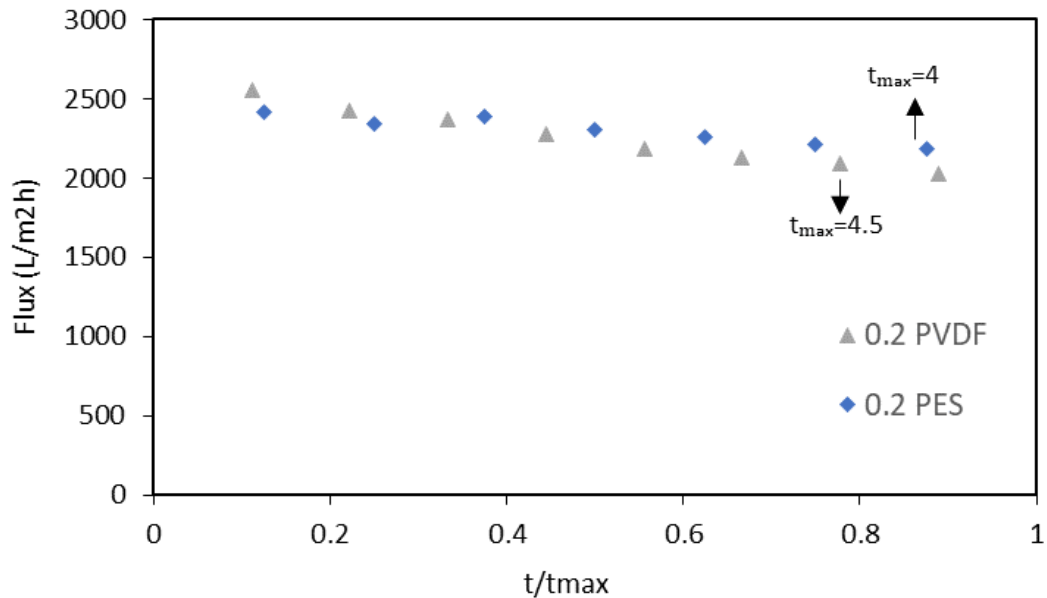


Figure 21. Flux decline of the 0.2 PVDF and 0.2 PES membranes at a pressure of 14 psi and 8 psi, respectively, and similar initial flux.

The rejection of target particles after the FPW pre-treatment through aeration (AP) improved considerably, removing more than 70% of iron and silica for the two 0.2 μm MF membranes (Table 8), compared to the low rejection values in the NAP sample with values below 10%. Rejection of the 0.1 PVDF and 0.03 PES membrane is shown in Table A.1 (Appendix A). The rejection of TOC after the aeration treatment was negligible in contrast to the results of the untreated sample where some rejection was seen. The minimal removal of TOC after the aeration treatment revealed that the organics present in FPW samples are poorly retained in MF membranes. This might suggest that most of the organic compounds present in the aerated FPW sample are smaller than the pore size of the membranes (possibly in dissolved or colloidal form) passing readily through the pores. As noted before, organic substances can be detrimental in the drilling process as well as during membrane filtration treatment.

Table 8. Rejection of iron, silica, and TOC after aeration of the raw FPW.

Sample	Rejection of Iron (Fe)		Rejection of Silica (Si)		Rejection of TOC	
	Concentration (mg/L)	Observed Rejection %	Concentration (mg/L)	Observed Rejection %	Concentration (mg/L)	Observed Rejection %
Raw FPW	210 \pm 4.7	-	23.2 \pm 1.8	-	314 \pm 3.5	-
0.2 PVDF	47.3 \pm 0.9	77.5	6.4 \pm 0.1	72.5	314	0.0
0.2 PES	7.7 \pm 2.8	96.3	5.5 \pm 0.2	76.1	313 \pm 3.2	0.1

Figure 22 shows the difference in appearance among the feed solutions and the NAP and AP obtained after membrane filtrations. Figure 22A shows the appearance of the raw FPW, having a light-yellow color with dark suspended solids. Permeate 1 (non-aerated FPW) did not significantly differ in the appearance from the raw FPW feed, but the dark particles were clearly

removed during the MF. Figure 22B shows the FPW feed after the aeration treatment, having a highly turbid and orange color due to the oxidation of ferrous iron. Permeate 2 (aerated sample), on the other hand, shows an evident improvement in the quality of the solution with a much clearer appearance.

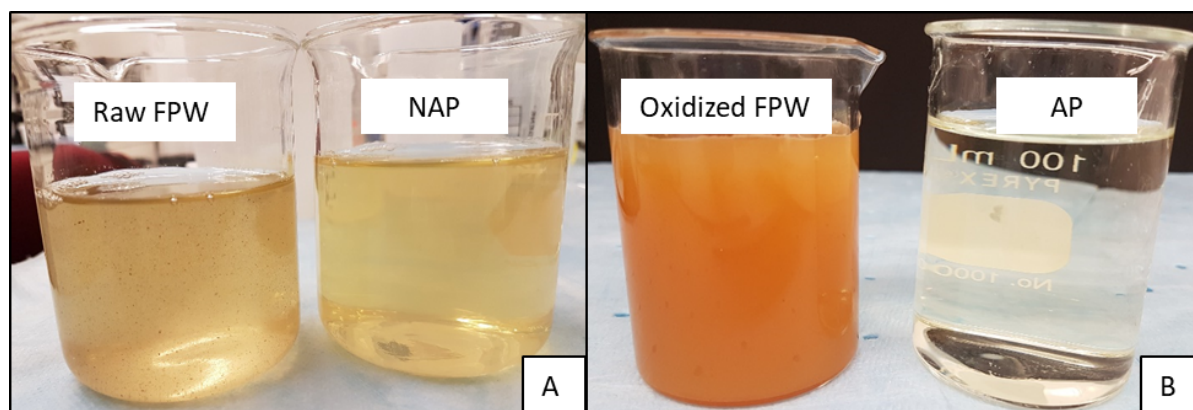


Figure 22. A) Appearance of the feed (raw FPW) and non-aerated permeate (NAP) solutions. B) Appearance of the FPW after the aeration treatment (oxidized FPW) used as a feed in MF and UF analysis, and the aerated permeate (AP) solution.

3.2.5 Fouling Characterization Before and After Aeration Treatment

Fouling mechanisms affecting the four polymeric membranes before and after the aeration treatment were investigated using Hermia's model (Hermia, 1982). Relevant data are presented only for the two MF membranes (0.2 PVDF and 0.2 PES) as they have shown a more effective performance, having higher filtration fluxes and lower consumption of energy compared to the smaller pore size membranes (0.1 μm and 0.03 μm).

Fouling mechanisms were identified at different filtration stages only for the raw FPW, i.e., an initial stage when more substantial flux reduction occurs, and a final stage where flux has

stabilized, reaching almost steady-state, as it has been suggested by many researchers that distinct mechanisms can be present at different filtration stages (Zhou et al., 2015; Wang and Tarabara, 2008). Figures 23 and 24 show that the two filtration stages obtained for the two membranes studied had similar characteristics with a high fouling tendency during the filtration of the raw FPW. Fouling mechanisms of the 0.1 PVDF and 0.03 PES are shown in Figure A.1 (Appendix A). In the initial stage (first ten minutes of filtration, Figure 23) the main fouling mechanism was cake filtration formation for both MF membranes (0.2 PVDF and 0.2 PES), which is represented by the highest regression correlation factors (R^2) of 0.9993 and 0.9988, respectively. Intermediate pore blocking also seems to be an important factor in the reduction of permeate flux, with R^2 values of 0.9744 and 0.9740 for the 0.2 PVDF and 0.2 PES membranes, respectively. These results indicate a high concentration of solutes at the membrane surface as well as the presence of particles in the feed solution of larger size than the membrane pores. Although the other two mechanisms, standard pore blocking and complete pore blocking, also had high R^2 values (~ 0.94 and ~ 0.90), the models suggest that they are less likely to play a major role in the fouling of the membranes during the initial filtration stage. Many authors have suggested that the primary cause of severe fouling during MF and UF operations is due to the organic content from the feed solutions. Cassini et al. (2011) and Lee et al. (2004), for example, observed that severe UF-MF fouling was caused by the presence of colloidal and macromolecular organic components, having both hydrophilic and hydrophobic characters in the treatment of waste and natural waters.

Figure 24 shows the fouling mechanisms of the later stage for the untreated FPW. Similar fouling characteristics were observed for the later stage (final filtration time) than the initial stage for the two MF membranes. Although the most predominant fouling mechanism is still the cake layer formation for the 0.2 PVDF membrane, with an R^2 value of 0.9984, in the 0.2 PES membrane,

the intermediate pore blocking was the main fouling mechanism with an R^2 value of 0.9982. At the later stage, the higher influence of the other two fouling mechanisms is also evident, especially the standard pore blocking, presenting high R^2 values of 0.9901 and 0.9943 for the two MF membranes. Complete pore blocking also generated a good fit to the experimental data with $R^2 > 0.97$. These results evidence the heterogeneous composition of the feed solution with a combination of large and small particles depositing on the surface and in the pores of the polymeric membranes. He et al. (2014) also evaluated the fouling mechanisms of an FPW sample from the Marcellus Formation, and found that at the initial stage pore-blocking was the main mechanism, while cake filtration seemed to be more important in the later stage, although their studies were based on the Ho and Zidney (1999) fouling approach. The authors also indicated that the main reason for fouling in a sample with high ionic strength is due to the presence of submicron particles, e.g., iron, that are likely stabilized in solution by an organic coating. Results in this study are also consistent with the principal cause of fouling being the organic compounds found in the feed solution.

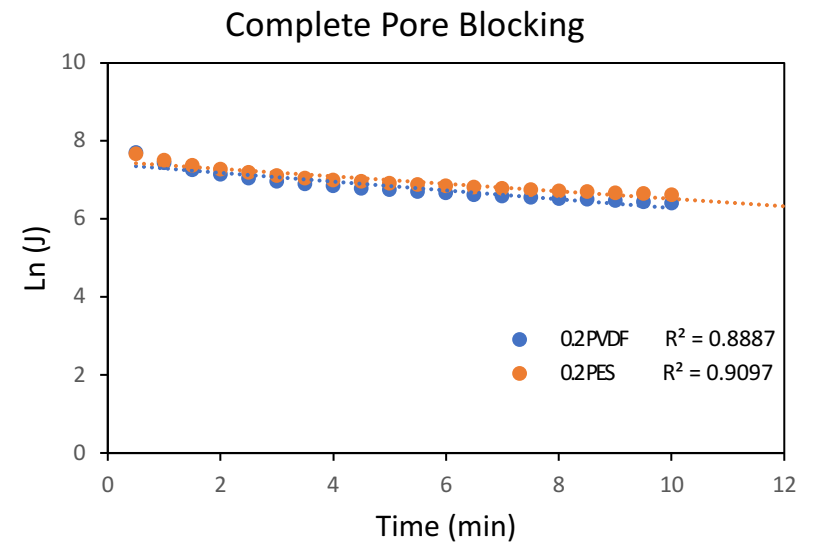
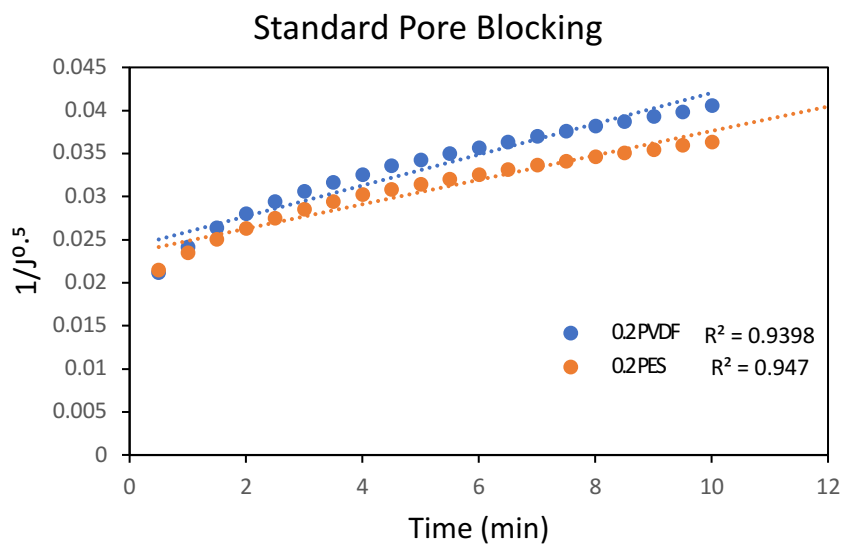
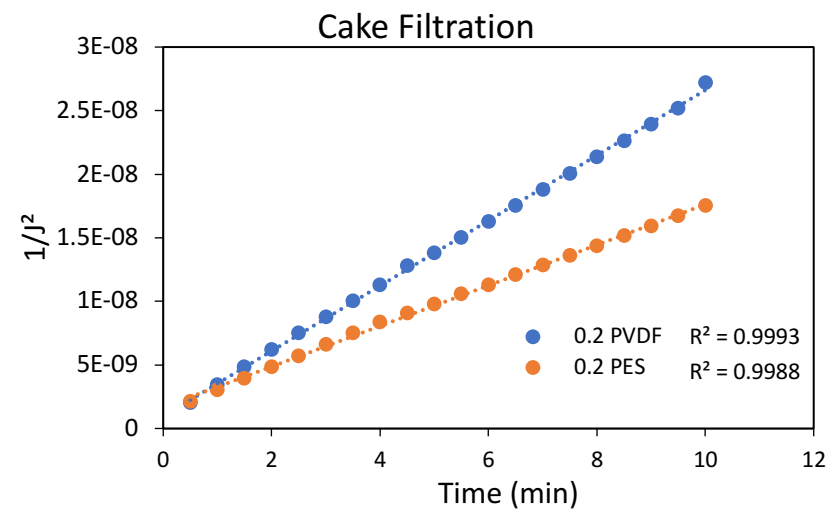
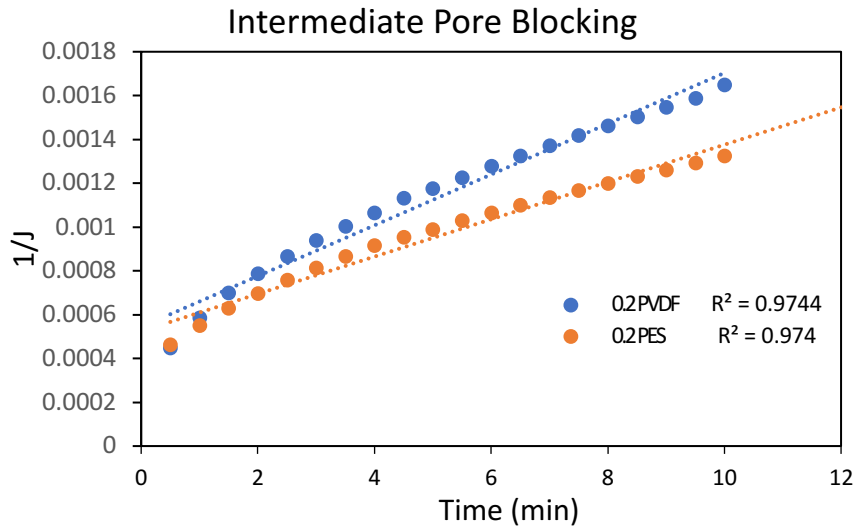


Figure 23. Fouling mechanisms at the initial stage after filtration of non-aerated FPW according to Hermia's model.

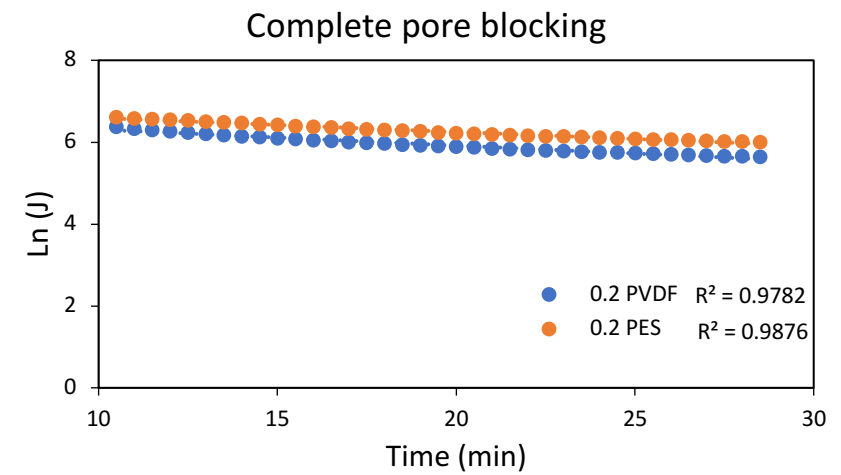
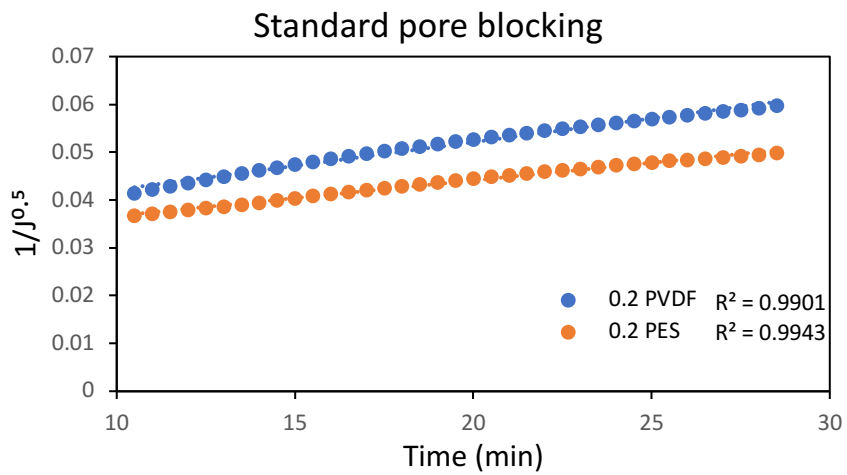
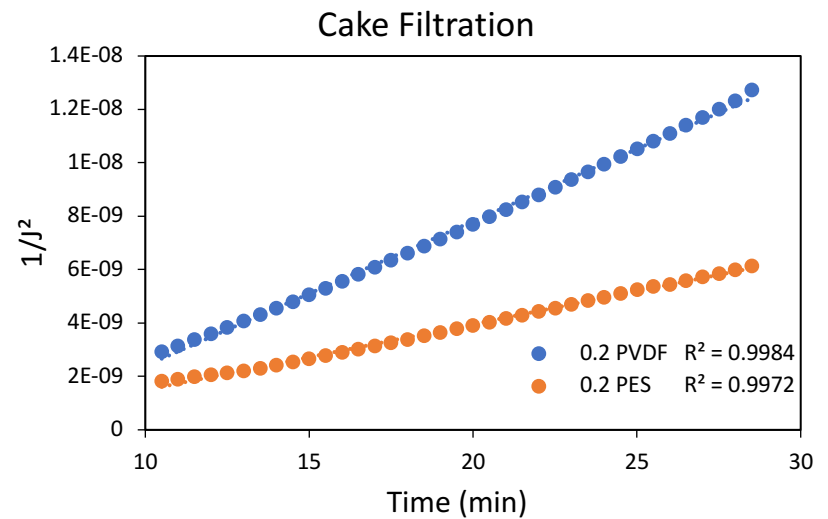
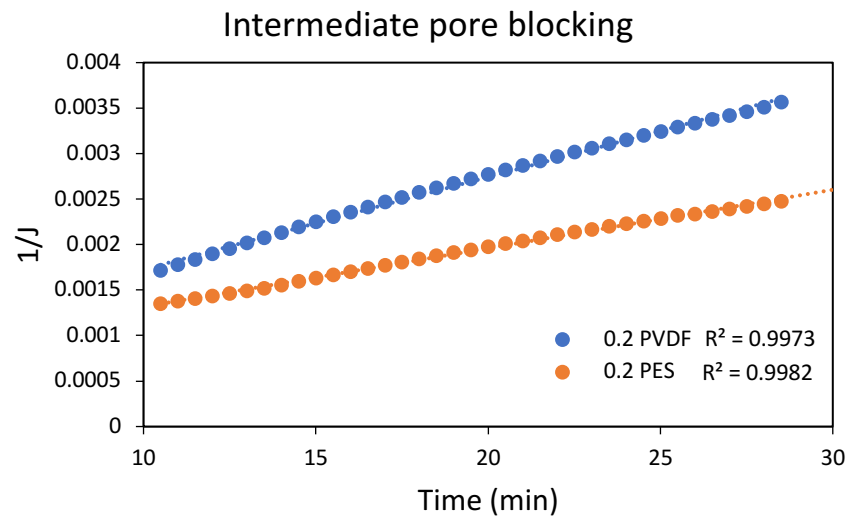


Figure 24. Fouling mechanisms at the later stages of the non-aerated FPW for the 0.2 PVDF and 0.2 PES membranes.

Figure 25 shows the fouling mechanisms for only one filtration stage of the treated FPW because of the rapid flux after the aeration treatment. The fouling mechanisms (R^2 values) generated from the two membranes (0.2 PVDF and 0.2 PES) are slightly different between each other. Fouling mechanisms of the aerated FPW using the 0.1 PVDF and 0.03 PES membranes are shown in Figure A.2 (Appendix A). For instance, the predominant mechanism for the 0.2 PVDF membrane corresponded to cake filtration formation while the dominant mechanism in the 0.2 PES membrane was intermediate pore blocking. The four mechanisms in this membrane (0.2 PES) seem to influence the membrane fouling, all displaying R^2 values of around 0.95. No significant differences were found for the experiments before and after the aeration treatment. It is also worth noting that these results are similar to the previous experiments (without the aeration treatment) for the later stage of the filtration, where the four mechanisms gave reasonable fits to the data, showing again that fouling of FPW it is a complex process where more than one mechanism might be responsible for the flux decline.

The high R^2 values originating in all four fouling mechanisms is usually associated with the poor removal of colloids and fine particles. This was also observed by Kong et al. (2017) during the UF of an FPW sample obtained from the Fuling shale gas play (China). Cassini et al. (2011) also noted that during the filtration of wastewater the flux decline was the result of various fouling mechanisms acting at the same time.

Cheryan (1998) noted that in some fouling studies comparing PVDF and PES membranes, the PVDF might be more or less prone to adsorption or fouling by organics than the PES membrane depending on the degree of hydrophilicity, i.e., the smaller the contact angle, the lower the degree of membrane fouling. The author concluded that the hydrophilic character of a membrane is not the only factor affecting fouling, but that other membrane or water factors such as surface

roughness and feed concentration can also play important roles in membrane fouling, thus affecting also flux decline.

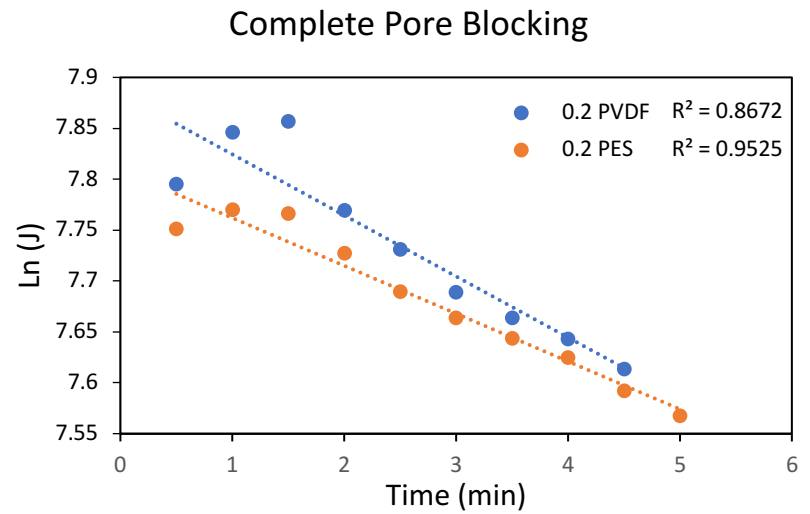
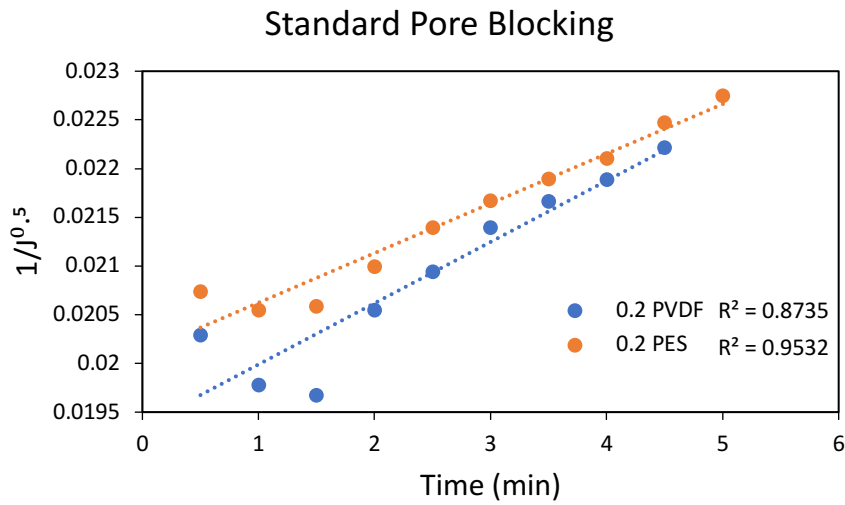
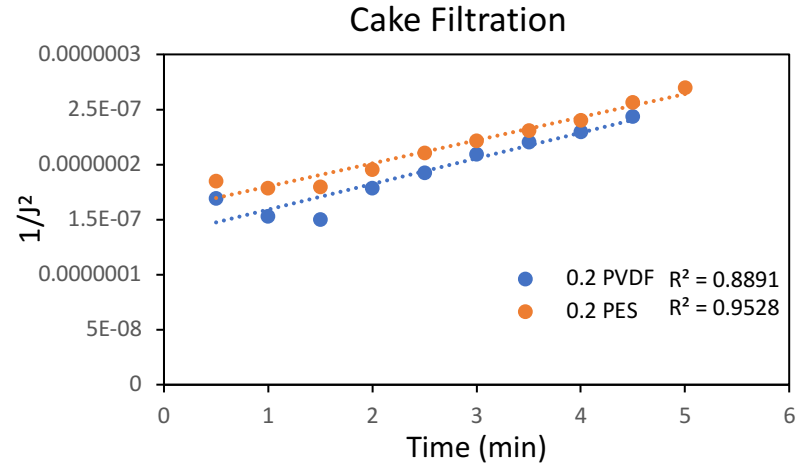
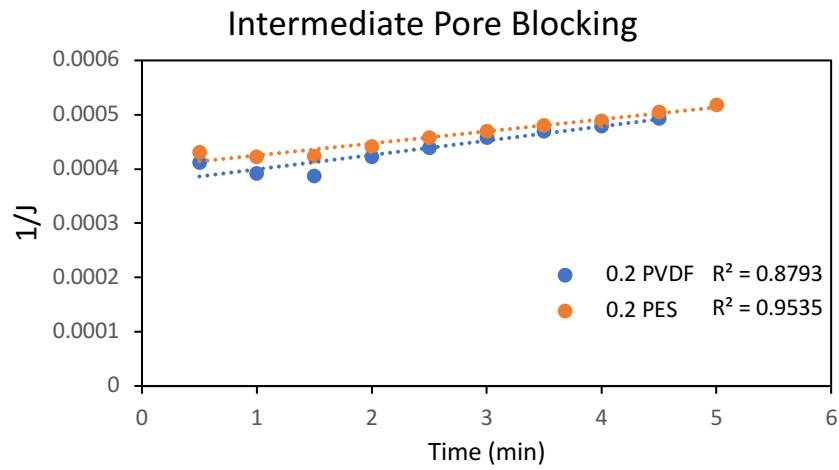


Figure 25. Fouling mechanisms after the aeration treatment for the 0.2 PVDF and 0.2 PES membranes.

Deposition of the particles on the membrane surfaces before and after the aeration treatment are shown in Figure 26. Before the aeration, the particles retained in all polymeric membranes have a brownish color and are tightly held on the surface, which may explain the high flux decline when there is no pre-treatment of the FPW. Conversely, after the aeration treatment, there is an evident change in the particles retained on the four membranes, having an orange-color and attached loosely on the membrane surface. The difference seen on the particles retained on the membrane surfaces before and after aeration might be explained by one of these mechanisms: 1) during the aeration process some of the organic bonds were broken, and some of these organics were likely adsorbed on the surface of the newly form iron oxides; 2) the aeration treatment increase the particle size for some of the materials present in the FPW samples such as iron and silica, forming larger clusters of precipitates, 3) a higher degree of deposition of inorganic particles with respect to the organic substances on the membrane which could have decreased the direct interaction between the organic constituents from the feed solution and the membrane surface, 4) the reduction of fouling after the aeration treatment could also be explained by the degradation of some hydrophilic compounds, specifically polyacrylamide (PAM) as described recently by Xiong et al. (2018) who suggests that this polymer may be the main cause of membrane fouling. The results found in this thesis also indicate the relevant role of the organic compounds in the fouling of the untreated FPW and how the aeration may have improved the permeation flux and rejection.

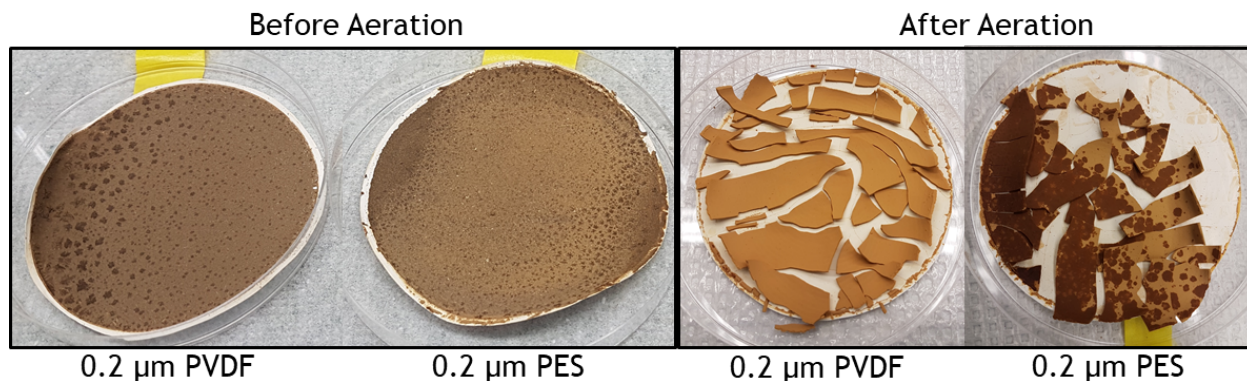


Figure 26. Particles deposited on the surface of the MF membranes before and after the aeration treatment.

The morphology of the particles before and after the aeration treatment deposited on the membrane surfaces was qualitatively analyzed by FESEM-EDS. The overall composition of the particles retained on the 0.2 PES membrane before and after the aeration treatment was determined by EDS analysis (Figure 27). Similar results were obtained for all the membranes, and a representative image is shown. The major difference observed between the two systems (untreated and treated FPW) was the higher concentration of iron after the aeration treatment as more amorphous iron oxides precipitated from solution, which it is expected to occur. Also, some of the elements present before aeration such as barium, calcium, and sulfur were not detected in the aerated sample likely because of the elevated amount of iron oxides that could mask the signal of those elements.

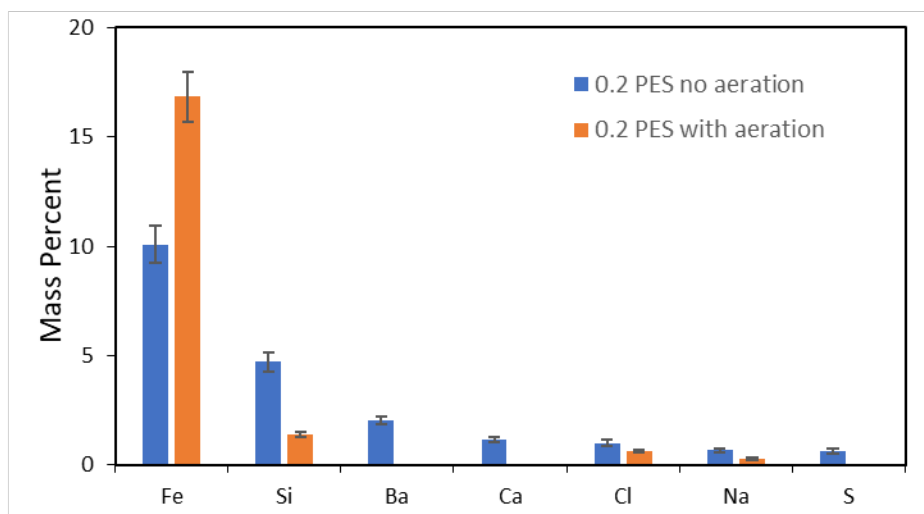
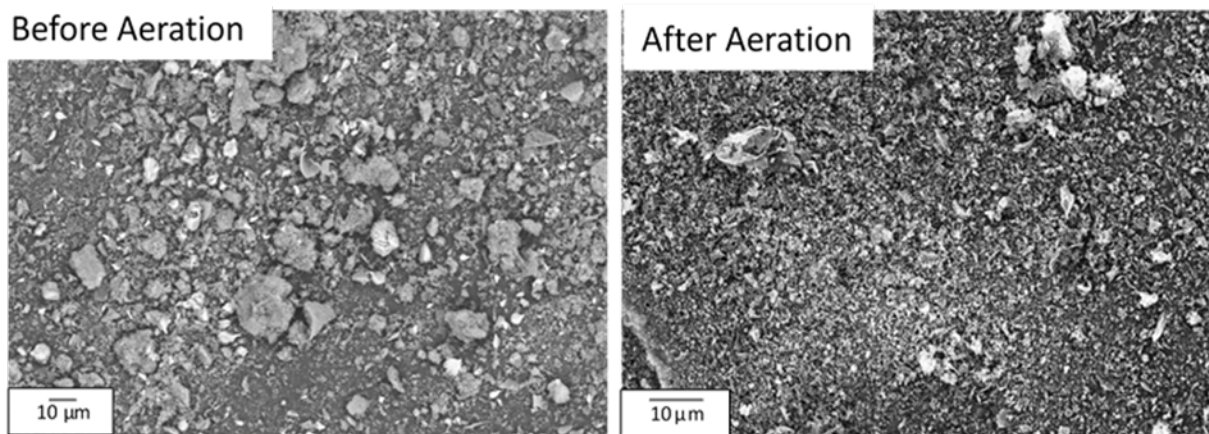


Figure 27. Overall composition of particles retained on the 0.2 PES membrane before and after aeration.

Figure 28 shows some of the most common particles retained on the membrane surface after the filtration process. No significant differences were found before and after the aeration treatment, although after the aeration treatment it was more common to find the elongated tubular shapes illustrated in Figure 28A, composed mainly of iron and oxygen and in small proportion silicon. Some authors have suggested that at lower pH, precipitation of goethite is more favorable. Therefore, it is possible that goethite could form under these experimental conditions. Similar particles were found by Lokare et al. (2017) who evaluated the fouling effects of FPW samples from the Marcellus play in direct contact membrane distillation processes. He et al. (2014) also

reported that the particles retained on their MF membranes were composed mainly by Fe. The carbon signal in the samples is largely attributed to the carbon coating and the carbon tape used for holding the samples.

Figure 28B shows typical clusters of needle-like shapes that are consistent with particles composed of barium, strontium, and sulfur, as determined by EDS analysis. This elemental configuration likely corresponds to the strontium sulfate mineral (celestine, SrSO_4) and barium sulfate (barite, BaSO_4), or it could be a solid solution composed of Ba-Sr- SO_4 , which it can form in brine solutions (Brower, 1973). He et al. (2014) also reported barite precipitation during their MF experiments but noted that these particles were not likely to influence the fouling of polymeric microfiltration membranes.

Figure 29 shows the XRD patterns obtained from the analysis performed on the non-aerated and aerated samples to corroborate the FESEM-EDS findings. The XRD peaks for the non-aerated sample matched the barium sulfate phase which may correspond to barite, also seen in the EDS results. No peaks matching celestine were observed. Other diffraction peaks corresponded to crystal phases of quartz, halite, and spinel. The spinel peak, however, did not appear to be part of the suit of crystals in the FPW solids, and no similar elements were detected in the SEM-EDS images. Instead, those peaks could correspond to some other type of crystalline iron oxide. Contrarily, the XRD patterns for the aerated sample showed only a few peaks that likely correspond to the NaCl phase halite. This finding supports the observation that most of the iron phases found in the aerated sample correspond to amorphous iron hydroxides, and that their high concentration could be masking the signal of other possible crystalline materials, additionally agreeing with the SEM-EDS results.

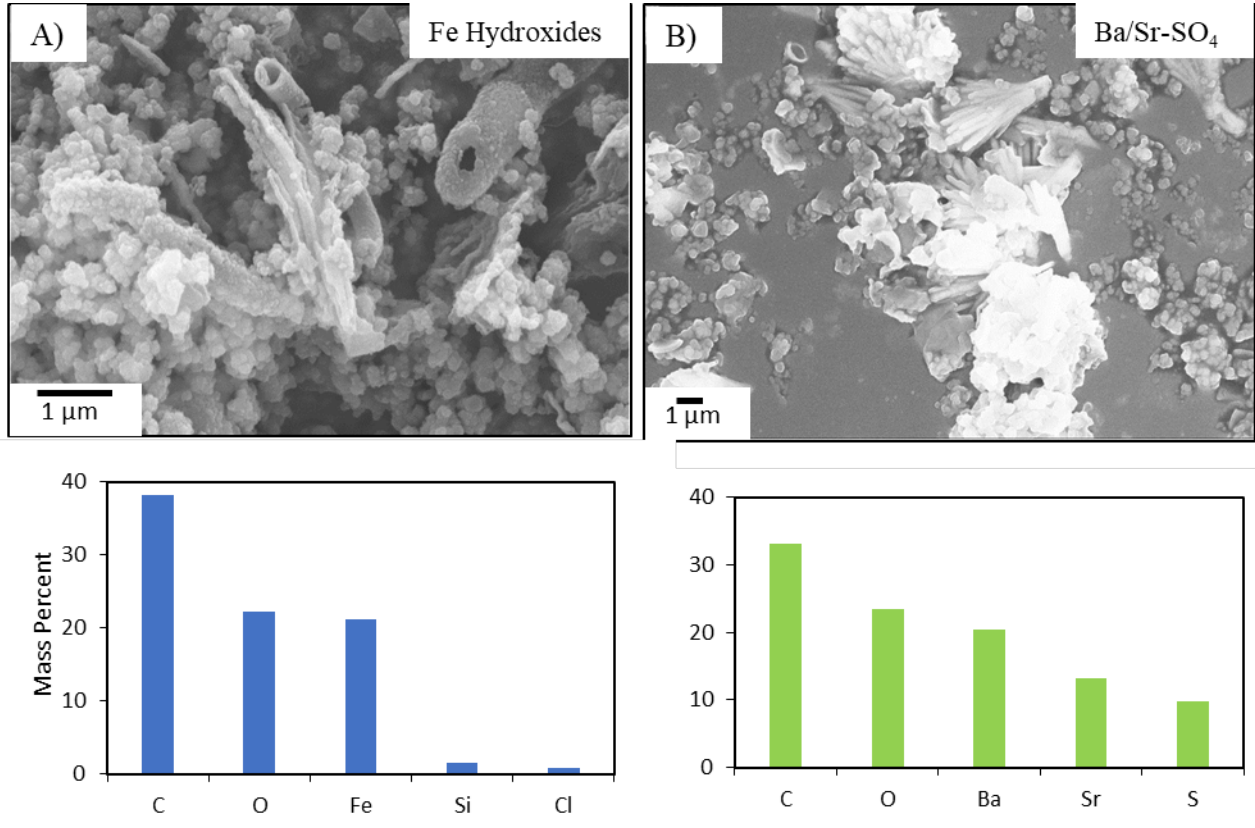


Figure 28. A) clusters of iron oxides smaller than 1 micron and tubular iron oxides. A) clusters of needle-like shapes of Ba/Sr-SO₄ (possibly barite and celestine). Similar particles were observed before and after the aeration treatment for all the membrane filtrations.

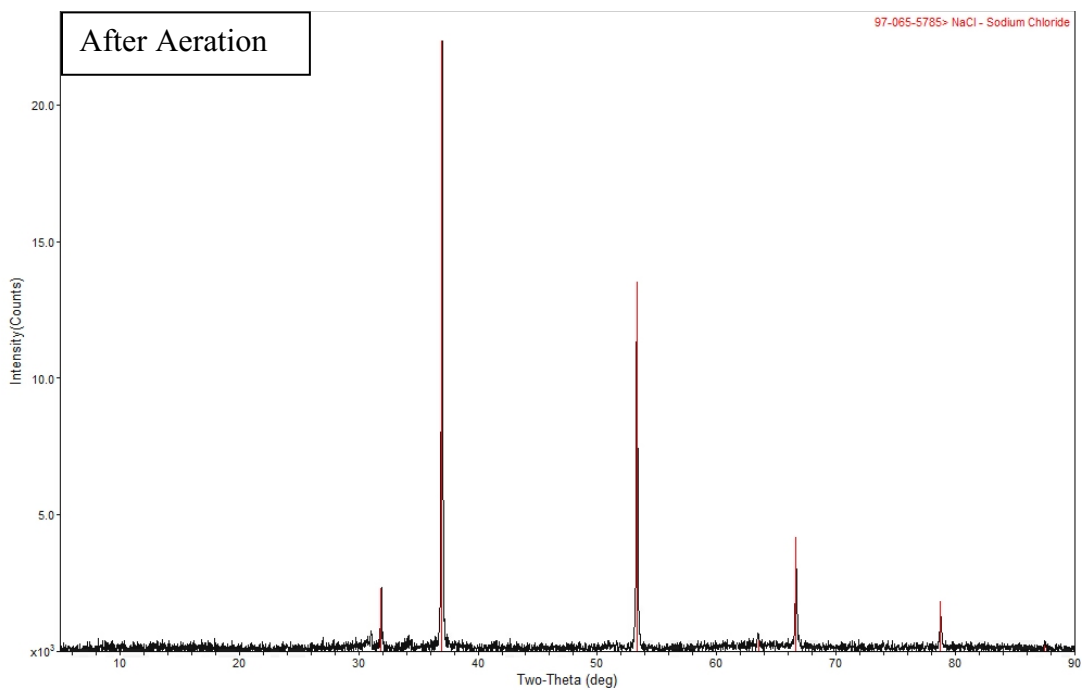
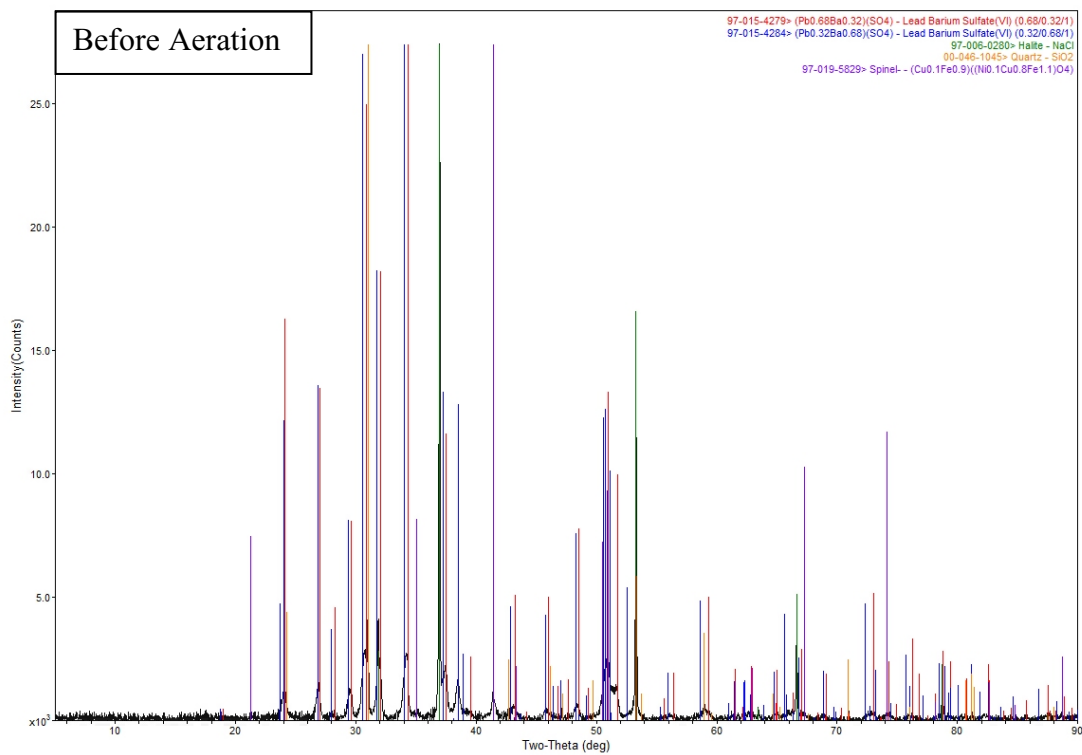


Figure 29. XRD of the samples before and after aeration treatment.

Figure 30 shows the surface of the 0.2 PES membrane before and after the aeration treatment. The image of the membrane before aeration revealed a damaged surface, where the pores are somewhat deformed due to the fouling layer deposited on it. The cake deposited on the membrane surface from the non-aerated sample appears more compacted than do particles deposited on the membrane from FPW samples that underwent aeration pre-treatment. The surface of the membrane after aeration shows the pores considerably less disturbed, where the morphology of the pores is still clearly visible with open-circular shape. The crystalline material shown on the membrane after aeration is predominantly sodium chloride.

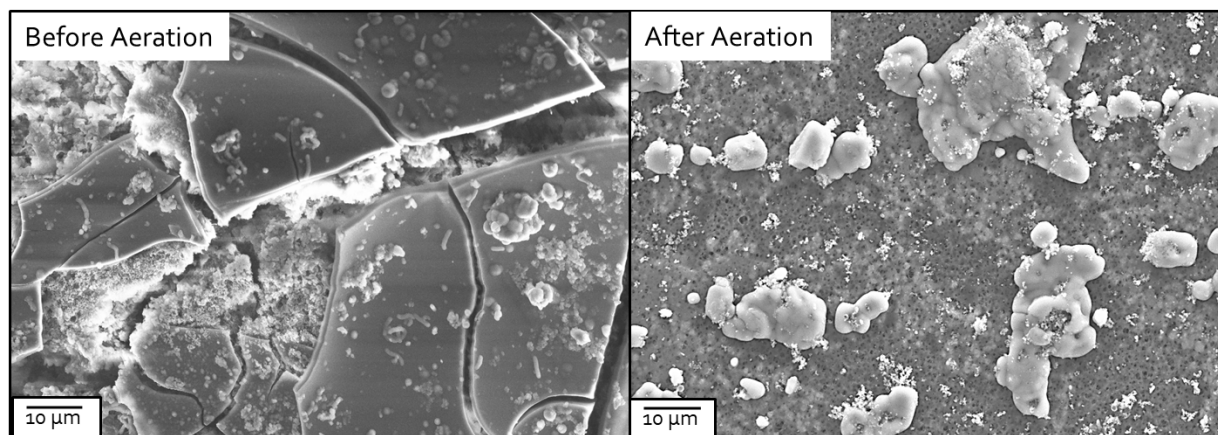


Figure 30. Surface of the 0.2 PES membrane before and after the aeration treatment.

Cross-sections of the four polymeric membranes were also analyzed by FESEM-EDS, and here data are presented for the 0.2 PVDF and 0.2 PES membranes. Figure 31 shows cross sections of the clean (unused) and fouled membranes before and after the aeration treatment. The image of the cross-section of the unused 0.2 PES membrane was not possible to obtain, as this membrane was more flexible and challenging to break compared as compared to the 0.2 PVDF membrane, which was more brittle. The 0.2 PES membranes used in the filtration experiments before and after the aeration treatment, on the other hand, were possible to break using the technique described in the Methods section, although some deformation may have occurred during the breaking process. In order to break the membranes, all of them were soaked in liquid nitrogen for about 5 min before splitting in half, but because the 0.2 PES membranes were more ductile, they were left for a longer period (10 to 15 min).

The SEM images corroborated the results obtained from the fouling mechanisms, wherein larger particles were retained on the membrane surface while colloidal material likely passes through the membrane pores. A few particles were observed in the cross-section of the 0.2 PVDF membrane (Fig 24 B and C) which likely obstruct the pores and decrease the filtration flux. The used 0.2 PES membranes did not have a significant number of particles on the wall pores, which again corroborates the main fouling mechanisms, cake filtration and intermediate pore blocking, as shown from the fouling plots. The composition of the particles found in the 0.2 PVDF and 0.2 PES membranes was analyzed by EDS and showed similar results to the particles retained on the membrane surface. Iron, oxygen, silica, sodium, and chloride were the most predominant elements. It has been noted by Gryta (2007) that the structure of iron oxides compounds is mainly porous, which therefore may not affect the permeability of the membranes considerably. This idea supports the hypothesis of this study that the organic constituents may be more important in impacting

membrane permeability and fouling, and ultimately in reducing the permeate flux during microfiltration and ultrafiltration operations.

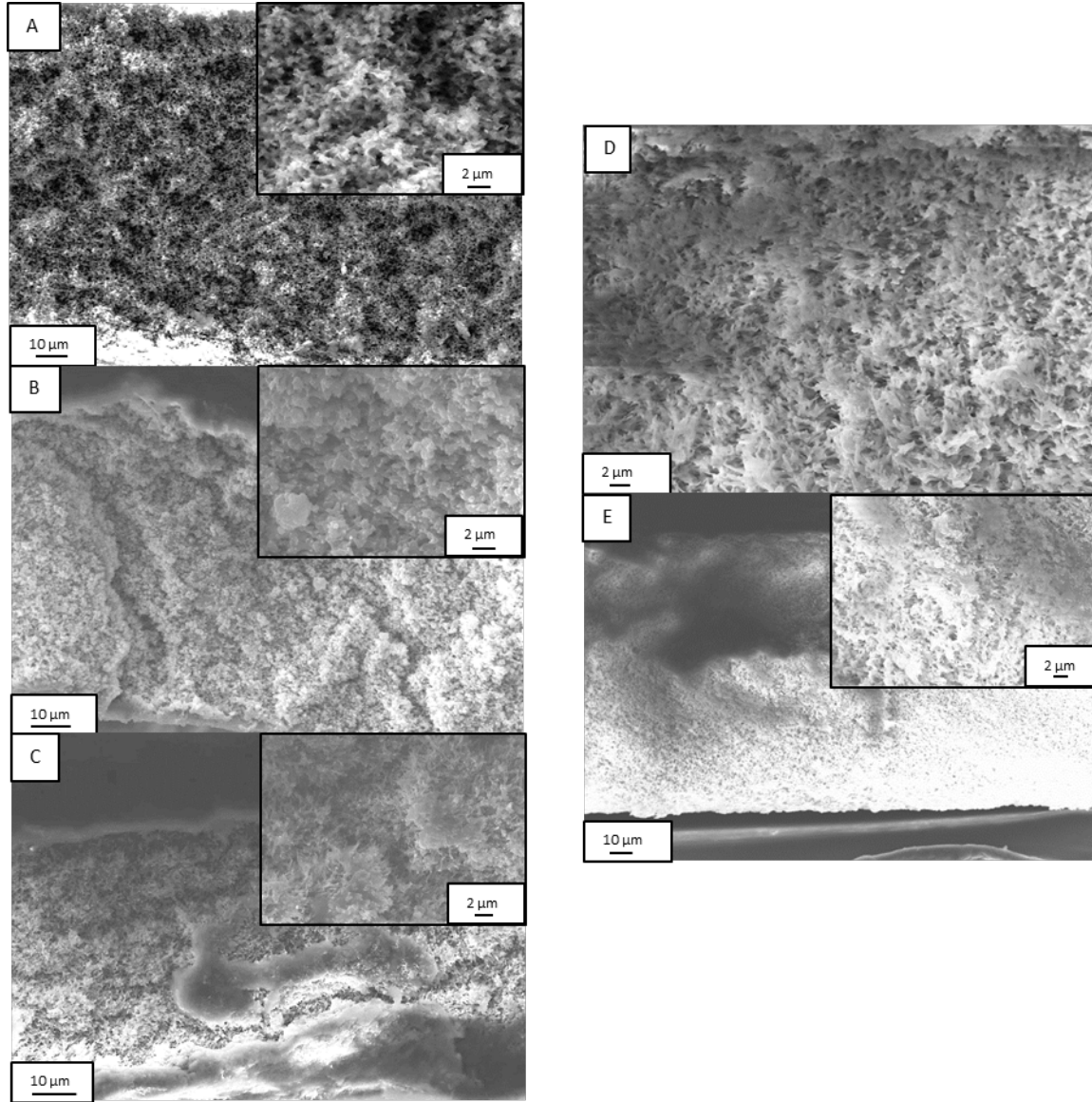


Figure 31. Cross section of the 0.2 PVDF (left side) and 0.2 PES (right side) membranes. A. cross-section of the unused 0.2 PVDF membrane. B. Cross-section of the 0.2 PVDF membrane after filtration of raw FPW. C. Cross-section of the 0.2 PVDF membrane after filtration of the oxidized FPW. D. Cross-section of the 0.2 PES membrane after filtration of raw FPW. D. Cross-section of the 0.2 PES membrane after filtration of the oxidized FPW.

3.3 Environmental Implications of FPW treatment

3.3.1 Total Digestion and Sequential Extraction from Solids Before and After Aeration Treatment

Total digestion of solids with hydrofluoric acid (HF) for metals quantification and alkaline fusion for Si (Figure 32) showed only small differences in the metal content between the non-aerated and the aerated precipitates. The most significant change observed for the aerated sample compared to the non-aerated sample was the higher iron concentration, which increased by more than two times from 112 mg/g to 255.32 mg/g, consistent with the SEM-EDS results. The content of elements such as B and Cr also increased after aeration from 871.44 ug/g and 51.90 ug/g to 1188.07 ug/g and 1003.94 ug/g, respectively. The high concentration of Cr observed in the aerated sample, however, could be attributed to contamination from the experimental setup during the aeration process. On the other hand, other major elements such as Si, S, K, Sr, and Ba did not have a proportionate increase to iron in the aerated sample, which might be explained as a result of a dilution effect caused by iron precipitation.

Sequential extraction performed on the solids obtained before and after aeration revealed similar patterns in the metal content and distribution for the 6-step method employed in the study (Figure 32; details in Tables B.2 and B.3, Appendix B). The exchangeable (acid soluble) fraction contains mainly mono- and divalent elements such as Li, K, and Ca, containing more than 80% of the total amount. This indicates that those major elements might be easy to mobilize in the case of FPW spills, although it is not expected that these elements represent a threat to the environment. Sr and B were also partially found in the exchangeable fraction (~40%) being relatively easy to mobilize. Sr in the exchangeable fraction after aeration was more soluble, corresponding to almost

60% of the total. Similar results were observed for Mn, for which 17% was in the exchangeable fraction before aeration, while after aeration it increased to 40%. B, Zn, and Cu are the most dominant elements found in the carbonate fraction with percentages of 43%, 55%, and 27%, respectively, possibly sorbed on CaCO₃ surfaces (Mesquita et al., 2000), especially for the non-aerated sample. The aerated sample had lower values for B and Zn of 27% and 33%, respectively, while Cu remained at a similar abundance (30%). The percentage of iron found in the carbonate fraction was about 25% before aeration while after aeration it decreased to less than 10%.

The reducible fraction (amorphous Mn and Fe oxides) is directly related to the release of metals including Fe, Cu, Zn, Mo, and Pb, primarily after aeration. For instance, before aeration around 62% of iron was found in the reducible fraction while after aeration it increased to 88%. This is important, as a high abundance of iron in the sample could possibly serve as a pathway of organic or inorganic removal by adsorption on precipitated iron oxides. This may explain the higher content of Mo, Zn, Cu, and Pb found in the Fe/Mn oxides fraction (>15%). Similarly, B and P also increase in percentage after aeration in this fraction with percentages of 36% and 13%, respectively. The non-aerated sample had lower fractions of B (14%) and P (18%). Some studies have shown that B might be better adsorbed on amorphous iron oxides at low pH (<8) (Goldberg and Glaubig, 1985), which might explain the increase of B with the aeration as more iron oxides precipitated.

The oxidizable fraction did not play a major role in the release of metals, perhaps because organics did not contain a large fraction of the metals. Nevertheless, more than 20% of the P, S, Cu, and Mo were contained in this fraction, both before and after aeration. The content of P decreased almost by half from 64% to 32% after aeration. Contrarily, Ba increased after aeration from 17% to more than 20%. The next fraction (crystalline Fe) is considered more stable. It shows

similar results to the previous oxidizable fraction, with little release of metals. This result is perhaps not surprising, considering the low amounts of crystalline substances in the samples, as shown by the XRD results. The release of Mn (42%, 22%) and S (25%, 13%) before and after aeration might be due to their association with the amorphous iron oxides which were not completely attacked during the reducible fraction, or due to the presence of small quantities of crystalline iron oxides which were detected in the non-aerated sample through the XRD patterns. As suggested by a number of authors, using only one step for iron removal might be insufficient when there is a high content of this element in the sample, and may instead require more than one treatment to complete its extraction (Gleyzes et al., 2002).

The residual fraction to extract elements from the crystalline lattice of alumino-silicates and recalcitrant compounds is usually performed using strong acids (HF-HNO₃-HCl) (Gleyzes et al., 2002). No significant differences were found between the aerated and non-aerated samples. As expected, large amounts of Si and Al were found, with more than 74% of the total element concentrations for both samples. The major difference observed in this fraction is a decrease in the content of elements such as Sr, Ba, and Pb from 35%, 45%, and 33%, respectively, in the non-aerated sample to less than 10% for all elements in the aerated sample.

As most of the metals are present in the last four fractions, they are considered not very mobile or available because they are associated with stable organic or inorganic substances. Both samples, however, might release more easily macronutrients and micronutrients such as K, Ca, Mn, Ba, Li, and Sr. Thus, the release of contaminants may require considerable changes in the environmental conditions.

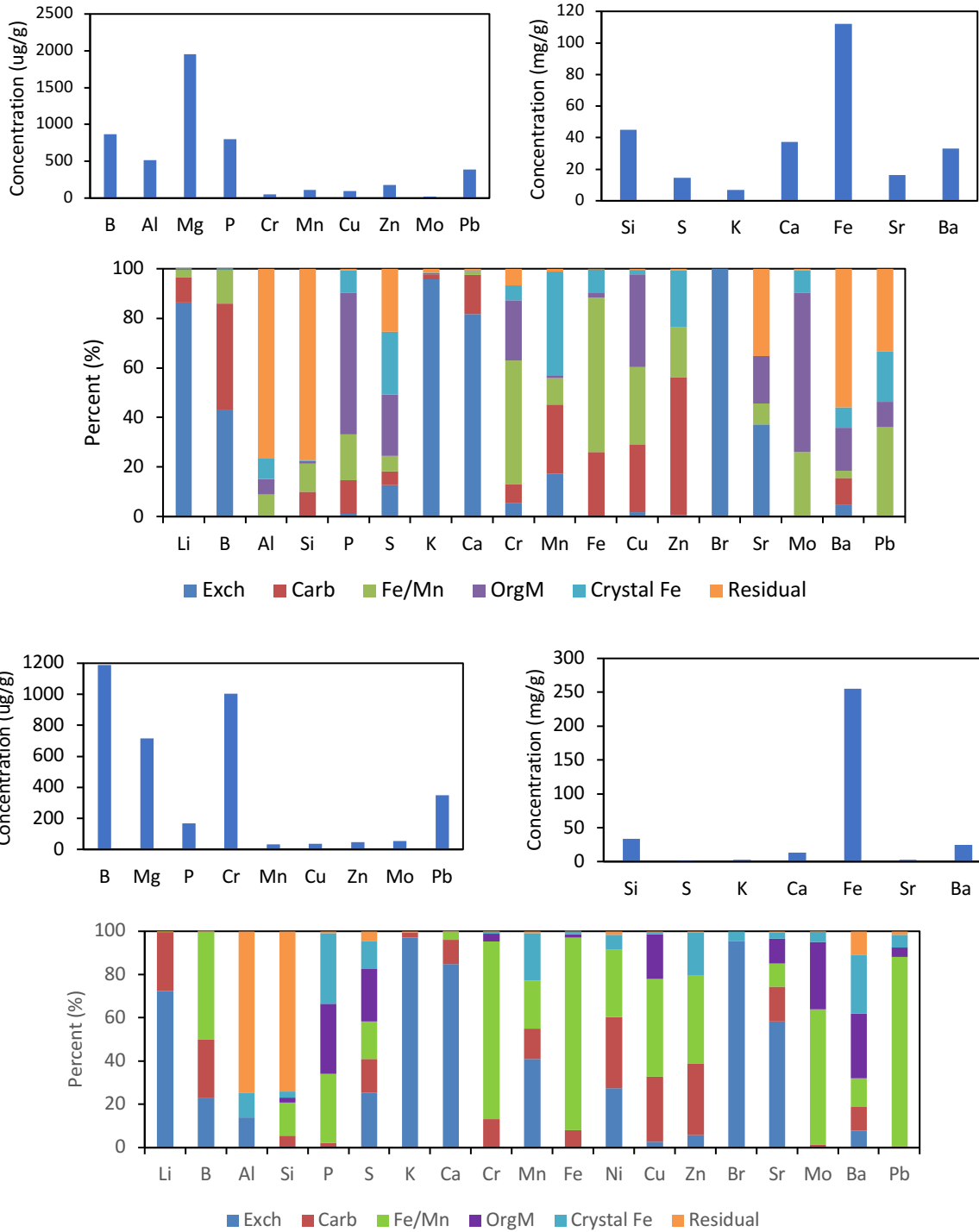


Figure 32. Sequential extraction results of solids before and after the aeration treatment. Total digestion for each sample is presented above the graph.

3.3.2 Polycyclic Aromatic Hydrocarbons (PAHs) analysis

Organic compounds present in FPW samples are a complex mixture of hydrophobic and hydrophilic substances of low and high molecular weights (Xiong et al., 2018), where some of them can present a threat to natural ecosystems. PAHs, for instance, are of concern due to their potential toxicity to aquatic species (Long et al., 1995). In this study, PAHs were quantified for both the aqueous (W) and the sediment (S) fractions in the raw FPW as well as in the permeates collected from the filtration through the 0.2 PES membranes before and after the aeration treatment. The total concentrations of 13 of the 16 USEPA priority PAHs and 4 alkyl PAHs species detected from each FPW sample (raw, NAP, AP) are reported in Figure 33 and Table 9. The units in ng/L are used for representing the concentrations in both the water and sediment fractions to facilitate their comparison and to sum them up (W+S) as the total organics from each FPW sample (raw, NAP, AP). The sediment fraction thus corresponds to the concentration of PAHs sorbed to the precipitates if they were resuspended to the original solution volume.

Significant differences were found in the concentration of parent and alkyl PAHs species in the raw FPW compared to the NAP and AP samples for both the aqueous and sediment fractions. The overall total concentration of PAHs (13 USEPA and 4-alkyl PAHs) in the raw FPW (W+S) was approximately 40 times higher (958.64 ng/L) than in the NAP (24.23 ng/L) and AP (20.04 ng/L) samples. It is worth nothing that although the total PAHs concentrations (13 USEPA and 4-alkyl PAHS) were approximately the same in the NAP and AP solutions, their distribution in the aqueous and sediment fraction was considerably different. In fact, the PAHs in the aqueous fraction of the AP was about 18 times lower (0.55 ng/L) as compared to the aqueous fraction in the NAP (9.72 ng/L). In general, the 13- and 4 alkyl-PAHs were more abundant in the sediment fraction, with values ranging from 60% to 98%, than in the aqueous fraction, ranging from 2% to

40%, for all the samples analyzed. These results are contrary to the results found by He et al. (2018), where the 13-PAHs were mainly in the aqueous phase. He et al. (2017b) reported about 50% of total PAHs being adsorbed to suspended solids from another Duvernay FPW sample. However, their sample had a higher PAHs concentration than this study, evidencing the variability of organic and inorganic content in FPW. This variability could be attributed to compositional variations among wells, or it might be the consequence of the analysis time of their sample compared to the sample used in this study, i.e., the fluid used in this study could have been exposed to the atmosphere for longer periods, allowing for the formation of amorphous ferric (oxy)hydroxide precipitates, which consequently sorb more PAHs.

Some differences were found in the predominance of PAHs species, especially between the raw FPW compared to the two treated water samples. The most abundant parent PAHs in the raw FPW sample were benzo[b]fluoranthene and fluorene with total concentrations (W+S) of 120 ng/L and 106 ng/L, respectively. The two dominant 4-alkyl species in the raw FPW were methyl/dimethyl phenanthrene. The most abundant parent PAHs in the NAP and AP sample were fluorene and phenanthrene. In these two samples, the concentration for benzo[b]fluoranthene was not detected, indicating that most of this compound was removed effectively by the MF membrane. The most abundant 4-alkyl species for the two treated samples corresponded to 1-methylfluorene with a higher total concentration (W+S) in the AP sample as compared to the NAP; however, 1-methylfluorene was below the detection limit in the aqueous fraction of the AP, while there remained a detectible concentration in the NAP sample (2.3 ng/L).

The overall removal of total PAHs (W+S) was similar for the two filtration experiments (NAP and AP). Removal of total PAHs (W+S) with 0.2 PES membrane in the NAP and AP samples accounted for about 97% and 98%, respectively. Most of the individual PAHs species

were reduced by more than 90% in both samples. These results revealed that MF processes could be effectively used for removing potentially toxic PAHs from FPW generated in hydraulic fracturing operations.

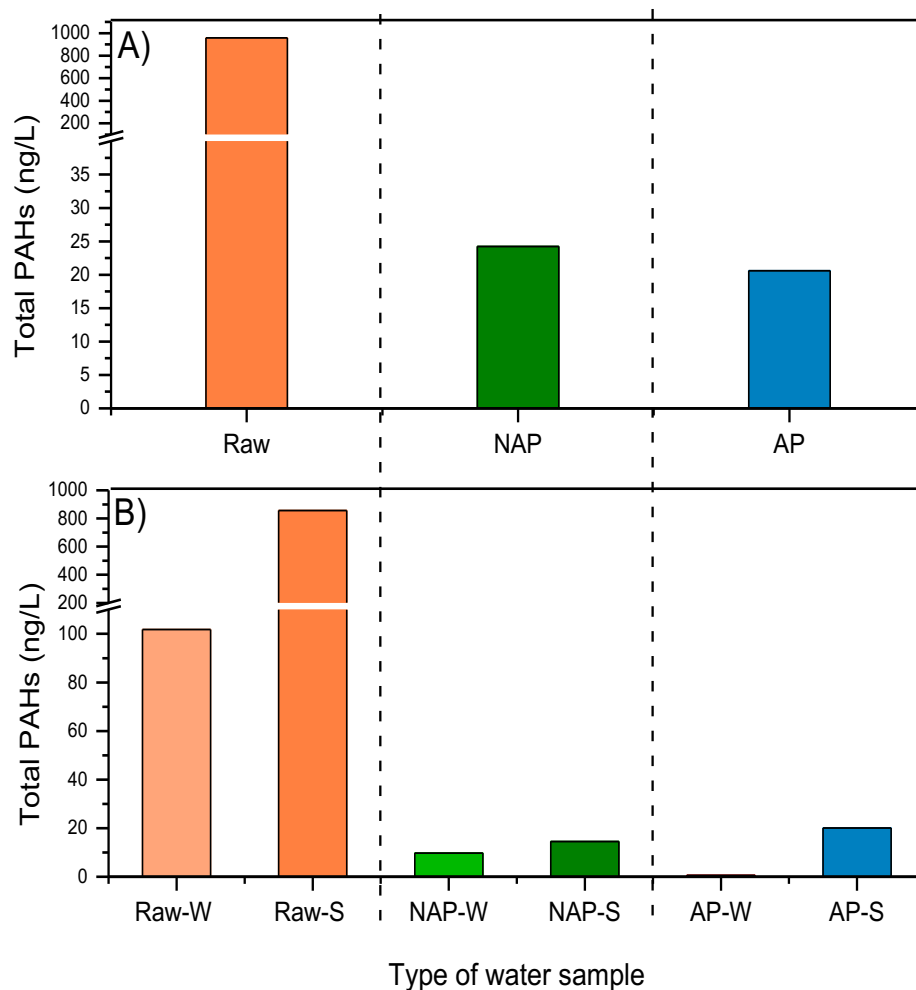


Figure 33. Total PAHs concentration. A) shows the total PAHs concentration from the untreated (Raw) FPW, the treated FPW by only-membrane filtration (Non-Aerated Permeate, NAP), and the FPW with the combined aeration-filtration treatment (Aerated Permeate, AP). B) shows the distribution of the total PAHs in the aqueous (W) and suspended sediment (S) fractions of the total in each FPW sample, respectively.

Table 9. Concentration of 13 USEPA priority parent PAHs, and 4 alkylated PAHs present in the FPW samples. Concentration in the aqueous (W) and the sediment (S) fractions, respectively. ND = Not Detected; MDL = Method Detection Limit.

Parent PAHs (ng/L)	Water MDL	Sediment MDL	Raw-W	Raw-S	Raw-W+S	NAP-W	NAP-S	NAP-W+S	AP-W	AP-S	AP-W+S
Fluorene	2.6	2.3	12	94	106	2.8	3.1	5.9	<MDL	3.8	3.8
Phenanthrene	4.8	2.9	40	44	84	<MDL	5	5	<MDL	4.5	4.5
Anthracene	0.58	0.19	ND	0.84	0.84	<MDL	ND	0	ND	<MDL	0
Fluoranthene	1.2	0.78	9.8	17	26.8	1.4	0.48	1.88	<MDL	0.54	0.54
Pyrene	1.5	3.7	12	53	65	1.9	<MDL	1.9	<MDL	<MDL	0
Benz[a]anthracene	0.052	0.13	3.8	24	27.8	0.33	0.43	0.76	0.31	0.19	0.5
Chrysene	0.072	0.23	3	60	63	ND	0.44	0.44	ND	ND	0
Benzo[b]fluoranthene	1.5	1	ND	120	120	ND	ND	0	ND	ND	0
Benzo[k+j]fluoranthene	0.17	0.41	ND	46	46	ND	ND	0	ND	ND	0
Benzo[a]pyrene	0.17	0.43	ND	ND	0	ND	ND	0	ND	ND	0
Indeno[1,2,3-cd]pyrene	0.06	0.18	ND	ND	0	ND	ND	0	ND	ND	0
Benzo[g,h,i]perylene	0.061	1	ND	29	29	ND	ND	0	ND	ND	0
Dibenz[a,h]anthracene	0.094	0.24	ND	ND	0	ND	ND	0	ND	ND	0
Total USEPA 13 PAHs			80.60	487.84	568.44	6.43	9.45	15.88	0.31	9.03	9.34
Total USEPA 13 PAHs%			14%	86%	100%	40%	60%	100%	3%	97%	100%
Alkyl PAHs (ng/L)											
1-Methylfluorene	0.78	0.78	9.6	80	89.6	2.3	3.7	6	<MDL	9.8	9.8
1-Methylphenanthrene	0.11	0.37	6.1	100	106.1	0.99	1	1.99	0.24	1	1.24
3,6-Dimethylphenanthrene	0.07	0.17	5.5	170	175.5	ND	0.36	0.36	ND	0.21	0.21
1-Methylpyrene	0.05	0.12	ND	19	19	ND	ND	0	ND	ND	0
Total 4 alkylated PAHs			21.20	369.00	390.2	3.29	5.06	8.35	0.24	11.01	11.25
Total 4 alkylated PAHs%			5%	95%	100%	38%	62%	100%	2%	98%	100%
Total PAHs			101.80	856.84	958.64	9.72	14.51	24.23	0.55	20.04	20.59

3.3.3 Toxicological Analysis on Zebrafish Embryos (*Danio rerio*)

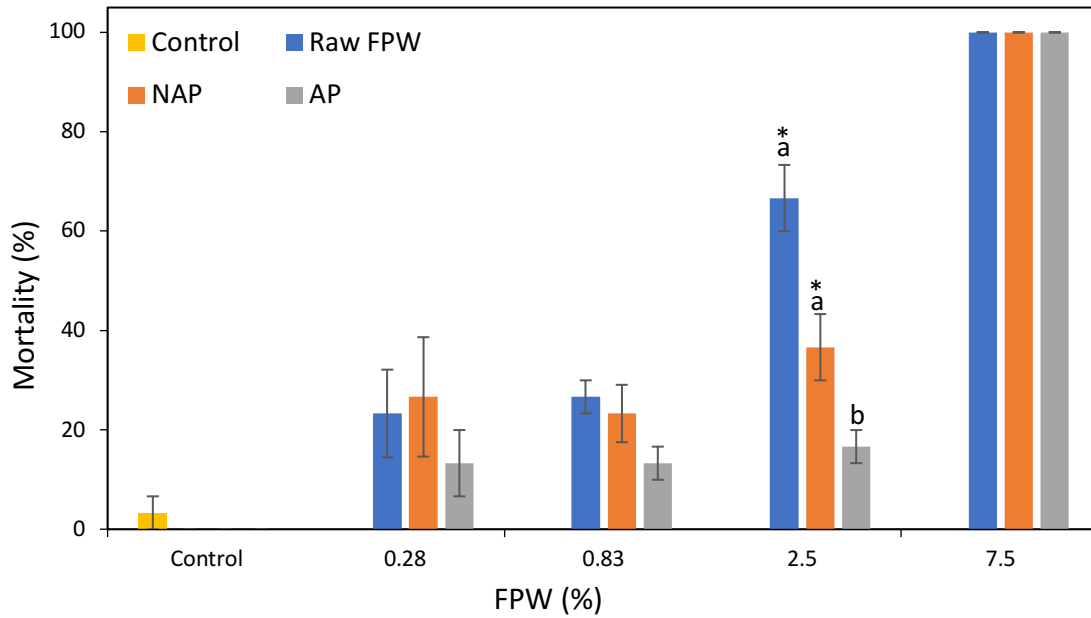
To investigate the effects of the water treatments, i.e., microfiltration and aeration combined with microfiltration using the 0.2 PES membranes, a toxicity test was conducted using zebrafish embryos species were. To do so, embryos were exposed to the permeates obtained from the two filtration treatments (before and after aeration) and compared to the raw FPW exposure as well as a control water at different water ratios, for a total time of 96 h. Figure 34 shows adverse effects (mortality and pericardial edema) observed in the zebrafish embryos caused by each water sample and their respective dilution groups.

The raw FPW sample exhibited higher mortality rates in three dilution groups, i.e., 0.28%, 0.83%, and 2.5% corresponding to the percentages of 23%, 27%, and 67%, respectively (Figure 34A). The aerated permeate, on the other hand, showed much lower mortality with only 13%, 13%, and 16% for the 0.28%, 0.83%, and 2.5% dilutions, respectively. The non-aerated permeate also showed reduced mortality at the 0.83% and 2.5% dilutions (20% and 36% and, respectively) as compared to the raw FPW, but higher than the combined aeration-MF treatment. The statistical analysis by one-way ANOVA showed that the mortality parameter was significantly different ($p < 0.05$) for the aerated permeate sample as compared to the raw FPW and the non-aerated permeate. No significant differences were found between the non-aerated permeate and the raw FPW. The most concentrated dilution group (7.5%) for all three FPW sample preparations exhibited a 100% mortality of the embryos after 24 h exposure. The primary factor of the high mortality in the 7.5% dilution group could be attributed to the high salinity, as suggested by He et al. (2017b) when assessing the effects of a sample treated by activated charcoal, where the results showed that the elevated content of salts was the main cause of the zebrafish embryos' toxicity.

The reduction of embryos with pericardial edema (PE), was clearly observed in the exposure group of the AP sample for the three lower dilutions (0.28%, 0.83%, and 2.5%) with values ranging from 3 to 6% of the embryos affected, as compared to the higher percentages in the raw FPW (6-20%) and Non-aerated Permeate solutions (6-33%) (Figure 34B). The lower fraction of embryos affected with PE observed in the raw FPW as compared to the non-aerated permeate for the 2.5% dilution group might be the result of the higher mortality in the raw FPW at the initial stage of the experiment. Significant differences were found between the NAP and the AP samples. Spinal malformations effects were also observed in the raw FPW and the non-aerated permeate sample, but no significant differences were found among the groups (Figure B.1, Appendix B).

The LC_{50} results are presented in Figure 35 and Table 10. LC_{50} values did not differ significantly between the raw FPW and the non-aerated FPW samples. The aerated permeate showed the highest LC_{50} value (3.61 ± 0.41) compared to the other two samples (raw FPW and NAP), indicating lower acute lethal toxic effects. The lowest LC_{50} value (1.85 ± 0.25) corresponded to the raw FPW where a higher number of embryos were adversely affected by the untreated water. During the exposure experiments, it was observed that some orange-colored particles, consistent with iron oxides, began to precipitate in the raw FPW and to a lesser extent in the NAP sample after 24 h. These precipitates were then strongly attached to the embryo's chorion, having the potential to directly affect their normal growth because the iron oxides particles and substances adsorbed to them may interact directly with the embryos. These results again support the hypothesis noted by He et al. (2017b), where raw FPW samples were more lethal to embryos than were sediment-free treated FPW samples. Our results also suggest that the aeration treatment and subsequent microfiltration could be used efficiently to diminish potential risks to aquatic organisms that might be associated to FPW produced in the hydraulic fracturing industry.

A)



B)

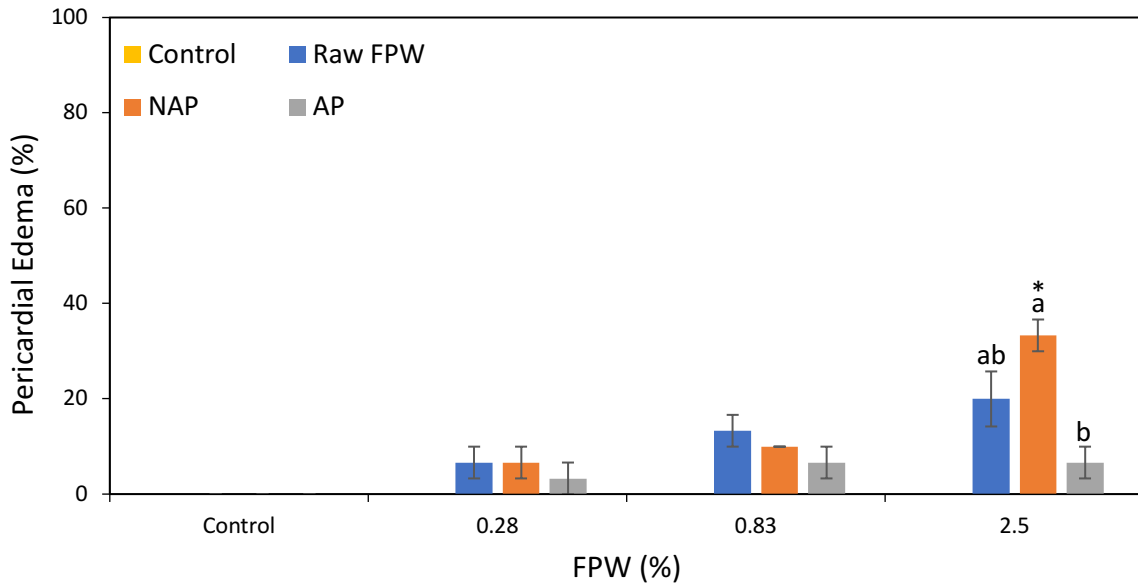


Figure 34. Effects in zebrafish embryo of the filtration and filtration-aeration treatments compared to the raw FPW sample after 96 h of exposure. A control water was also compared.

NAP: non-aerated permeate, AP: aerated permeate A) Mortality of exposed embryos. B) Pericardial Edema results. Significant differences ($p < 0.05$) among each dilution are shown by different letters using one-way ANOVA. Significant differences between the control and dilutions is represented by (*).

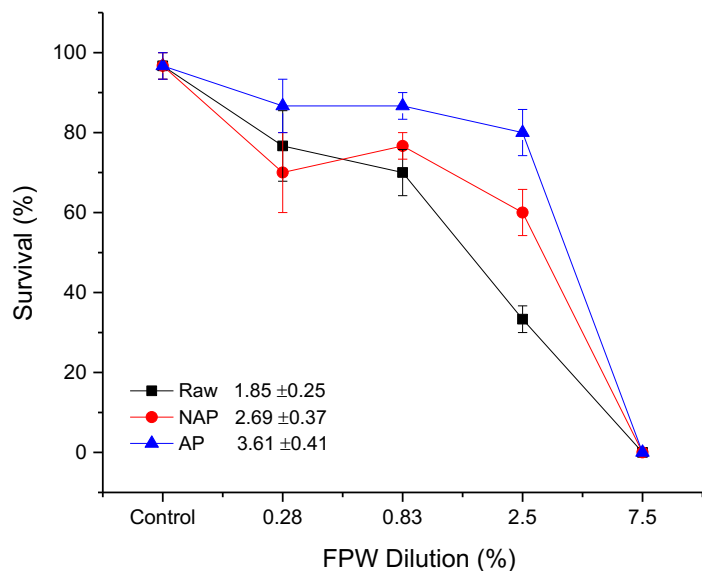


Figure 35. LC₅₀ curves for the exposed zebrafish embryos to the three different FPW solutions.

Table 10. LC₅₀ data and analysis through the Litchfield-Wilcoxon method where significant differences are shown by different letters.

No. of Death Embryos (10 embryos per well, in triplicates)			
Dilution %	Raw FPW	Non-aerated Permeate	Aerated Permeate
Control	1	1	1
0.28	7	9	4
0.83	9	7	4
2.5	20	12	6
7.5	30	30	30
Statistical analysis - LC₅₀			
Upper 95%	2.3537	3.4503	4.4626
LC ₅₀	1.8537	2.697	3.6076
Lower 95%	1.3527	1.94	2.7526
f	1.3201	1.3334	1.2738
(logf) ²	0.0145	0.0156	0.0110
Sig.	a	a	b

3.3.4 Microbial Communities Present in FPW Solids

The microbiology of the two solid samples recovered through MF with the 0.2 PES membrane before and after the aeration treatment was analyzed to identify any distinct communities. Some differences with respect to class and family composition between the aerated and non-aerated samples are presented in Figure 36, and microbial diversity and richness are shown in Table 11. See table B.4 (Appendix B) for a list of the complete taxa found in the precipitates. Bacteria dominated in both samples, although Archaea are observed in the non-aerated sample. The two samples were characterized by a high abundance of the bacterial class *Clostridia* and at the genus level, related to *Halanaerobium*, with an abundance of 43% and 49% in the aerated and the non-aerated samples, respectively. Significant differences found in the non-aerated sample corresponded to the more abundant genus of *Flexistipes* (family *Deferribacteraceae*), which is strictly an anaerobic heterotroph found in brines with at least 3% NaCl (Fiala et al., 1990). The non-aerated sample was also richer in sequences related to the Archaea class *Methanomicrobia*, related to *Methanohalophilus* at the genus level (Paterek and Smith, 1988). This genus corresponds to moderately halophilic and anaerobic methanogens (0.5-2 M NaCl). On the other hand, the aerated sample showed a higher abundance of the genus *Fuchsiella* (family *Halobacteroidaceae*) which are haloalkaliphilic and anaerobic (optimal pH >8.5) that can grow chemolithoautotrophically and chemoorganotrophically (Zhilina et al., 2012; Zhilina et al., 2015). The genus *Modicisalibacter* (family *Halomonadaceae*) was also rich in the aerated sample. *Modicisalibacter* is an aerobic, halophilic bacterium that was previously found in oilfield-water (Gam et al., 2007). Some of the microorganisms present in the samples have been reported to potentially degrade hydrocarbons compounds under extreme saline environments like that of oilfield brines, which include the genera *Pseudomonas* and *Ralstonia* (Mnif et al., 2011).

Modicisalibacter was also shown to degrade phenols (Bonfa et al., 2013). In general, the aeration treatment slightly favored the production of more aerobic species as compared to the non-aerated sample.

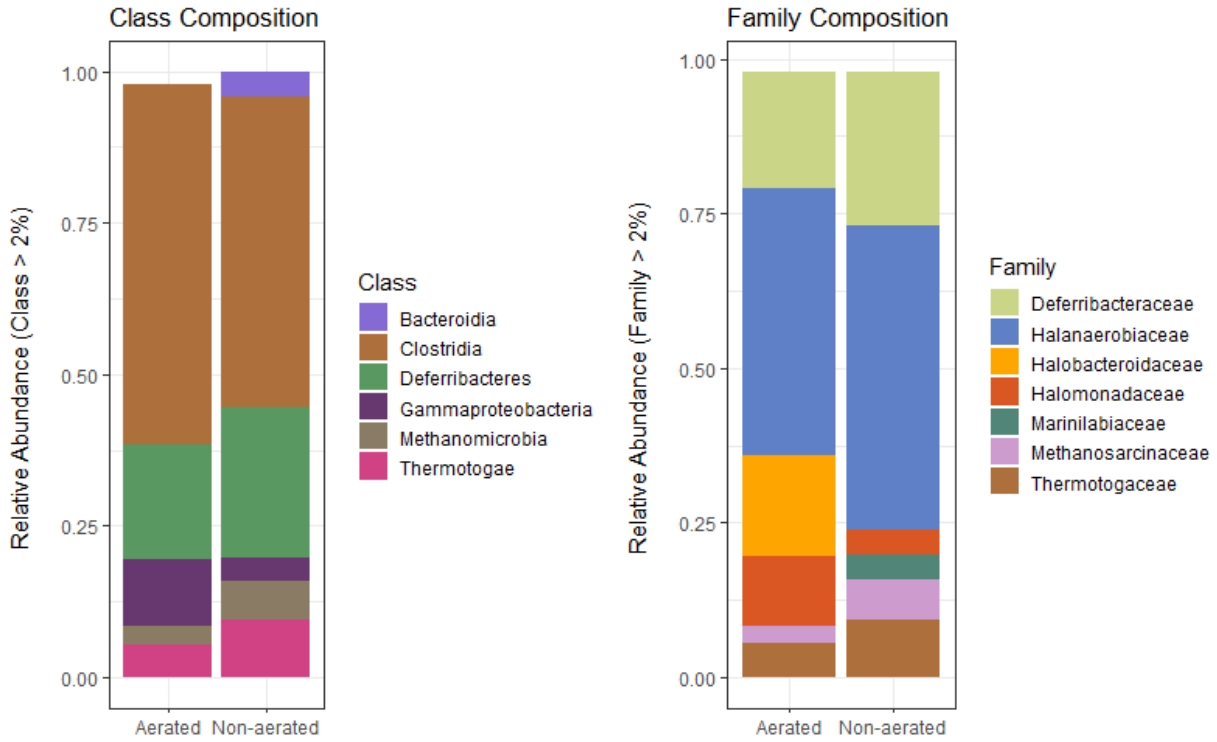


Figure 36. Microbial communities of the treated and untreated sediments collected after microfiltration with the 0.2 PES membrane.

Table 11. Richness and diversity of the microbial community for the two FPW solids (before and after aeration).

Sample	Number of OTUs	Chao1	Shannon	Inv. Simpson
Aerated	28	31.33	2.15	6.99
Non-aerated	24	24.60	2.08	6.21

4. Conclusions

Membrane technologies continue to gain increasing relevance in the oil and gas industry as an effective alternative to treat flowback and produced water for reuse and recycling in subsequent hydraulic fracturing operations. However, the severe fouling tendency and low permeate flux recovery during the microfiltration and ultrafiltration of raw FPW with polymeric membranes, observed in this study and from previous research (He et al., 2014; Xiong et al., 2016; Jiang et al., 2013). These issues, in turn, have been an obstacle for the direct use of membranes in FPW treatment. Therefore, to control or diminish the fouling phenomenon and increase the fluid flux, some type of water pre-treatment is needed before filtration. In this study, aeration was applied to an FPW sample recovered from the Duvernay Formation to enhance the microfiltration and ultrafiltration operations. It was found that the raw (untreated) FPW caused a considerable reduction of flux decline, ranging from more than 40% to more 90%, in the first 10 to 15 min when employing MF or UF alone. Low rejection values (below 10%) were observed for iron and silica, and the majority of the TOC rejection (6.1 - 7.8%) was attributed to adsorption on the gel layer formed during the filtration experiments with the untreated FPW for all four polymeric membranes. Contrarily, the aeration pre-treatment improved the MF and UF operations, with the permeate flux decreasing by less than 20% as compared to the initial flux for the three MF and one UF membranes tested. As a consequence, the filtration time improved over 50% for all the membranes, reflecting a more efficient process when aeration was used as a pre-treatment. The rejection results also showed that removal of particulate matter comprised of mainly iron and silica increased considerably to more than 70%. During the aeration experiments, it was found that the TOC concentration decreased from 400 mg/L to 314 mg/L in the first 30 min, which is likely the result of volatilization and possibly of some adsorption onto the surfaces of iron oxides.

The main fouling mechanisms identified for the non-aerated and the aerated FPW samples were cake filtration and intermediate pore blocking. It is worth noting that for the aerated sample, the four mechanisms modeled all had reasonable fits as confirmed by the R^2 correlation values, especially for the 0.2 PES membrane (~ 0.95), possibly due to the rapid permeation flux in a relatively short period of time (< 5 min). The SEM images and corresponding photographs evidenced a better-preserved membrane surface after the aeration treatment, showing that the particles are more loosely attached on the membranes if aeration is applied, as compared to the raw FPW where the solids formed a tightly-held layer on the membrane surface. These differences might be attributed specifically to changes in the organic constituents during and after the aeration, where it is hypothesized that some of the bonds were broken down and that a fraction of the organics was adsorbed onto the iron oxides. An additional possibility is that the ratio of organics to iron oxides decreased considerably in the aerated sample, resulting in less interaction of organics with the membranes. Finally, comparison among the four polymeric membranes used in these experiments with both untreated and treated FPW demonstrated that the 0.2 μm PES membrane had a higher performance than the other three membranes, with lower energy consumption, i.e., lower TMP.

The analysis of the PAHs showed that the raw FPW sample had higher concentrations of total species, for both the aqueous (101.8 ng/L) and the sediment fractions (856.8 ng/L), than did the non-aerated sample (9.7 ng/L, 14.5 ng/L), and a far lower concentration in the aerated-filtered samples only for the aqueous fraction (0.14 ng/L). After the aeration treatment, the fractionation of PAHs was mainly associated to the sediment fraction (27.8 ng/L). The determination of PAHs also confirmed that MF could efficiently remove a high percentage ($> 80\%$) of the parent and alkyl PAHs species, presumably by removing the suspended solids (composed mainly of iron oxides

and silica) from the FPW solution, for both the untreated and treated samples. The toxicological studies showed that mortality and other adverse effects on zebrafish embryo were substantially reduced with the combined aeration and MF treatments, which principally removed the suspended solids. These results confirmed that the combined treatment (aeration-MF) might be applied to reduce some potentially toxic pollutants and enhance the flowback and produced water quality for reuse in fracturing technologies in an economically viable way.

5. Future Work

Based on the experimental results obtained for the non-aerated and aerated FPW samples additional future studies could be pursued to enrich this research and help better understand some of the causes of membrane fouling. Special attention should be given to the degradation, volatilization, or other changes that might have occurred to the organic substances in the FPW during the aeration process, which clearly influenced their interaction with the membrane surface. Some important aspects are listed here:

1. Additional organic characterization, such as Thermo Gravimetric Analyses (TAG), size exclusion chromatography (SEC), fluorescence excitation-emission matrix (EEM), and other evaporation methods to identify and corroborate degradation of some organic polymers used in the fracturing fluids mixture such as polyacrylamide. As Xiong et al. (2018) suggested, degradation of polyacrylamide reduced significantly the fouling of MF membranes. This degradation was significantly affected by ferrous iron and the presence of dissolved oxygen.
2. Studying the possibility of biodegradation of some organic compounds, perhaps promoted through the aeration treatment, and searching for more effective methods to remove organics from the permeate.
3. Future studies to correlate membrane types to fouling potential should use a wider variety of FPW, especially to conduct fouling analysis with the aerated solutions. Additionally, comparisons among different FPW samples from other gas plays (e.g., the Montney Formation) would help to evaluate the effectiveness of the combined aeration-microfiltration treatment developed here. This could aid in obtaining more insights about the interactions between the foulants and the membranes.

4. Analysis of the possible adsorption and desorption mechanisms of some metals (e.g., Zn, Ni, Cu) and organics on the iron oxides surface during and after the aeration which not only can affect the reuse of the fluid in new fracturing wells, but also are closely linked to the solution toxicity.
5. Evaluating and identifying the possibility that new compounds, such as degradation products from organics or halogenated compounds, are possibly being formed during the aeration process, which could represent a hazard to the environment.
6. Implementing a cross-flow filtration system to evaluate how creating some turbulence in the feed could decrease concentration polarization and even reduce membrane fouling by increasing permeate flux.
7. Testing various mechanical, thermal, or chemical cleaning methods to identify the most appropriate techniques to restore flux on the different polymeric MF and UF membranes tested here before and after the aeration. Such a study could also provide additional information to corroborate the efficiency of the aeration pre-treatment.
8. Testing different membrane processes in series, starting with MF membranes, to remove suspended solids and following this treatment with a membrane distillation system (MD) or forward osmosis (FO) system that uses the pre-treated (aeration) FPW as a feed. Such a study may obtain a higher-water quality that could be reused in other industrial activities (e.g., agriculture).

References

- Abualfaraj, N., Gurian, P.L. and Olson, M.S., 2014. Characterization of Marcellus shale flowback water. *Environmental Engineering Science*, 31(9), pp.514-524.
- AER (Alberta Energy Regulator), 2016. Annual report 16/17. <https://www.aer.ca/documents/reports/AER2016-17AnnualReport.pdf>
- AER (Alberta Energy Regulator), 2017. Water use performance. <http://www.aer.ca/protecting-what-matters/holding-industry-accountable/industry-performance/water-use-performance>.
- Alberta Oil and Gas Industry, 2017. Alberta oil & gas industry - Quarterly update. https://www.albertacanada.com/files/albertacanada/OilGas_QuarterlyUpdate_Summer2017.pdf.
- Alessi, D.S., Zolfaghari, A., Kletke, S., Gehman, J., Allen, D.M. and Goss, G.G., 2017. Comparative analysis of hydraulic fracturing wastewater practices in unconventional shale development: Water sourcing, treatment and disposal practices. *Canadian Water Resources Journal/Revue canadienne des ressources hydriques*, 42(2), pp.105-121.
- Alzahrani, S. and Mohammad, A.W., 2014. Challenges and trends in membrane technology implementation for produced water treatment: A review. *Journal of Water Process Engineering*, 4, pp.107-133.
- Annevelink, M.P.J.A., Meesters, J.A.J. and Hendriks, A.J., 2016. Environmental contamination due to shale gas development. *Science of the Total Environment*, 550, pp.431-438.
- Arthur, J.D., Bohm, B.K., Coughlin, B.J., Layne, M.A. and Cornue, D., 2009, January. Evaluating the environmental implications of hydraulic fracturing in shale gas reservoirs. In *SPE Americas E&P environmental and safety conference*. Society of Petroleum Engineers.
- Bai, B., Carlson, K., Prior, A. and Douglas, C., 2015. Sources of variability in flowback and produced water volumes from shale oil and gas wells. *Journal of Unconventional Oil and Gas Resources*, 12, pp.1-5.

- Bai, B., Goodwin, S. and Carlson, K., 2013. Modeling of frac flowback and produced water volume from Wattenberg oil and gas field. *Journal of Petroleum Science and Engineering*, 108, pp.383-392.
- Benko, K.L. and Drewes, J.E., 2008. Produced water in the Western United States: geographical distribution, occurrence, and composition. *Environmental Engineering Science*, 25(2), pp.239-246. U.S.
- Blauch, M.E., Myers, R.R., Moore, T., Lipinski, B.A. and Houston, N.A., 2009, January. Marcellus shale post-frac flowback waters-Where is all the salt coming from and what are the implications? In *SPE Eastern Regional Meeting*. Society of Petroleum Engineers.
- Blewett, T.A., Delompré, P.L., He, Y., Folkerts, E.J., Flynn, S.L., Alessi, D.S. and Goss, G.G., 2017. Sublethal and reproductive effects of acute and chronic exposure to flowback and produced water from hydraulic fracturing on the water flea *Daphnia magna*. *Environmental Science & Technology*, 51(5), pp.3032-3039.
- Bonfá M. R. L., Grossman M. J., Piubeli F., Mellado E., Durrant L. R. (2013). Phenol degradation by halophilic bacteria isolated from hypersaline environments. *Biodegradation* 24, 699–709.
- Boschee, P., 2014. Produced and flowback water recycling and reuse: economics, limitations, and technology. *Oil and Gas Facilities*, 3(01), pp.16-21.
- Bowen, W.R., Calvo, J.I. and Hernandez, A., 1995. Steps of membrane blocking in flux decline during protein microfiltration. *Journal of Membrane Science*, 101(1-2), pp.153-165.
- Bromley, D., 2015. Water Energy Food: Our Existence Will Require Natural Gas. In *Food, Energy, and Water* (pp. 161-182).
- Brower, E., 1973. Synthesis of barite, celestite and barium-strontium sulfate solid solution crystals. *Geochimica et Cosmochimica Acta*, 37(1), pp.155-158.
- Burke, S.P. and Banwart, S.A., 2002. A geochemical model for removal of iron (II)(aq) from mine water discharges. *Applied geochemistry*, 17(4), pp.431-443.
- Butkovskyi, A., Bruning, H., Kools, S.A., Rijnaarts, H.H. and Van Wezel, A.P., 2017. Organic pollutants in shale gas flowback and produced waters: identification, potential ecological

- impact, and implications for treatment strategies. *Environmental science & technology*, 51(9), pp.4740-4754.
- CAPP (Canadian Association of Petroleum Producers), 2018. Canada's Energy Resources. <https://www.capp.ca/canadian-oil-and-natural-gas/canadas-petroleum-resources>.
- Cassini, A.S., Tessaro, I.C. and Marczak, L.D.F., 2011. Ultrafiltration of wastewater from isolated soy protein production: Fouling tendencies and mechanisms. *Separation Science and Technology*, 46(7), pp.1077-1086.
- Cheremisinoff, N.P. and Davletshin, A., 2015. *Hydraulic fracturing operations: Handbook of environmental management practices*. John Wiley & Sons.
- Cheryan, M., 1998. *Ultrafiltration and microfiltration handbook*. CRC press.
- Chong, J. and Simikian, M., 2014. *Shale gas in Canada: Resource potential, current production and economic implications*. Library of Parliament= Bibliothèque du Parlement.
- Clark, C.E. and Veil, J.A., 2009. *Produced water volumes and management practices in the United States* (No. ANL/EVS/R-09-1). Argonne National Lab. (ANL), Argonne, IL (United States).
- Clark, C.E., Horner, R.M. and Harto, C.B., 2013. Life cycle water consumption for shale gas and conventional natural gas. *Environmental science & technology*, 47(20), pp.11829-11836.
- CCA (Council of Canadian Academies). Expert Panel on Harnessing Science and Technology to Understand the Environmental Impacts of Shale Gas Extraction, 2014. *Environmental impacts of shale gas extraction in Canada*. Council of Canadian Academies= Conseil des académies canadiennes.
- Cozzarelli, I.M., Skalak, K.J., Kent, D.B., Engle, M.A., Benthem, A., Mumford, A.C., Haase, K., Farag, A., Harper, D., Nagel, S.C. and Iwanowicz, L.R., 2017. Environmental signatures and effects of an oil and gas wastewater spill in the Williston Basin, North Dakota. *Science of The Total Environment*, 579, pp.1781-1793.

- Dang, H.T., Narbaitz, R.M., Matsuura, T. and Khulbe, K.C., 2006. A comparison of commercial and experimental ultrafiltration membranes via surface property analysis and fouling tests. *Water quality research journal of Canada*, 41(1), pp.84-93.
- Dong, X., Kleiner, M., Sharp, C.E., Thorson, E., Li, C., Liu, D. and Strous, M., 2017. Fast and simple analysis of MiSeq amplicon sequencing data with MetaAmp. *Frontiers in microbiology*, 8, p.1461.
- Drogos, D.L., 2016. Hydraulic fracturing: environmental issues. *Oxford University Press*.
- Ettensohn, F.R. and Barron, L.S., 1981. Tectono-climatic model for origin of Devonian-Mississippian black gas shales of east-central United States. *AAPG Bulletin*, 65(5), pp.923-923.
- Fajt, J.R., Burnett, D.B., Palmgren, T.H. and Danilov, A.G., 2013, March. Aeration and Microfiltration for Solids Removal of Produced Waters from the Barnett Shale. In *SPE Americas E&P Health, Safety, Security and Environmental Conference*. Society of Petroleum Engineers.
- Fakhru'l-Razi, A., Pendashteh, A., Abdullah, L.C., Biak, D.R.A., Madaeni, S.S. and Abidin, Z.Z., 2009. Review of technologies for oil and gas produced water treatment. *Journal of hazardous materials*, 170(2-3), pp.530-551.
- Ferrer, I. and Thurman, E.M., 2015. Chemical constituents and analytical approaches for hydraulic fracturing waters. *Trends in Environmental Analytical Chemistry*, 5, pp.18-25.
- Fiala, G., Woese, C.R., Langworthy, T.A., and Stetter, K.O. (1990) *Flexistipes sinusarabici*, a novel genus and species of eubacteria occurring in the Atlantis II Deep brines of the Red Sea. *Archives of Microbiology*, 154(2), pp.120-126.
- Folkerts, E.J., Blewett, T.A., He, Y. and Goss, G.G., 2017. Cardio-respirometry disruption in zebrafish (*Danio rerio*) embryos exposed to hydraulic fracturing flowback and produced water. *Environmental Pollution*, 231, pp.1477-1487.
- Gam, Z.B.A., Abdelkafi, S., Casalot, L., Tholozan, J.L., Oueslati, R., and Labat, M., 2007. *Modicisalibacter tunisiensis* gen. nov., sp. nov., an aerobic, moderately halophilic bacterium isolated from an oilfield-water injection sample, and emended description of the

- family Halomonadaceae Franzmann et al. 1989 emend Dobson and Franzmann 1996 emend. Ntougias et al. 2007. *International journal of systematic and evolutionary microbiology*, 57(10), pp.2307-2313.
- GBC Scientific Equipment. 2013. The determination of aluminum, iron and silicon in rock samples. http://www.gbcscientific.com/appnotes/AA_app_note_001.pdf
- Gleyzes, C., Tellier, S. and Astruc, M., 2002. Fractionation studies of trace elements in contaminated soils and sediments: a review of sequential extraction procedures. *TrAC Trends in Analytical Chemistry*, 21(6-7), pp.451-467.
- Goldberg, S. and Glaubig, R.A., 1985. Boron Adsorption on Aluminum and Iron Oxide Minerals 1. *Soil Science Society of America Journal*, 49(6), pp.1374-1379.
- Gooddy, D.C. and Hinsby, K., 2008. Organic quality of groundwaters. *Natural groundwater quality*, pp.59-70.
- Goss, G., Alessi, D., Allen, D., Gehman, J., Brisbois, J., Kletke, S., Zolfaghari, A., Notte, C., Thompson, Y., Hong, K. and Covalski, V., 2015. Unconventional wastewater management: a comparative review and analysis of hydraulic fracturing wastewater management practices across four North American basins.
- Gregory, K.B., Vidic, R.D. and Dzombak, D.A., 2011. Water management challenges associated with the production of shale gas by hydraulic fracturing. *Elements*, 7(3), pp.181-186.
- Gryta, M., 2007. Effect of iron oxides scaling on the MD process performance. *Desalination*, 216(1-3), pp.88-102.
- Haluszczak, L.O., Rose, A.W. and Kump, L.R., 2013. Geochemical evaluation of flowback brine from Marcellus gas wells in Pennsylvania, USA. *Applied Geochemistry*, 28, pp.55-61.
- He, C. and Vidic, R.D., 2016. Application of microfiltration for the treatment of Marcellus Shale flowback water: Influence of floc breakage on membrane fouling. *Journal of Membrane Science*, 510, pp.348-354.

- He, C., Wang, X., Liu, W., Barbot, E. and Vidic, R.D., 2014. Microfiltration in recycling of Marcellus Shale flowback water: Solids removal and potential fouling of polymeric microfiltration membranes. *Journal of Membrane Science*, 462, pp.88-95.
- He, Y., Folkerts, E.J., Zhang, Y., Martin, J.W., Alessi, D.S. and Goss, G.G., 2017a. Effects on Biotransformation, Oxidative Stress and Endocrine Disruption in Rainbow Trout (*Oncorhynchus mykiss*) Exposed to Hydraulic Fracturing Flowback and Produced Water. *Environmental Science & Technology*.
- He, Y., Flynn, S.L., Folkerts, E.J., Zhang, Y., Ruan, D., Alessi, D.S., Martin, J.W. and Goss, G.G., 2017b. Chemical and toxicological characterizations of hydraulic fracturing flowback and produced water. *Water Research*, 114, pp.78-87.
- He, Y., Sun, C., Zhang, Y., Folkerts, E.J., Martin, J.W. and Goss, G.G., 2018. Developmental Toxicity of the Organic Fraction from Hydraulic Fracturing Flowback and Produced Waters to Early Life Stages of Zebrafish (*Danio rerio*). *Environmental science & technology*, 52(6), pp.3820-3830.
- Hermia, J. (1982). Constant pressure blocking filtration laws: application to power-law non-Newtonian fluids. *Trans. Inst. Chem. Eng.*, 60a, 183 - 187.
- Ho, C.C. and Zydney, A.L., 1999. Effect of membrane morphology on the initial rate of protein fouling during microfiltration. *Journal of Membrane Science*, 155(2), pp.261-275.
- Ho, C.C. and Zydney, A.L., 2000. A combined pore blockage and cake filtration model for protein fouling during microfiltration. *Journal of colloid and interface science*, 232(2), pp.389-399.
- Hongprasith, N., Dolkittikul, N., Apiboonsuwan, K., Pungrasmi, W. and Painmanakul, P., 2016. Study of different flexible aeration tube diffusers: Characterization and oxygen transfer performance. *Environmental Engineering Research*, 21(3), pp.233-240.
- Howe, K.J. and Clark, M.M., 2002. Fouling of microfiltration and ultrafiltration membranes by natural waters. *Environmental science & technology*, 36(16), pp.3571-3576.
- Howe, K.J., Marwah, A., Chiu, K.P. and Adham, S.S., 2007. Effect of membrane configuration on bench-scale MF and UF fouling experiments. *Water research*, 41(17), pp.3842-3849.

- Hussain, A., Minier-Matar, J., Janson, A., Gharfeh, S. and Adham, S., 2014, January. Advanced technologies for produced water treatment and reuse. In *IPTC 2014: International Petroleum Technology Conference*.
- IER (Institute for Energy Research), 2012; U.S. Leads World in Natural Gas Production from Hydraulic Fracturing. <https://instituteforenergyresearch.org/analysis/u-s-leads-world-in-natural-gas-production-from-hydraulic-fracturing/>
- IEA (International Energy Agency), 2014. World Energy Outlook 2014, *OECD/IEA, Paris*. <https://www.iea.org/publications/freepublications/publication/WEO2014.pdf>
- Jackson, R.B., Lowry, E.R., Pickle, A., Kang, M., DiGiulio, D. and Zhao, K., 2015. The depths of hydraulic fracturing and accompanying water use across the United States. *Environmental science & technology*, 49(15), pp.8969-8976.
- Jackson, R.B., Vengosh, A., Carey, J.W., Davies, R.J., Darrah, T.H., O'sullivan, F. and Pétron, G., 2014. The environmental costs and benefits of fracking. *Annual Review of Environment and Resources*, 39, pp.327-362.
- Jiang, Q., Rentschler, J., Perrone, R. and Liu, K., 2013. Application of ceramic membrane and ion-exchange for the treatment of the flowback water from Marcellus shale gas production. *Journal of Membrane Science*, 431, pp.55-61.
- Kassotis, C.D., Iwanowicz, L.R., Akob, D.M., Cozzarelli, I.M., Mumford, A.C., Orem, W.H. and Nagel, S.C., 2016. Endocrine disrupting activities of surface water associated with a West Virginia oil and gas industry wastewater disposal site. *Science of the Total Environment*, 557, pp.901-910.
- Kim, K.M., Woo, S.H., Lee, J.S., Park, H.S., Park, J. and Min, B.R., 2015. Improved Permeate Flux of PVDF Ultrafiltration Membrane Containing PVDF-g-PHEA Synthesized via ATRP. *Applied Sciences*, 5(4), pp.1992-2008.
- Kim, S., Omur-Ozbek, P., Dhanasekar, A., Prior, A. and Carlson, K., 2016. Temporal analysis of flowback and produced water composition from shale oil and gas operations: Impact of frac fluid characteristics. *Journal of Petroleum Science and Engineering*, 147, pp.202-210.

- King, G.E., 2012. Hydraulic fracturing 101: what every representative, environmentalist, regulator, reporter, investor, university researcher, neighbor, and engineer should know about hydraulic fracturing risk. *Journal of Petroleum Technology*, 64(04), pp.34-42.
- Kondash, A.J., Albright, E. and Vengosh, A., 2017. Quantity of flowback and produced waters from unconventional oil and gas exploration. *Science of the Total Environment*, 574, pp.314-321.
- Kong, F.X., Chen, J.F., Wang, H.M., Liu, X.N., Wang, X.M., Wen, X., Chen, C.M. and Xie, Y.F., 2017. Application of coagulation-UF hybrid process for shale gas fracturing flowback water recycling: Performance and fouling analysis. *Journal of Membrane Science*, 524, pp.460-469.
- Ladewig, B. and Al-Shaeli, M.N.Z., 2017. Fundamentals of membrane bioreactors. *Springer*.
- Lammer, E., Carr, G.J., Wendler, K., Rawlings, J.M., Belanger, S.E. and Braunbeck, T., 2009. Is the fish embryo toxicity test (FET) with the zebrafish (*Danio rerio*) a potential alternative for the fish acute toxicity test?. *Comparative Biochemistry and Physiology Part C: Toxicology & Pharmacology*, 149(2), pp.196-209.
- Lebas, R.A., Shahan, T.W., Lord, P. and Luna, D., 2013, February. Development and use of high-TDS recycled produced water for crosslinked-gel-based hydraulic fracturing. *In SPE Hydraulic Fracturing Technology Conference. Society of Petroleum Engineers*.
- Lee, N., Amy, G., Croue, J.P. and Buisson, H., 2004. Identification and understanding of fouling in low-pressure membrane (MF/UF) filtration by natural organic matter (NOM). *Water research*, 38(20), pp.4511-4523.
- Lester, Y., Ferrer, I., Thurman, E.M., Sitterley, K.A., Korak, J.A., Aiken, G. and Linden, K.G., 2015. Characterization of hydraulic fracturing flowback water in Colorado: Implications for water treatment. *Science of the Total Environment*, 512, pp.637-644.
- Li, H., 2013. Produced water quality characterization and prediction for Wattenberg field. MSc. thesis. *Colorado State University*.
- Li, X., Coles, B. J., Ramsey, M. H., & Thornton, I., 1995. Sequential extraction of soils for multielement analysis by ICP-AES. *Chemical Geology*, 124(1), pp.109-123.

- Lim, A.L. and Bai, R., 2003. Membrane fouling and cleaning in microfiltration of activated sludge wastewater. *Journal of membrane science*, 216(1-2), pp.279-290.
- Liu, Z., Li, Q., Wu, Q., Kuo, D.T., Chen, S., Hu, X., Deng, M., Zhang, H. and Luo, M., 2017. Removal efficiency and risk assessment of polycyclic aromatic hydrocarbons in a typical municipal wastewater treatment facility in Guangzhou, China. *International journal of environmental research and public health*, 14(8), p.861.
- Lokare, O.R., Tavakkoli, S., Wadekar, S., Khanna, V. and Vidic, R.D., 2017. Fouling in direct contact membrane distillation of produced water from unconventional gas extraction. *Journal of Membrane Science*, 524, pp.493-501.
- Long, E.R., Macdonald, D.D., Smith, S.L. and Calder, F.D., 1995. Incidence of adverse biological effects within ranges of chemical concentrations in marine and estuarine sediments. *Environmental management*, 19(1), pp.81-97.
- Magi, E., Bianco, R., Ianni, C. and Di Carro, M., 2002. Distribution of polycyclic aromatic hydrocarbons in the sediments of the Adriatic Sea. *Environmental pollution*, 119(1), pp.91-98.
- Maguire-Boyle, S.J., Huseman, J.E., Ainscough, T.J., Oatley-Radcliffe, D.L., Alabdulkarem, A.A., Al-Mojil, S.F. and Barron, A.R., 2017. Superhydrophilic Functionalization of Microfiltration Ceramic Membranes Enables Separation of Hydrocarbons from Frac and Produced Water. *Scientific reports*, 7(1), p.12267.
- Mallevalle, J., Odendaal, P.E. and Wiesner, M.R. eds., 1996. Water treatment membrane processes. American Water Works Association.
- Mantell, M.E., 2011, March. Produced water reuse and recycling challenges and opportunities across major shale plays. In *Proceedings of the technical workshops for the hydraulic fracturing study: water resources management*. EPA (Vol. 600, pp. 49-57).
- McGroddy, S.E. and Farrington, J.W., 1995. Sediment porewater partitioning of polycyclic aromatic hydrocarbons in three cores from Boston Harbor, Massachusetts. *Environmental Science & Technology*, 29(6), pp.1542-1550.

- McMurdie, P.J. and Holmes, S., 2013. phyloseq: an R package for reproducible interactive analysis and graphics of microbiome census data. *PloS one*, 8(4), p.e61217.
- Mesquita, M.E., Silva, J.V.E., Branco, M.C. and Sequeira, E.M., 2000. Copper and zinc competitive adsorption: desorption in calcareous soils. *Arid soil research and rehabilitation*, 14(1), pp.27-41.
- Millero, F.J., Sotolongo, S. and Izaguirre, M., 1987. The oxidation kinetics of Fe (II) in seawater. *Geochimica et Cosmochimica Acta*, 51(4), pp.793-801.
- Mnif, S., Chamkha, M., Labat, M. and Sayadi, S., 2011. Simultaneous hydrocarbon biodegradation and biosurfactant production by oilfield-selected bacteria. *Journal of applied microbiology*, 111(3), pp.525-536.
- Mohammadi, T., Kazemimoghadam, M. and Saadabadi, M., 2003. Modeling of membrane fouling and flux decline in reverse osmosis during separation of oil in water emulsions. *Desalination*, 157(1-3), pp.369-375.
- Mondal, S., 2016. Polymeric membranes for produced water treatment: an overview of fouling behavior and its control. *Reviews in Chemical Engineering*, 32(6), pp.611-628.
- Morgan, B. and Lahav, O., 2007. The effect of pH on the kinetics of spontaneous Fe (II) oxidation by O₂ in aqueous solution—basic principles and a simple heuristic description. *Chemosphere*, 68(11), pp.2080-2084.
- Mulholland, P.J., 2003. Large-scale patterns in dissolved organic carbon concentration, flux, and sources. In *Aquatic Ecosystems* (pp. 139-159).
- Müller, S., Totsche, K.U. and Kögel-Knabner, I., 2007. Sorption of polycyclic aromatic hydrocarbons to mineral surfaces. *European Journal of Soil Science*, 58(4), pp.918-931.
- NEB (National Energy Board), 2017. Energy Futures 2017 Supplement: Natural Gas Production.
- Network, C.W., 2015. Water and hydraulic fracturing: Where knowledge can best support decisions in Canada.
- NRCAN, 2018. Natural gas facts. <https://www.nrcan.gc.ca/energy/facts/natural-gas/20067>

- O.E.C.D., 2011. Towards Green Growth: Monitoring progress. <https://www.oecd.org/greengrowth/greening-energy/49157219.pdf>
- Oliveira, M.E. and Franca, A.S., 1998. Simulation of oxygen mass transfer in aeration systems. *International communications in heat and mass transfer*, 25(6), pp.853-862.
- Orem, W., Tatu, C., Varonka, M., Lerch, H., Bates, A., Engle, M., Crosby, L. and McIntosh, J., 2014. Organic substances in produced and formation water from unconventional natural gas extraction in coal and shale. *International Journal of Coal Geology*, 126, pp.20-31.
- Paterek, J.R., and Smith, P.H., 1988. *Methanohalophilus mahii* gen. nov., sp. nov., a methylotrophic halophilic methanogen. *International Journal of Systematic and Evolutionary Microbiology*, 38(1), pp.122-123.
- PTAC (Petroleum Technology Alliance Canada), 2017. Tight oil and shale gas innovation roadmap. <https://www.ptac.org/wp-content/uploads/2017/05/TOGIN-Roadmap-Report-05May2017.pdf>.
- Quast, C., Pruesse, E., Yilmaz, P., Gerken, J., Schweer, T., Yarza, P., Peplies, J. and Glöckner, F.O., 2012. The SILVA ribosomal RNA gene database project: improved data processing and web-based tools. *Nucleic acids research*, 41(D1), pp.D590-D596.
- R Core Team, 2017. R: A language and environment for statistical computing. Vienna, Austria: R Foundation for Statistical Computing [WWW document]. <https://www.R-project.org/>.
- Radhi, A.A. and Borghei, M., 2017. Effect of aeration then granular activated carbon on removal efficiency of TOC, COD and Coliform, Fecal coliform for "Sorkheh Hesar Canal" water.
- Rahm, B.G., Bates, J.T., Bertoia, L.R., Galford, A.E., Yoxtheimer, D.A. and Riha, S.J., 2013. Wastewater management and Marcellus Shale gas development: Trends, drivers, and planning implications. *Journal of environmental management*, 120, pp.105-113.
- Rivard, C., Lavoie, D., Lefebvre, R., Séjourné, S., Lamontagne, C. and Duchesne, M., 2014. An overview of Canadian shale gas production and environmental concerns. *International Journal of Coal Geology*, 126, pp.64-76.

- Rokosh, C.D., Lyster, S., Anderson, S.D.A., Beaton, A.P., Berhane, H., Brazzoni, T., Chen, D., Cheng, Y., Mack, T., Pana, C. and Pawlowicz, J.G., 2012. Summary of Alberta's shale- and siltstone-hosted hydrocarbon resource potential. *Energy Resources Conservation Board, ERCB/AGS Open File Report*, 6, p.327.a.
- Krishnamurti, S. R., G & M. Huang, P & Rees, K & M. Kozak, L & P. W. Rostad, H. (1995). Speciation of particulate-bound Cadmium of soils and its bioavailability. *Analyst*. 120, pp.659-665.
- Saba, B., 2014. Potential treatment options for hydraulic fracturing return fluids: a review. *ChemBioEng Reviews*, 1(6), pp.273-279.
- Sampath, M., Shukla, A. and Rathore, A.S., 2014. Modeling of filtration processes—microfiltration and depth filtration for harvest of a therapeutic protein expressed in *Pichia pastoris* at constant pressure. *Bioengineering*, 1(4), pp.260-277.
- Sick, B.A., 2014. Characterization and treatment of produced water from Wattenberg oil and gas wells fractured with slickwater and gel fluids. MSc. thesis. Colorado State University.
- Speight, J.G., 2016. *Handbook of Hydraulic Fracturing*. John Wiley & Sons.
- Stepan, D.J., Shockey, R.E., Kurz, B.A., Kalenze, N.S., Cowan, R.M., Ziman, J.J. and Harju, J.A., 2010. Bakken water opportunities assessment—Phase 1. *University of North Dakota Energy and Environmental Research Center for North Dakota Industrial Commission Oil and Gas Research Council*. <http://www.undeerc.org/bakken/pdfs/FracWaterPhaseIreport.pdf>.
- Stoakes, F.A. and Creaney, S., 1985. Sedimentology of a carbonate source rock: the Duvernay Formation of Alberta Canada.
- Stookey, L.L., 1970. Ferrozine- a new spectrophotometric reagent for iron. *Analytical chemistry*, 42(7), pp.779-781.
- Stringfellow, W.T., Domen, J.K., Camarillo, M.K., Sandelin, W.L. and Borglin, S., 2014. Physical, chemical, and biological characteristics of compounds used in hydraulic fracturing. *Journal of hazardous materials*, 275, pp.37-54.

- Stumm, W. and Lee, G.F., 1961. Oxygenation of ferrous iron. *Industrial & Engineering Chemistry*, 53(2), pp.143-146.
- Tamura, H., Goto, K. and Nagayama, M., 1976. The effect of ferric hydroxide on the oxygenation of ferrous ions in neutral solutions. *Corrosion Science*, 16(4), pp.197-207.
- Tessier, A., Campbell, P.G. and Bisson, M., 1979. Sequential extraction procedure for the speciation of particulate trace metals. *Analytical chemistry*, 51(7), pp.844-851.
- Todd DK and Mays LW. 2005. Groundwater Hydrology. John Wiley & Sons, New York.
- U.S.EIA (Energy Information Administration), 2016. International energy outlook 2016. Natural gas, Chapter 3. https://www.eia.gov/energyexplained/index.php?page=natural_gas_where
- U.S.EPA (US Environmental Protection Agency) n.d. Aeration and Air Stripping, accessed June 2018. <https://iaspub.epa.gov/tdb/pages/treatment/treatmentOverview.do>
- U.S.EPA (US Environmental Protection Agency), 2016. Hydraulic Fracturing for Oil and Gas: Impacts from the Hydraulic Fracturing Water Cycle on Drinking Water Resources in the United States.
- von Gunten, K., Hamilton, S.M., Zhong, C., Nesbø, C., Li, J., Muehlenbachs, K., Konhauser, K.O. and Alessi, D.S., 2018. Electron donor-driven bacterial and archaeal community patterns along forest ring edges in Ontario, Canada. *Environmental microbiology reports*.
- Wang, F. and Tarabara, V.V., 2008. Pore blocking mechanisms during early stages of membrane fouling by colloids. *Journal of colloid and interface science*, 328(2), pp.464-469.
- Wang, J., Wang, C., Huang, Q., Ding, F. and He, X., 2015. Adsorption of PAHs on the sediments from the yellow river delta as a function of particle size and salinity. *Soil and Sediment Contamination: An International Journal*, 24(2), pp.103-115.
- Wheeler, M.W., Park, R.M. and Bailer, A.J., 2006. Comparing median lethal concentration values using confidence interval overlap or ratio tests. *Environmental Toxicology and Chemistry: An International Journal*, 25(5), pp.1441-1444.
- Xiong, B., Roman-White, S., Piechowicz, B., Miller, Z., Farina, B., Tasker, T., Burgos, W., Zydney, A.L. and Kumar, M., 2018. Polyacrylamide in hydraulic fracturing fluid causes

- severe membrane fouling during flowback water treatment. *Journal of Membrane Science*, 560, pp.125-131.
- Xiong, B., Zydney, A.L. and Kumar, M., 2016. Fouling of microfiltration membranes by flowback and produced waters from the Marcellus shale gas play. *Water research*, 99, pp.162-170.
- Yilmaz, P., Parfrey, L.W., Yarza, P., Gerken, J., Pruesse, E., Quast, C., Schweer, T., Peplies, J., Ludwig, W. and Glöckner, F.O., 2013. The SILVA and “all-species living tree project (LTP)” taxonomic frameworks. *Nucleic acids research*, 42(D1), pp.D643-D648.
- Zhang, Y., Shotyk, W., Zaccone, C., Noernberg, T., Pelletier, R., Bicalho, B., Froese, D.G., Davies, L. and Martin, J.W., 2016. Airborne petcoke dust is a major source of polycyclic aromatic hydrocarbons in the Athabasca Oil Sands Region. *Environmental science & technology*, 50(4), pp.1711-1720.
- Zhilina, T.N., Zavarzina, D.G., Detkova, E.N., Patutina, E.O., and Kuznetsov, B.B., 2015. *Fuchsiella ferrireducens* sp. nov., a novel haloalkaliphilic, lithoautotrophic homoacetogen capable of iron reduction, and emendation of the description of the genus *Fuchsiella*. *International journal of systematic and evolutionary microbiology*, 65(8), pp.2432-2440.
- Zhilina, T.N., Zavarzina, D.G., Panteleeva, A.N., Osipov, G.A., Kostrikina, N.A., Tourova, T.P., and Zavarzin, G.A., 2012. *Fuchsiella alkaliacetigena* gen. nov., sp. nov., an alkaliphilic, lithoautotrophic homoacetogen from a soda lake.
- Zhou, J., Wandera, D. and Husson, S.M., 2015. Mechanisms and control of fouling during ultrafiltration of high strength wastewater without pretreatment. *Journal of Membrane Science*, 488, pp.103-110.
- Ziemkiewicz, P.F. and He, Y.T., 2015. Evolution of water chemistry during Marcellus Shale gas development: A case study in West Virginia. *Chemosphere*, 134, pp.224-231.
- Zolfaghari, A., Tang, Y., Holyk, J., Binazadeh, M., Dehghanpour, H. and Bearinger, D., 2015, September. Advances in flowback chemical analysis of gas shales. In *SPE Annual Technical Conference and Exhibition*. Society of Petroleum Engineers.

Appendix A.

Additional Data of Membrane Filtration

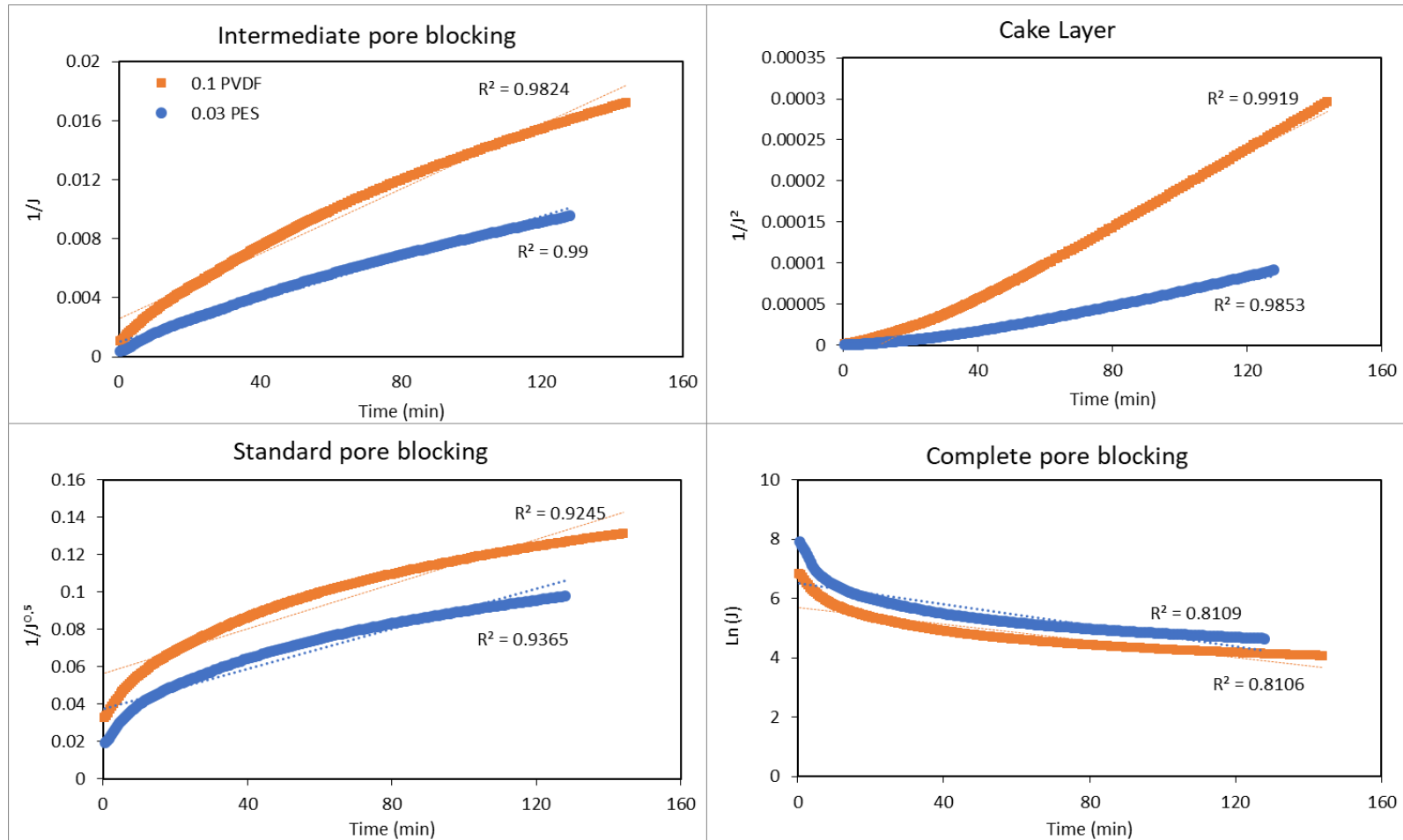


Figure A.1. Fouling mechanisms of the non-aerated FPW sample using the 0.1 PVDF and 0.03 PES membranes.

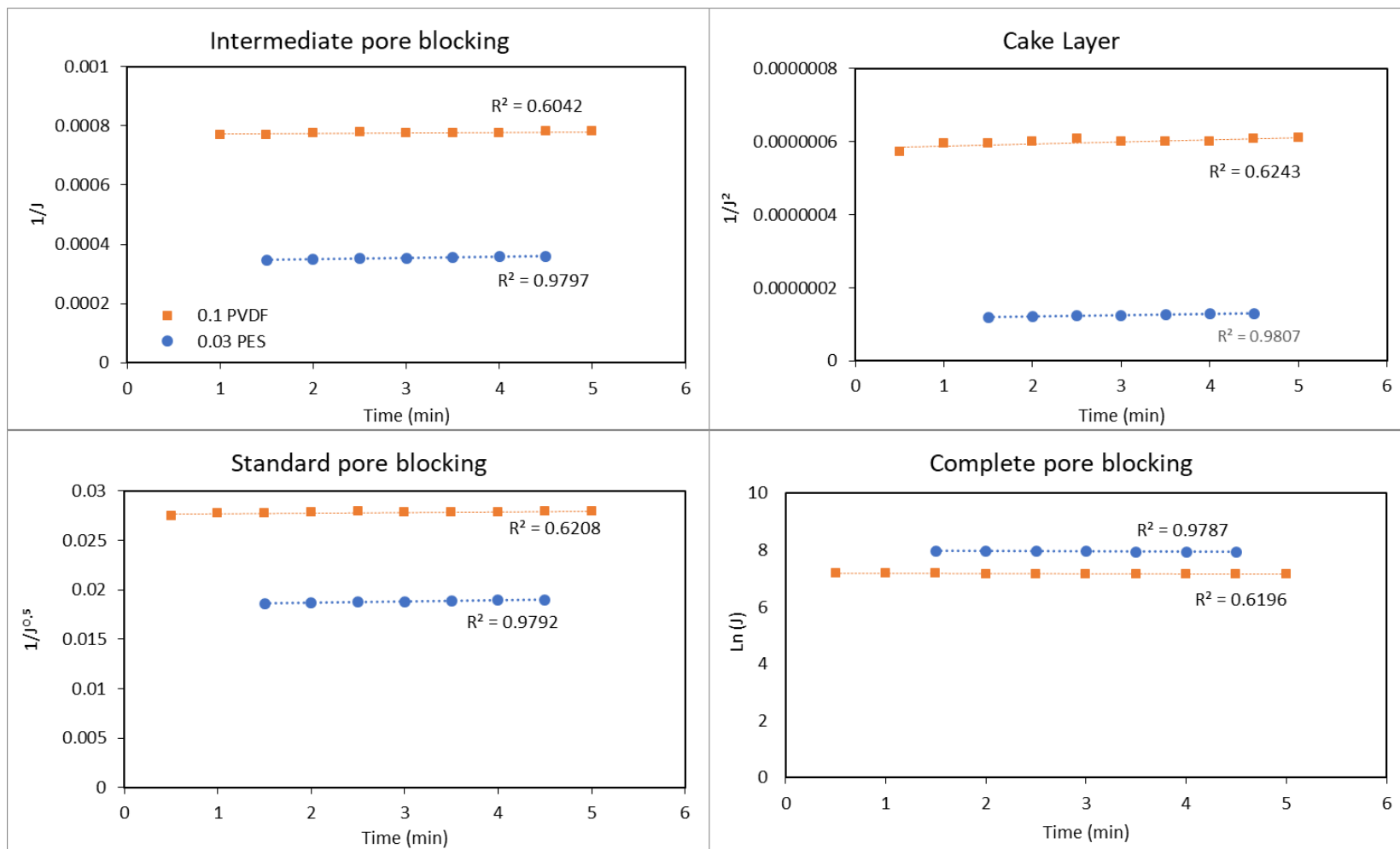


Figure A.2. Fouling mechanisms of the aerated FPW sample using the 0.1 PVDF and 0.03 PES membranes.

Table A.1. Rejection of Iron and Silica using the 0.1 PVDF and 0.03 PES membranes.

Sample	Rejection of Iron (Fe)		Rejection of Silica (Si)	
	Concentration (mg/L)	Observed Rejection %	Concentration (mg/L)	Observed Rejection %
Raw FPW	210 ± 4.7		23.2 ± 1.8	
0.1 PVDF	6.8	96.7	BDL	>99
0.03 PES	5.6	97.3	BDL	>99

Appendix B.

Additional FPW Analyses

Table B.1. Charge balance of the FPW sample.

Element	meq
Na ⁺	2328
Li ⁺	5.87
Ca ²⁺	382
K ⁺	48.96
Sr ²⁺	20.18
Mg ²⁺	57.68
Fe ²⁺	7.52
Ba ²⁺	0.14
Mn ²⁺	0.19
Zn ²⁺	0.037
Pb ²⁺	0.0013
Cl ⁻	2894
Br ⁻	2.76
B ⁻	7.32

Table B.2. Sequential extraction results for the non-aerated FPW precipitates. Exch: exchangeable. Carb: bound to carbonates. Fe/Mn: bound to amorphous iron and manganese oxides. OrgM: bound to organic matter. Crystal Fe: Crystalline iron oxides.

Element	Masses	Method	Exch (ug/g)	Carb (ug/g)	Fe/Mn (ug/g)	OrgM (ug/g)	Crystal Fe (ug/g)	Residual (ug/g)	Total	Recovery FPW (%)
Li	7/7	No gas	138.61	16.42	4.99	0.00	0.12	0.16	160.30	160.02
B	11/11	No gas	345.05	341.29	111.05	0.00	0.88	0.65	798.92	91.68
Al	27/27	No gas	0.00	0.00	23.32	16.38	21.55	201.06	262.30	51.00
Si	28/28	He	46.96	4431.50	5151.37	502.27	50.50	34781.22	44963.82	105.21
P	31/31	O ₂	7.48	93.31	124.79	390.87	60.08	5.31	681.84	85.23
S	32/48	O ₂	909.14	405.26	434.17	1772.38	1815.73	1817.08	7153.76	65.55
K	39/39	No gas	6967.91	154.61	0.00	21.69	31.62	108.96	7284.79	127.55
Ca	40/40	H ₂	28078.32	5490.52	533.53	46.16	78.38	183.84	34410.75	135.18
Cr	52/52	No gas	2.95	3.88	25.84	12.68	3.05	3.51	51.91	100.01
Mn	55/55	No gas	18.85	30.01	11.40	0.90	45.51	1.22	107.89	95.92
Fe	56/56	No gas	175.98	25311.96	61056.54	1663.31	9384.94	227.54	97820.27	88.24
Cu	63/63	No gas	1.99	32.59	36.77	44.13	2.16	0.50	118.15	118.13
Zn	66/66	No gas	1.12	99.43	36.55	0.00	41.26	1.21	179.57	100.28
Br	79/79	He	122.27	0.00	0.00	0.00	0.00	0.00	122.27	72.10
Sr	88/88	No gas	3347.11	0.00	747.61	1711.43	ADL	3169.28	8975.42	66.75
Mo	95/95	He	0.00	0.00	5.65	13.96	1.93	0.17	21.70	94.76
Ba	138/138	He	2194.03	4614.72	1269.73	7656.78	3590.25	24620.25	43945.75	161.70
Pb	208/208	No gas	0.00	0.00	134.20	38.23	75.11	124.74	372.28	95.88

Table B.3. Sequential extraction results for the aerated FPW precipitates in triplicates. Exch: exchangeable. Carb: bound to carbonates. Fe/Mn: bound to amorphous iron and manganese oxides. OrgM: bound to organic matter. Crystal Fe: Crystalline iron oxides.

Element	Masses	Method	Exch (ug/g)	Carb(ug/g)	Fe/Mn (ug/g)	OrgaM(ug/g)	Crystal Fe (ug/g)	Residual (ug/g)	Total	Recovery FPW (%)
Li	7/7	No gas	40.26 ± 2.4	15.14 ± 3.2	<0.1	<0.1	<0.1	0.14 ± 0.09	55.59 ± 1.5	162.46
B	11/11	No gas	305.75 ± 7.3	353.70 ± 17.9	658.07 ± 10.5	<0.1	<0.1	0.51 ± 0.06	1318.07 ± 7.6	110.94
Al	27/27	He	8.41 ± 3.9	<0.1	<0.1	<0.1	7.01 ± 2.2	45.20 ± 4.3	60.62 ± 3.4	0.00
Si	28/28	No gas	139.65 ± 11.5	1716.83 ± 209	5140.02 ± 506	818.69 ± 88.7	913.09 ± 32.5	24968.65 ± 580	33696.93 ± 232	105.21
P	31/31	O ₂	0.40 ± 0.15	3.66 ± 0.9	56.03 ± 0.4	56.72 ± 6.5	57.47 ± 8.0	1.37 ± 0.09	175.65 ± 3.0	103.46
S	32/48	O ₂	555.40 ± 7.3	341.70 ± 12.5	377.58 ± 9.3	530.81 ± 8.8	284.15 ± 23.1	96.34 ± 13.6	2185.95 ± 9.5	107.08
K	39/39	He	3567.80 ± 66.3	84.09 ± 1.4	<0.1	<0.1	<0.1	25.26 ± 2.1	3677.15 ± 38.3	139.20
Ca	40/40	H ₂	14055.14 ± 206	1864.26 ± 73.6	651.18 ± 15.7	<0.1	3.07 ± 0.7	5.96 ± 1.5	16579.61 ± 76	120.82
Cr	52/52	He	0.19 ± 0.1	143.41 ± 5.9	895.32 ± 6.1	39.23 ± 3.8	11.96 ± 2.0	0.81 ± 0.05	1090.92 ± 2.7	108.66
Mn	55/55	No gas	15.53 ± 0.3	5.37 ± 0.06	8.38 ± 1.13	<0.1	8.37 ± 0.4	0.34 ± 3.4	37.99 ± 1.3	120.95
Fe	56/56	He	63.35 ± 4.6	17535.19 ± 901	192526.3 ± 1678	351.9	2992.64 ± 302	41.55 ± 2.7	216649.86 ± 566	84.85
Cu	63/63	He	1.08 ± 0.2	11.93 ± 0.3	17.91 ± 0.8	8.21 ± 0.6	0.39 ± 0.01	0.19 ± 0.07	39.70 ± 0.3	113.24
Zn	66/66	No gas	2.73 ± 0.12	15.35 ± 0.7	19.07 ± 0.92	<0.1	9.13 ± 0.2	<0.1	46.51 ± 0.4	100.72
Br	79/79	No gas	146.68 ± 8.7	<0.1	<0.1	<0.1	6.78 ± 0.3	<0.1	153.46 ± 7.6	90.49
Sr	88/88	No gas	1918.77 ± 24.9	525.74 ± 17.9	355.31 ± 7.8	375.81 ± 10.1	94.34 ± 7.9	21.29 ± 2.6	3291.26 ± 9.9	108.18
Mo	95/95	No gas	0.00	0.81 ± 0.1	36.45 ± 0.4	18.24 ± 0.4	2.84 ± 0.4	<0.1	58.39 ± 0.3	105.01
Ba	138/138	No gas	1919.3 ± 45.2	2670.82 ± 124.5	3223.75 ± 75.5	7307.46 ± 157.1	6640.75 ± 338	2649.20 ± 338	24411.54 ± 196	100.33
Pb	208/208	No gas	0.00	2.72 ± 0.07	327.58 ± 2.2	16.14 ± 2.7	22.14 ± 2.4	6.07 ± 0.8	374.64 ± 1.5	107.61

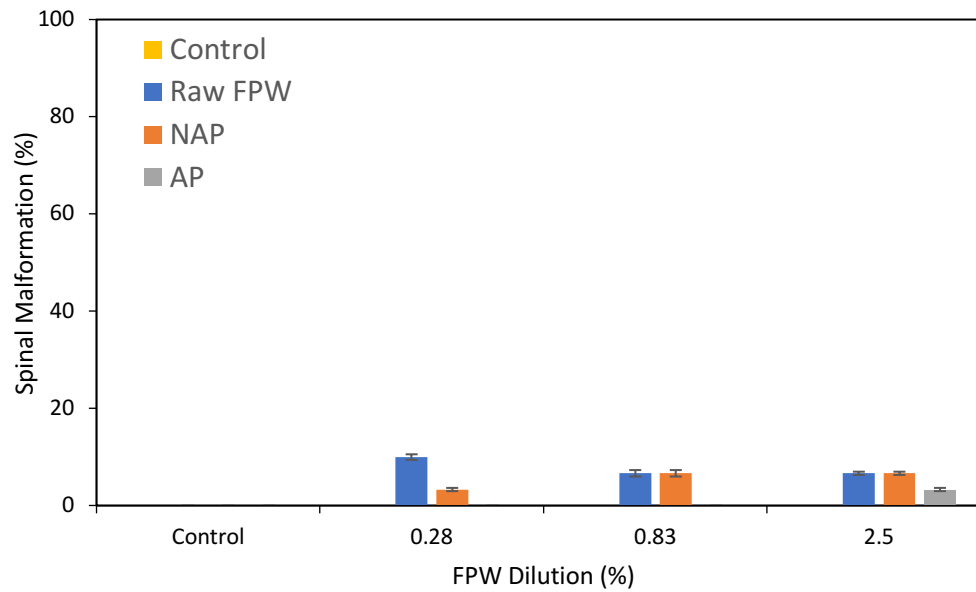


Figure B.1. Spinal malformation effects in zebrafish embryo using the non-aerated permeate (NAP) and the aerated permeate (AP) compared to the raw FPW sample after 96 h of exposure. A control water was also compared.

Table B.4. Summary table of all taxa found in the two precipitate samples. Taxa with single reads and unknowns are not shown.

Total	Aerated (%)	Non-aerated (%)	Taxonomy
159650	42.595	48.642	Bacteria; Firmicutes; Clostridia; Halanaerobiales; Halanaerobiaceae; Halanaerobium;
74324	18.560	24.555	Bacteria; Deferribacteres; Deferribacteres; Deferribacterales; Deferribacteraceae; Flexistipes;
34213	14.833	1.844	Bacteria; Firmicutes; Clostridia; Halanaerobiales; Halobacteroidaceae; Fuchsiella;
28676	10.862	3.908	Bacteria; Proteobacteria; Gammaproteobacteria; Oceanospirillales; Halomonadaceae; Modicisalibacter;
24665	5.382	9.318	Bacteria; Thermotogae; Thermotogae; Thermotogales; Thermotogaceae; Geotoga;
14934	2.829	6.288	Archaea; Euryarchaeota; Methanomicrobia; Methanosarcinales; Methanosarcinaceae; Methanohalophilus;
5147	1.716	1.053	Bacteria; Firmicutes; Clostridia;
5125	1.200	1.813	Bacteria; Bacteroidetes; Bacteroidia; Bacteroidales; Marinilabiaceae; Marinilabilia;
4785	0.709	2.311	Bacteria; Bacteroidetes; Bacteroidia; Bacteroidales; Marinilabiaceae; Anaerophaga;
2548	1.112	0.126	Bacteria; Firmicutes; Clostridia; Halanaerobiales; Halobacteroidaceae; Orenia;
312	0.066	0.121	Bacteria; Firmicutes; Clostridia; Halanaerobiales;
245	0.107	0.012	Bacteria; Proteobacteria; Betaproteobacteria; Burkholderiales; Burkholderiaceae; Ralstonia;
24	0.010	0.002	Bacteria; Proteobacteria; Betaproteobacteria; Burkholderiales; Burkholderiaceae; Burkholderia;
19	0.008	0.001	Bacteria; Proteobacteria; Gammaproteobacteria; Pseudomonadales; Pseudomonadaceae; Pseudomonas;
18	0.008	0.001	Bacteria; Proteobacteria; Gammaproteobacteria; Pseudomonadales; Moraxellaceae; Acinetobacter;
3	0.001	0.001	Bacteria; Proteobacteria; Betaproteobacteria; Nitrosomonadales; Gallionellaceae;
3	0.001	0.001	Bacteria; Proteobacteria; Gammaproteobacteria; Alteromonadales; Shewanellaceae; Shewanella;
2	0.001	0.000	Bacteria; Bacteroidetes; Bacteroidia; Bacteroidales; Prevotellaceae; Prevotella;
2	0.001	0.000	Bacteria; Proteobacteria; Alphaproteobacteria; Sphingomonadales; Sphingomonadaceae; Sphingomonas;
2	0.000	0.001	Bacteria; Proteobacteria; Gammaproteobacteria; 1013-28-CG33;
2	0.001	0.000	Bacteria; Proteobacteria; Gammaproteobacteria; Xanthomonadales; Xanthomonadaceae; Stenotrophomonas;